The Dissertation Committee for Ping Du Certifies that this is the approved version of the following dissertation:

Influence of Engineered Particulate Lactose On The Performance of DPI Formulations

Committee:

Hugh D. C. Smyth, Supervisor

James W. McGinity

Robert O. Williams, III

Noel T. Clemens

Christopher R. Frei

Influence of Engineered Particulate Lactose On The Performance of DPI Formulations

by

Ping Du, B.S.; M.S.

Dissertation

Presented to the Faculty of the Graduate School of
The University of Texas at Austin
in Partial Fulfillment
of the Requirements
for the Degree of

Doctor of Philosophy

The University of Texas at Austin
May, 2015

Acknowledgements

Graduate study and dissertation could not be completed merely by one person. A number of people I have met and interacted with during my four years' study in The University of Texas at Austin all made contribution and paved the road to the success for me.

I want to express my deep gratitude to my supervisor Dr. Hugh D. C. Smyth for giving me the great opportunity to work in such a great group and for his generous support in my research projects, internships and my active activities in student organizations. Dr. Smyth's broad and deep knowledge in pharmaceutics, formulation and pulmonary delivery inspired my interest and innovation in my dissertation research. Being in your research group is an invaluable experience of my life and I could not appreciate more. Special thanks to my dissertation committee members, Dr. James W. McGinity, Dr. Robert O. Williams III, Christopher R. Frei and Dr. Noel T. Clemens, for their encouragement in my study and invaluable guidance in the scope of my research projects. I am especially thankful to Dr. James W. McGinity, and Dr. Robert O. Williams III for their enthusiasm and experiences in pharmaceutics, and their professional advice in my career development. I also appreciate Dr. Jason McConville, my first supervisor for giving me the opportunity to study in University of Texas at Austin, so that I could reunite with Ju Du, my husband.

I am grateful to the assistance and encouragement from Dr. Feng Zhang, Dr. Zhengrong Cui, Dr. Solomon Stavchansky, and Dr. Carlton Erickson, the faculty members in Pharmaceutics Division or College of Pharmacy.

Ju Du, my dear husband, is always encouraging and thinks things in the positive site. Being able to study in UT-Austin and especially in the same lab with Ju Du is a great memory and invaluable experience for us. I am especially grateful to all the labmates for their friendship, generosity and support in my research and student activity work. Particularly, I would like to thank Mr. Ashkan Yazdi, Mr. Matt Herpin, and Dr. Andy Maloney for discussing problems I met in my research projects. I thank Dr. Nihal Bandara, Dr. Srimahitha Kaliki, Mr. Daniel Moraga and Ms. Tania Baham ́ndez for their warm friendship and always willing to share with me about their interesting life experiences.

I am especially grateful to all the current and past fellow graduate students including Dr. Bo Lang, Dr. Yibo Wang, Dr. Xinran Li, Dr. Justin Keen, Dr. Justin Hughey, Dr. Ryan Bennett, Dr. Amit Kumar, Mr. Michael Sandoval, Mr. Jim Bynum, Mr. Julien Maincent, Mr. Sachin Thakkar, Mr. Abdul (dayel) Abdulaziz, Mr. Chris Brough, Ms. Soraya Hengsawas, Mr. Siyuan Huang, Mr. Justin LaFountaine, Mr. Youssef Naguib, Ms. Leena Prasad, Ms. Solange Valdes, Ms. Abbie Miller.

My life won't be so easier and colorful without the assistance from the enthusiastic staff members in College of Pharmacy, especially Ms. Stephanie Crouch, Ms. Yolanda Abasta, Ms. Claudia McClelland and Ms. Parker Jane A. for their help.

Finally, I would like to thank my parents for their support in my decision to study abroad and unconditional love through this journey. My parents' spirit in hard working always encourage me and inspire me to move forward, which is the foundation of my success.

Influence of Engineered Particulate Lactose On The Performance of DPI Formulations

Ping Du, Ph.D.

The University of Texas at Austin, 2015

Supervisor: Hugh D. C. Smyth

Development of dry powder inhaler (DPI) formulations for respiratory diseases, such as Tuberculosis (TB), is challenging. The major limitation of current marketed DPIs is low delivery efficiency. In addition, delivered dose variation is also a challenging problem in the development and design of DPI formulations due to the poor flowability and dispersibility of the powder formulation. Furthermore, antibiotic drugs used in TB or other respiratory infectious diseases have to be administered in a relatively large dose for pulmonary delivery. However, currently there is no high dose conventional lactose based DPI formulations available. Therefore, I propose an innovative approach to solve these problems through the engineering of particulate lactose by wet granulation.

Lactose is the commonly used carrier particle for DPI formulations. Although it was widely believed that carrier particles with smaller diameters were preferable to maximize aerosolization efficiency (the ability of the drugs to be delivered to the lung), it was found recently that lactose carriers with large size also can improve aerosol performance, especially when combined with greater surface roughness and an appropriately designed inhaler device.

In the first study, after the engineered particulate lactose was manufactured, the relationship between the physico-chemical properties, e.g. size, of the granulated lactose and the DPI aerosol performance was investigated. It was concluded that poorer or enhanced dispersion performance is not an inherent property to the significantly large size of granulated lactose carriers as previously contended. Relatively large granulated lactose has improved flowability and increased surface roughness with increasing size fraction, which were properties for formulating high drug loaded DPI formulations. It was found that the aerosol performance of the high drug loaded DPI formulation depended significantly on the specific APIs and also the inhalation flow rate used in the cascade impactor study. DPI aerosol performance is the interplay of formulation, patient inhalation effort and device design. The device design was therefore modified and optimized to further improve the aerosol performance. In the end, with the optimized device and granulated lactose as the carrier, a high drug loaded rifampicin DPI formulation with improved aerosol performance (fine particle fraction around 70%), better blending uniformity and potential low systemic toxicity was achieved.

Table of Contents

List of Tables

List of Figures

Chapter 1: Introduction

1.1 EXCIPIENTS IN DRY POWDER INHALERS

In their broadest definition, excipients are the constituents of pharmaceutical dosage forms that are not the active substance. In general they serve a wide range of purposes including coloring agents, antioxidants, preservatives, adjuvants, stabilizers, thickeners, emulsifiers, solubilizers, permeation enhancers, flavoring and aromatic substances as well many other enabling roles. They are even defined as broadly as the constituents of the outer covering of the medicinal products, e.g. gelatin capsules[1]. But what is the purpose of using excipients in dry powder inhaler formulations? To answer this, it is useful to trace the history of modern dry powder inhalers and discuss briefly the mechanisms of operation of these devices and the underlying physics.

US patent 2470296 describes perhaps the first modern commercial dry powder inhaler, the Abbott Aerohalor. This patent application from 1948 provides the first description of how drug powders and additives or excipients might influence the performance of an inhaler device. Specifically, fields describe his invention as being more accurate and had improved performance when the drug (penicillin) was mixed with some other ingredient that functioned as a diluent or vehicle[2, 3]. From these beginnings one can identify the next major advance in dry powder inhalers as the paper by Bell and coworkers (1971) that describes issues of powder dispersion and flow as it related to the Fison's Spinhaler that was patented in 1970 [4, 5]. This landmark paper changed the way the aerosol scientists thought of inhalers and the influence of the work is still present in the

multitude of scientific works that focus on dry powder inhalers today. For the first time, it was suggested the addition of coarse carrier particles to the fine particles in the formulation in order to improve the powder flow. For example, cromolyn sodium after micronization was reduced to a mean aerodynamic diameter of 2.6 μm and resulted in poor powder flow and difficulty in emptying from the capsule. However, results were shown where powder flow was considerably improved when mixed with 70% w/w of coarse lactose in the range 30-60 μm. Another longstanding legacy introduced in the paper was the concept of using standard hard gelatin capsule for the dose storage. In this way the powder was protected against the environment unlike previous technologies such as the Aerohalor. This paper also illustrated that vibratory motion was necessary for powder aerosolization. These features are still readily observable in modern inhalers. The impact of powder particle size on discharge of powder from the gelatin capsule also was studied. For this study, eight different lactose powders sizes were tested, ranging from 4 to 400 μm. Their results showed the best performance was obtained with a size range of 70-100 μm.

From these beginnings one can see the origins of today's dry powder inhaler technologies from device and formulation design. We can begin to answer some of the central questions about excipients in dry powder inhalers: Why do we need excipients? Almost all commercialized DPIs and many of those in development utilize lactose as an excipient. Lactose as an excipient has two main functions: (1) aiding in the dilution and powder flow necessary for metering of the dose into capsules or blister cavities, and (2) aiding in particle entrainment and in particle deaggregation during airflow across the device improving lung deposition efficiencies. Dose metering and particle deaggregation

are two critical steps in successful powder delivery to the airways that are difficult to achieve. Pure micronized particles suffer from complex adhesion and cohesion forces resulting in aggregation. These adhesive forces are primarily van der waals in origin [6] and at the size ranges of respirable particles these forces dominate over gravitational forces that are responsible for much of the physical behavior of much larger sized particulate systems. Individually, van der waals forces are weak, but collectively there can be strong – analogous to Velcro™. Strong aggregation arises in micronized powders because their surface areas are large and the masses are very low. For example, 500 mcg dose of micronized fluticasone contains the total equivalent surface area as the U.S. one dollar bill. The mass of each particle however is in the low picogram range. Therefore a major challenge is to facilitate the relatively modest airflow of inhalation to overcome the high surface areas and associated energies that result in strong particle-particle adhesion. Because the particles themselves carry such a low mass, the transfer of forces to induce breakage of these interparticulate forces are the major limitation in dry powder inhaler systems. However, as seen with the Aerohalor and the Spinhaler™, mixing the micronized drug with an excipient improves the balance so that deaggregation can occur to a sufficient extent that clinical benefit can be achieved from these and similar devices.

Why do we use lactose as the primary excipient in DPIs? Table 1.1 is a list of commercially available inhalation grade lactose (Figure 1.1) on the market [7, 8]. The literature does not reveal a clear picture of why lactose itself was initially chosen. Over the years reasons have been given that include the fact that it is less hygroscopic than many other polyols, it is readily available in a variety of pre-engineered morphologies, densities, and it is easily processed by a number of different manufacturing methods. The

established safety profile is obviously important today but would not have been as established when lactose was first chosen forty or so years ago. It seems that lactose may be our excipient of choice today because Bell and coworkers showed that it was promising as a DPI excipient.

Despite its obvious widespread use and apparent functionality in dry powder inhalers, lactose does not yet solve the major challenges for DPIs today. Dose consistency is poor with dry powder inhalers. In general, the dose depends on the inhalation flow rate achieved by the patient. In addition, it is well known that manufacturing control and uniformity are extremely challenging with these products, particularly with the emergence of fixed dose combination products. The poor deaggregation efficiency achieved by modern DPIs is also a barrier to commercialization for therapeutics with either low potency or with narrow therapeutic indicies. Off-targeting of 60-80 percent of the drug payload is the current norm for both inhalers on the market and even for many of those in development. A large and growing body of literature has been generated on various aspects of DPI formulation design and excipient properties as scientists have tried to solve these issues. Lactose has been examined by looking at the influence of particle size [9, 10], surface area[11], particle shape [9, 12], effects of crystallinity [13], surface adhesion forces [14] and surface energetics [11], electrostatic effects [15, 16], influence of impurities [17], amongst other aspects. Table 1.2 provides a summary of the physicochemical properties of lactose extensively investigated and their influence on DPI performance. Despite the multitude of detailed investigations our understanding of DPIs has improved only gradually and many critical unknowns still exist. For instance the mechanisms of powder blend statics and dynamics (i.e. the adhesion step) are largely

unknown. The dispersion mechanisms (i.e. deaggregation step) has received greater attention but this remains speculative and importantly, few, if any, analytical methods have been found that provide sufficient predictive power of formulation performance and insights into quality of the system.

What is needed for improving DPI quality and performance? The aerosol performance of DPIs is a function of the adhesive (drug-lactose) and cohesive forces (drug-drug). Strong adhesive forces between lactose and drug facilitate homogenous blending, but may result in poor drug particle dispersion from carrier surface. On the other hand, strong cohesive forces, which lead to easier carrier-drug deaggregation, may reduce blending stability and cause product variability. What is needed are methods that identify the important parameters predictive of powder performance. Several methodologies and techniques have been applied to estimate particulate interactions, such as atomic force microscopy (AFM)[50, 51], inverse gas chromatography (IGC)[52, 53], powder flow indices [44], and newly developed blending dynamics[9]. powder flow properties with aerosol performance have investigated with the hope of allowing rapid selection and optimization of formulations. Angle of repose, Carr's compressibility index (CI), and Hausner ratio (HR) are static powder flow indices of pharmaceutical solids. The angle of repose (a) reflects interparticulate adhesion and friction forces. As the adhesion and friction forces increase, the angle of repose increases with a greater resistance to flow. Free-flowing powders have less than 40 ° angle of repose; while angle of repose greater than 50 ° indicates poor flowability [54]. Dynamic powder flow measurement methods include dynamic angle of repose, also called rotating drum method [55], and vibrating spatula method [56]. In the rotating drum method, powders slowly rotate in the drum and

avalanches happen when angle of repose is exceeded during rotation. The dynamic angle of repose, Θ, oscillates around a mean angle. Powder rheology too has recently received attention and, similar to flow measurements, allow improved manufacturing and aerosolization performance to be quickly screened.

All analytical methods mentioned above, although providing snapshots and insight into surface interactions, have been limited by tedious procedures and irreproducibility. While AFM scrutinizes the system on the single particle scale (microscale) and IGC probes the bulk powder (macroscale), methods which span these scales have not yet been developed. Mixing studies may be employed to screen DPI formulations, which are performed in blending uniformity validation routinely. These approaches remain empirical however, and require different scales of scrutiny in order to develop a mechanistic understanding of the formulation performance.

As a result of the limitations of current lactose carriers and their innate variability in some manufactured products, alternative processing methodologies have been explored. Spray drying is most commonly used to optimize dry powder formulations, which can be used to process not only small molecules[54] but also macromolecules[55, 56]. Engineered carriers (spray dried, recrystallized, etc.) have also been extensively studied in past decades [26, 29, 57-61]. Despite these extensive efforts, few particle technology approaches have progressed into the clinic. Potential developmental and regulatory issues have slowed their advancement: regulatory burden of developing novel excipients, stability concerns due to presence of significant amorphous material, cost of processing, low

potency of powders, and large volumes of low density powders required for relevant dosing.

An emerging approach to solve variability and improve performance is to eliminate lactose from the system. Lactose, though ubiquitous and proven, might be considered technology limiting for DPIs. Despite intensive investigation, few studies have shown lactose formulations to achieve moderate dispersion performance with flow independence. Moreover, as a natural product, it proved a formidable challenge to control for many DPI manufacturers. However, to eliminate lactose, one must find alternatives that will assume it primary function: dose metering and entrainment enhancement. Selvam et al. developed excipient free novel powder inhaler with passive flutter induced dispersion. The flutter induced dispersion mechanism could achieve more efficient deaggregation and improved dispersion performance [62]. 3M Drug Delivery Systems (St. Paul, MN) developed a novel microstructured carrier tape (MCT) inhaler (Taper®), which delivers a dose range of 50-1500 μg without excipients [63]. This device uses external energy to aerosolize the powder. Respira Therapeutic's devices are passive, and eliminate lactose carriers, replacing this with a much larger bead platform to dramatically change efficiency of aerosolization. The drug-coated bead, sufficiently large such that it is retained within the device maximizes the energy transfer from the patient's inhalation into the micronized drug powder. Respira's inhaler technologies achieve high performance (>80% fine particle fractions) coupled with patient inhalation independence down to pressure drops as low as1 kPa [35].

However, few technologies currently allow elimination of excipients. In addition, it is challenging to bring new excipients to FDA approved products. Even though high barriers exist, recently new excipients have been included in new products. Exubera®, contained spray dried powder composed of recombinant human insulin, and a novel excipient composition (sodium citrate, sodium hydroxide, mannitol and glycine)[64]. Mannkind, also with an insulin product, appears to have satisfied regulators that their novel excipient is also safe.

To summarize, excipients (mainly lactose) have a long and interesting history in DPI formulations. Despite a great deal of science, lactose based formulations still retain a significant tendency for "art". Many remarkably successful DPI products provide evidence of the function and utility of lactose. However, moving the field beyond the current state-of-the-art will require development of a better understanding of all mechanisms underlying DPI performance. This may require significant investment and, as a consequence of divergence of research programs, may be subjugated by unexpected and emerging disruptive technologies. Excipient free technologies, alternative excipients, or novel manufacturing processes may provide solutions to the current challenges facing development of DPIs.

1.2 TABLES

Table 1.1 List of inhalation grade lactose on market[8]

Lactose grade	Description	(0.5)(μm)	D(0.9)(μm)
Respitose ML001 (DFE Pharma)	Milled lactose monohydrate with broad PSD	55	170
Respitose ML006 (DFE Pharma)	Fine milled lactose monohydrate with narrow PSD	17	45
Respitose SV003 (DFE Pharma)	Sieved lactose monohydrate with narrow PSD	60	100
Respitose SV010 (DFE Pharma)	Coarse sieved lactose monohydrate with broad PSD	05	175
Lactohale 100 (Domo)	Sieved lactose monohydrate with narrow PSD and tomahawk shaped particles with smooth surface	25-145	200-250
Lactohale 200 (Domo)	Gently milled lactose monohydrate with irregular shaped particles	50-100	120-160
Lactohale 201 (Domo)	Hardly milled lactose monohydrate with narrow PSD	50-100	120-160
Lactohale 300 (Domo)	Micronized lactose monohydrate with narrow PSD	<5	<10
Inhalac 70 (Meggle)	Sieved crystalline lactose with narrow PSD	00	300
Inhalac 120 (Meggle)	Sieved crystalline lactose with narrow PSD	50	200
Inhalac 230 (Meggle)	Sieved crystalline lactose with narrow PSD	00	140
Anhydrous 120 MS (Sheffield Pharma Ingredients)	Sieved anhydrous lactose	-	-
Monohydrate 120 MS (Sheffield Pharma Ingredients)	Sieved monohydrate lactose	-	-

Table 1.1 List of inhalation grade lactose on market[8] (Continued)

Lactose grade	Description	(0.5)(μm)	D(0.9)(μm)
Anhydrous 40 M (Sheffield Pharma Ingredients)	Sieved anhydrous lactose	-	-
Monohydrate 400 M (Sheffield Pharma Ingredients)	Sieved monohydrate lactose	-	-
Monohydrate 80 M (Sheffield Pharma Ingredients)	Sieved monohydrate lactose	-	-
Monohydrate 120 M (Sheffield Pharma Ingredients)	Sieved monohydrate lactose	-	-

D(0.5), volume median diameter, the size of particle below which 50% particles lie,

D(0.9), the size of particle below which 90% of the powders lie

Table 1.2 Influence of the physical properties of lactose carriers studied on aerosol performance

Physical properties of lactose carriers	Summary	Ref
Particle size	Consensus existed that aerosol performance increases with decreased particle size. New discovery: large lactose carriers are not that bad.	[10, 17-28]
Particle shape and morphology	Lactose carriers with higher elongation ratio (ER) increase drug particles deposited into the lung. But carrier particles with higher ER have poorer flow properties.	[12, 13, 18, 26, 29]
Size distribution, fine lactose	Aerosol performance increases with increased fine lactose fraction. Removal of fine lactose from drug formulation leads to a decreased fine particle fraction.	[20, 24, 27, 28, 30-32]
Particle surface roughness	Surface roughness changes DPI performance by influencing the adhesion and friction forces between drug and lactose carriers. Conflicting reports exist depending on which dispersion mechanism predominates, fluid flow or mechanical impaction [22, 23].	[17, 18, 24, 33-36]
Surface energy	In vitro dispersion of the drug formulation is correlated with the surface energy interactions between lactose carrier and drug particles. Balanced surface interaction is required to achieve best performance.	[11, 37]
Electrostatic charge	Electrostatic charge affects drug delivery efficiency by altering powder adhesion. Affected by particle type, size, size distribution, amorphous content, inhaler, environmental humidity, handling and type of capsule used.	[16, 18, 38-43]

Table 1.2 Influence of the physical properties of lactose carriers studied on aerosol performance (Continued)

Physical properties of lactose carriers	Summary	Ref
Flow properties	Powder flow property is influenced by particle size, size distribution, morphology, surface roughness, porosity and density. Powder flowability has effects on powder packing, emptying rate and dosing accuracy and consistency.	26, 44-46
Polymorphism	Drug particle dispersion and deposition from coarse carrier: α-monohydrate>β-anhydrous>α-anhydrous. For fine lactose: β-anhydrous>α-monohydrate>α-anhydrous. Alpha lactose monohydrate is commonly used in dry powder formulations, especially DPIs currently available on the market	13, 16, 22, 47-49

1.3 FIGURES

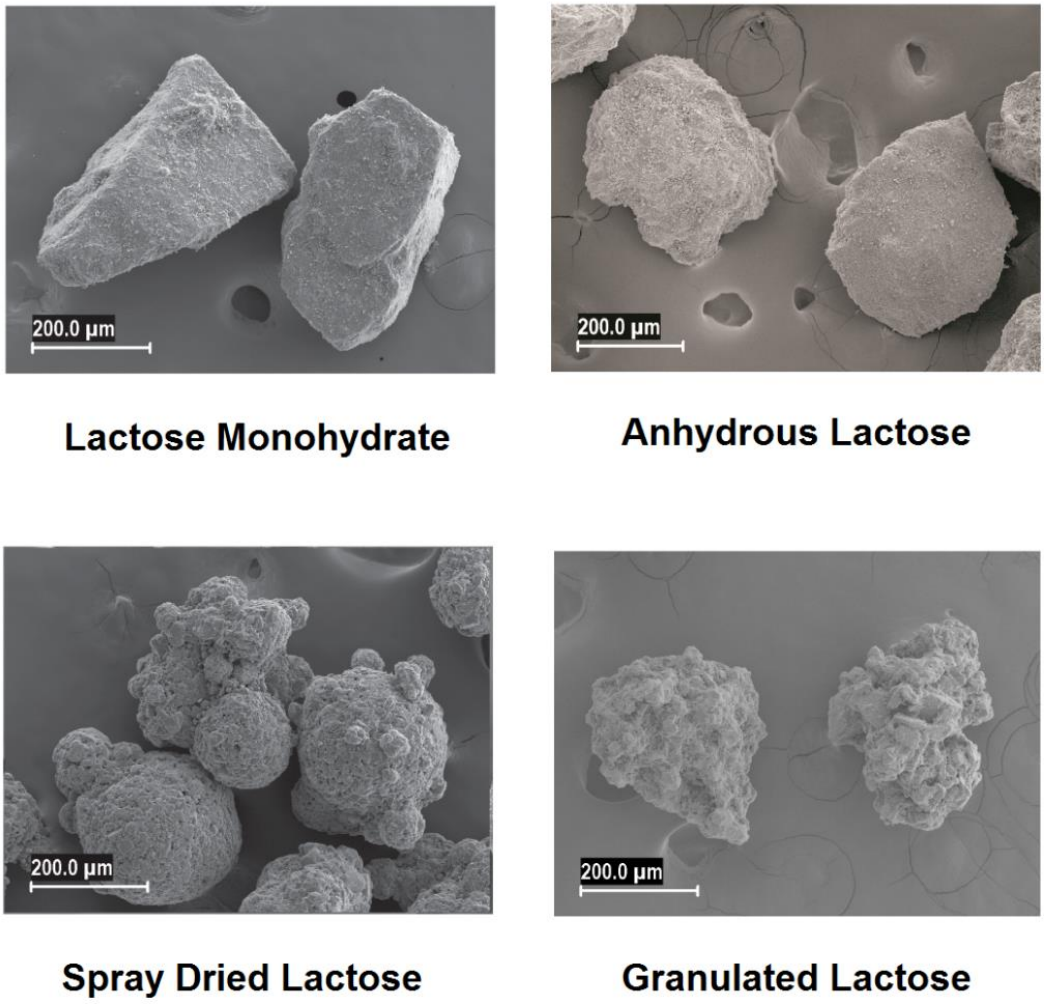

Figure 1.1 Representative Grade of Lactose

1.4 REFERENCES

1. EMEA. GUIDELINE ON EXCIPIENTS IN THE DOSSIER FOR APPLICATION FOR MARKETING AUTHORISATION OF A MEDICINAL PRODUCT 2006.

2. Fields MR, inventor; Abbott Laboratories, assignee. Inhalator. US Patent No. 2,470,297. USA1947.

3. Taplin GV, Cohen SH, Mahoney EE. Prevention of postoperative pulmonary infections; inhalation of micropowdered penicillin and streptomycin. Journal of the American Medical Association. 1948;138(1):4-8. Epub 1948/09/04.

4. Bell JH, Hartley PS, Cox JS. Dry powder aerosols. I. A new powder inhalation device. Journal of pharmaceutical sciences. 1971;60(10):1559-64. Epub 1971/10/01.

5. Altonnyan REC, inventor; Fisons Pharmaceuticals, assignee. Oral inhaler with spring biased, cam driven piercing device. US Patent No. 3, 518, 992. USA1970.

6. Hickey AJ. Pharmaceutical inhalation aerosol powder dispersion - An unbalancing act. American Pharmaceutical Review. 2003;6(4):106-10.

7. Pilcer G, Wauthoz N, Amighi K. Lactose characteristics and the generation of the aerosol. Advanced drug delivery reviews. 2012;64(3):233-56. Epub 2011/05/28.

8. Pilcer G, Amighi K. Formulation strategy and use of excipients in pulmonary drug delivery. International journal of pharmaceutics. 2010;392(1-2):1-19. Epub 2010/03/13.

9. Saleem I, Smyth H, Telko M. Prediction of dry powder inhaler formulation performance from surface energetics and blending dynamics. Drug development and industrial pharmacy. 2008;34(9):1002-10. Epub 2008/08/08.

10. Guenette E, Barrett A, Kraus D, Brody R, Harding L, Magee G. Understanding the effect of lactose particle size on the properties of DPI formulations using experimental design. International journal of pharmaceutics. 2009;380(1-2):80-8. Epub 2009/07/15.

11. Cline D, Dalby R. Predicting the quality of powders for inhalation from surface energy and area. Pharmaceutical research. 2002;19(9):1274-7. Epub 2002/10/31.

12. Kaialy W, Alhalaweh A, Velaga SP, Nokhodchi A. Effect of carrier particle shape on dry powder inhaler performance. International journal of pharmaceutics. 2011;421(1):12-23. Epub 2011/09/29.

13. Zeng XM, Martin GP, Marriott C, Pritchard J. The influence of crystallization conditions on the morphology of lactose intended for use as a carrier for dry powder aerosols. The Journal of pharmacy and pharmacology. 2000;52(6):633-43. Epub 2000/06/30.

14. Price R, Young PM, Edge S, Staniforth JN. The influence of relative humidity on particulate interactions in carrier-based dry powder inhaler formulations. International journal of pharmaceutics. 2002;246(1-2):47-59. Epub 2002/09/25.

15. Ali M, Mazumder MK, Martonen TB. Measurements of electrodynamic effects on the deposition of MDI and DPI aerosols in a replica cast of human oral-pharyngeal-laryngeal airways. Journal of aerosol medicine and pulmonary drug delivery. 2009;22(1):35-44. Epub 2008/09/20.

16. Murtomaa M, Mellin V, Harjunen P, Lankinen T, Laine E, Lehto VP. Effect of particle morphology on the triboelectrification in dry powder inhalers. International journal of pharmaceutics. 2004;282(1-2):107-14. Epub 2004/09/01.

17. de Boer AH, Hagedoorn P, Gjaltema D, Goede J, Kussendrager KD, Frijlink HW. Air classifier technology (ACT) in dry powder inhalation. Part 2. The effect of lactose carrier surface properties on the drug-to-carrier interaction in adhesive mixtures for inhalation. International journal of pharmaceutics. 2003;260(2):201-16. Epub 2003/07/05.

18. Podczeck F. The relationship between physical properties of lactose monohydrate and the aerodynamic behaviour of adhered drug particles. International journal of pharmaceutics. 1998;160(1):119-30.

19. Steckel H, Müller BW. In vitro evaluation of dry powder inhalers II: influence of carrier particle size and concentration on in vitro deposition. International journal of pharmaceutics. 1997;154(1):31-7.

20. Louey MD, Razia S, Stewart PJ. Influence of physico-chemical carrier properties on the in vitro aerosol deposition from interactive mixtures. International journal of pharmaceutics. 2003;252(1-2):87-98. Epub 2003/01/29.

21. Dickhoff BH, de Boer AH, Lambregts D, Frijlink HW. The effect of carrier surface and bulk properties on drug particle detachment from crystalline lactose carrier particles during inhalation, as function of carrier payload and mixing time. European journal of pharmaceutics and biopharmaceutics : official journal of Arbeitsgemeinschaft fur Pharmazeutische Verfahrenstechnik eV. 2003;56(2):291-302. Epub 2003/09/06.

22. Donovan MJ, Smyth HD. Influence of size and surface roughness of large lactose carrier particles in dry powder inhaler formulations. International journal of pharmaceutics. 2010;402(1-2):1-9. Epub 2010/09/08.

23. Donovan MJ, Kim SH, Raman V, Smyth HD. Dry powder inhaler device influence on carrier particle performance. Journal of pharmaceutical sciences. 2012;101(3):1097-107.

24. Zeng XM, Martin GP, Marriott C, Pritchard J. Lactose as a carrier in dry powder formulations: the influence of surface characteristics on drug delivery. Journal of pharmaceutical sciences. 2001;90(9):1424-34. Epub 2001/12/18.

25. Steckel H, Muller BW. In vitro evaluation of dry powder inhalers .2. Influence of carrier particle size and concentration on in vitro deposition. International journal of pharmaceutics. 1997;154(1):31-7.

26. Kaialy W, Martin GP, Larhrib H, Ticehurst MD, Kolosionek E, Nokhodchi A. The influence of physical properties and morphology of crystallised lactose on delivery of salbutamol sulphate from dry powder inhalers. Colloids and surfaces B, Biointerfaces. 2012;89:29-39. Epub 2011/10/04.

27. Podczeck F. Adhesion forces in interactive powder mixtures of a micronized drug and carrier particles of various particle size distributions. Journal of Adhesion Science and Technology 1998;12(12):1323-39.

28. Adi H, Larson I, Stewart PJ. Adhesion and redistribution of salmeterol xinafoate particles in sugar-based mixtures for inhalation. International journal of pharmaceutics. 2007;337(1-2):229-38. Epub 2007/02/17.

29. Larhrib HM, G. P. Prime, D. Marriott, C. Characterisation and deposition studies of engineered lactose crystals with potential for use as a carrier for aerosolised salbutamol sulfate from dry powder inhalers. European journal of pharmaceutical sciences : official journal of the European Federation for Pharmaceutical Sciences. 2003;19(4):211-21. Epub 2003/07/30.

30. Islam N, Stewart P, Larson I, Hartley P. Lactose surface modification by decantation: are drug-fine lactose ratios the key to better dispersion of salmeterol xinafoate from lactose-interactive mixtures? Pharmaceutical research. 2004;21(3):492-9. Epub 2004/04/09.

31. Young PM, Chan HK, Chiou H, Edge S, Tee TH, Traini D. The influence of mechanical processing of dry powder inhaler carriers on drug aerosolization performance. Journal of pharmaceutical sciences. 2007;96(5):1331-41. Epub 2007/04/25.

32. Guchardi R, Frei M, John E, Kaerger JS. Influence of fine lactose and magnesium stearate on low dose dry powder inhaler formulations. International journal of pharmaceutics. 2008;348(1-2):10-7. Epub 2007/08/11.

33. Islam N, Stewart P, Larson I, Hartley P. Surface roughness contribution to the adhesion force distribution of salmeterol xinafoate on lactose carriers by atomic force microscopy. Journal of pharmaceutical sciences. 2005;94(7):1500-11. Epub 2005/06/01.

34. Dickhoff BH, de Boer AH, Lambregts D, Frijlink HW. The interaction between carrier rugosity and carrier payload, and its effect on drug particle redispersion from adhesive mixtures during inhalation. European journal of pharmaceutics and biopharmaceutics : official journal of Arbeitsgemeinschaft fur Pharmazeutische Verfahrenstechnik eV. 2005;59(1):197-205. Epub 2004/11/30.

35. Flament MP, Leterme P, Gayot A. The influence of carrier roughness on adhesion, content uniformity and the in vitro deposition of terbutaline sulphate from dry powder inhalers. International journal of pharmaceutics. 2004;275(1-2):201-9. Epub 2004/04/15.

36. Young PM, Cocconi D, Colombo P, Bettini R, Price R, Steele DF, et al. Characterization of a surface modified dry powder inhalation carrier prepared by "particle smoothing". The Journal of pharmacy and pharmacology. 2002;54(10):1339-44. Epub 2002/10/25.

37. Hickey AJ, Mansour HM, Telko MJ, Xu Z, Smyth HD, Mulder T, et al. Physical characterization of component particles included in dry powder inhalers. I. Strategy review and static characteristics. Journal of pharmaceutical sciences. 2007;96(5):1282-301. Epub 2007/04/25.

38. Adi H, Kwok PC, Crapper J, Young PM, Traini D, Chan HK. Does electrostatic charge affect powder aerosolisation? Journal of pharmaceutical sciences. 2010;99(5):2455-61. Epub 2009/11/27.

39. Chow KT, Zhu K, Tan RB, Heng PW. Investigation of electrostatic behavior of a lactose carrier for dry powder inhalers. Pharmaceutical research. 2008;25(12):2822-34. Epub 2008/06/27.

40. Elajnaf A, Carter P, Rowley G. Electrostatic characterisation of inhaled powders: effect of contact surface and relative humidity. European journal of pharmaceutical sciences : official journal of the European Federation for Pharmaceutical Sciences. 2006;29(5):375-84. Epub 2006/09/06.

41. Young PM, Price R, Tobyn MJ, Buttrum M, Dey F. Effect of humidity on aerosolization of micronized drugs. Drug development and industrial pharmacy. 2003;29(9):959-66. Epub 2003/11/11.

42. Young PM, Price R, Tobyn MJ, Buttrum M, Dey F. The influence of relative humidity on the cohesion properties of micronized drugs used in inhalation therapy. Journal of pharmaceutical sciences. 2004;93(3):753-61. Epub 2004/02/06.

43. Zeng XM, MacRitchie HB, Marriott C, Martin GP. Humidity-induced changes of the aerodynamic properties of dry powder aerosol formulations containing different carriers. International journal of pharmaceutics. 2007;333(1-2):45-55. Epub 2006/10/27.

44. Hickey AJ, Mansour HM, Telko MJ, Xu Z, Smyth HD, Mulder T, et al. Physical characterization of component particles included in dry powder inhalers. II. Dynamic characteristics. Journal of pharmaceutical sciences. 2007;96(5):1302-19. Epub 2007/04/25.

45. Crowder T, Hickey A. Powder specific active dispersion for generation of pharmaceutical aerosols. International journal of pharmaceutics. 2006;327(1-2):65-72. Epub 2006/08/26.

46. Concessio NM, VanOort MM, Knowles MR, Hickey AJ. Pharmaceutical dry powder aerosols: correlation of powder properties with dose delivery and implications for pharmacodynamic effect. Pharmaceutical research. 1999;16(6):828-34. Epub 1999/07/09.

47. Kaialy W, Martin GP, Ticehurst MD, Momin MN, Nokhodchi A. The enhanced aerosol performance of salbutamol from dry powders containing engineered mannitol as excipient. International journal of pharmaceutics. 2010;392(1-2):178-88. Epub 2010/04/07.

48. Zeng XM, Martin AP, Marriott C, Pritchard J. The influence of carrier morphology on drug delivery by dry powder inhalers. International journal of pharmaceutics. 2000;200(1):93-106. Epub 2000/06/14.

49. Kawashima Y, Serigano T, Hino T, Yamamoto H, Takeuchi H. Effect of surface morphology of carrier lactose on dry powder inhalation property of pranlukast hydrate. 1998;172(1–2):188.

50. Davies MJ, Brindley A, Chen X, Doughty SW, Marlow M, Roberts CJ. A quantitative assessment of inhaled drug particle-pulmonary surfactant interaction by atomic force microscopy. Colloids and surfaces B, Biointerfaces. 2009;73(1):97-102. Epub 2009/06/09.

51. Kubavat HA, Shur J, Ruecroft G, Hipkiss D, Price R. Influence of primary crystallisation conditions on the mechanical and interfacial properties of micronised budesonide for dry powder inhalation. International journal of pharmaceutics. 2012;430(1-2):26-33. Epub 2012/03/28.

52. Davies M, Brindley A, Chen X, Marlow M, Doughty SW, Shrubb I, et al. Characterization of drug particle surface energetics and young's modulus by atomic force microscopy and inverse gas chromatography. Pharmaceutical research. 2005;22(7):1158-66. Epub 2005/07/20.

53. Tong HH, Shekunov BY, York P, Chow AH. Predicting the aerosol performance of dry powder inhalation formulations by interparticulate interaction analysis using inverse gas chromatography. Journal of pharmaceutical sciences. 2006;95(1):228-33. Epub 2005/11/30.

54. Duret C, Wauthoz N, Sebti T, Vanderbist F, Amighi K. New inhalation-optimized itraconazole nanoparticle-based dry powders for the treatment of invasive pulmonary aspergillosis. International journal of nanomedicine. 2012;7:5475-89. Epub 2012/10/25.

55. Tawfeek HM, Evans A, Iftikhar A, Mohammed AR, Shabir A, Somavarapu S, et al. Dry powder inhalation of macromolecules using novel PEG-co-polyester microparticle carriers. International journal of pharmaceutics. 2012. Epub 2012/11/06.

56. Traini D, Adi H, Valet OK, Young PM. Preparation and evaluation of single and co-engineered combination inhalation carrier formulations for the treatment of asthma. Journal of pharmaceutical sciences. 2012;101(11):4267-76. Epub 2012/08/29.

57. Schiavone H, Palakodaty S, Clark A, York P, Tzannis ST. Evaluation of SCF-engineered particle-based lactose blends in passive dry powder inhalers. International journal of pharmaceutics. 2004;281(1-2):55-66. Epub 2004/08/04.

58. Littringer EM, Mescher A, Schroettner H, Achelis L, Walzel P, Urbanetz NA. Spray dried mannitol carrier particles with tailored surface properties--the influence of carrier surface roughness and shape. European journal of pharmaceutics and biopharmaceutics : official journal of Arbeitsgemeinschaft fur Pharmazeutische Verfahrenstechnik eV. 2012;82(1):194-204. Epub 2012/05/19.

59. Beinborn NA, Lirola HL, Williams RO, 3rd. Effect of process variables on morphology and aerodynamic properties of voriconazole formulations produced by thin film freezing. International journal of pharmaceutics. 2012;429(1-2):46-57. Epub 2012/03/22.

60. Cheow WS, Ng ML, Kho K, Hadinoto K. Spray-freeze-drying production of thermally sensitive polymeric nanoparticle aggregates for inhaled drug delivery: effect of freeze-drying adjuvants. International journal of pharmaceutics. 2011;404(1-2):289-300. Epub 2010/11/26.

61. Maa YFP, S. J. Biopharmaceutical powders: particle formation and formulation considerations. Current pharmaceutical biotechnology. 2000;1(3):283-302. Epub 2001/07/27.

62. Selvam P, McNair D, Truman R, Smyth HD. A novel dry powder inhaler: Effect of device design on dispersion performance. International journal of pharmaceutics. 2010;401(1-2):1-6. Epub 2010/08/12.

63. Stephen W. Stein JKS, Mike J. Frits, James S. Stefely, cartographer Managing Excipient-Free DPI Delivery: An Laternative Approach with Reproducible Metering and Dosing2012.

64. White S, Bennett DB, Cheu S, Conley PW, Guzek DB, Gray S, et al. EXUBERA: pharmaceutical development of a novel product for pulmonary delivery of insulin. Diabetes technology & therapeutics. 2005;7(6):896-906. Epub 2006/01/03.

Chapter 2: Evaluation of Granulated Lactose as a Carrier for DPI Formulations 1: Effect of Granule Size[1]

Abstract

The objective of this study was to investigate the effect of large granulated lactose carrier particle systems on aerosol performance of dry powder inhaler formulations. Granulated lactose carriers with average sizes ranging from 200μm to1000μm were prepared and subsequently fractionated into separate narrow size powders. The fractionated granulated lactose (GL) samples were characterized in terms of size, specific surface area, surface roughness, morphology, density, flowability and solid state. The i*n vitro* aerosolization performance was performed on the different size fractions of GL samples from a commercial inhaler device (Aerolizer®) with a model formulation (2% w/w salbutamol sulphate). The cascade impaction parameters employed were 60L/min or 90L/min with standard (aperture size: 0.6mm) or modified piercing holes (aperture size: 1.2mm) of the inhaler loaded capsules. It was shown that the largest size fraction formulation (850-1000μm) had a slight improvement in the fine particle fraction (FPF) compared to immediately preceding size fractions, explained by a smaller adhesive force

[1]Parts of this chapter were taken from:

1) Ping Du, Ju Du, Hugh D. C. Smyth. (2014). "Evaluation of Granulated Lactose as a Carrier for DPI Formulations 1: Effect of Granule Size." AAPS PharmSciTech 15(6): 1417-1428.

Ping Du is the major contribution to the research and draft of the article. Ju Du and Hugh D. C. Smyth reviewed the manuscript and made some changes suitable for publications.

between drug and carrier. Compared to commercial piercing holes, enlarged piercing holes generated a slight decreasing trend of FPF as the lactose powder sizes increased from 200-250μm to 600-850μm, perhaps due to the reduced detachment force by flow forces. The size, surface roughness, density, flowability of lactose carrier as well as device design all contributed to the aerosol dispersion performance of granulated lactose based adhesive mixtures. It was concluded that poorer or enhanced dispersion performance is not an inherent property to the significantly large size of granulated lactose carriers as previously contended.

Keywords

DPI formulations; Granulated lactose; Carrier size; Carrier roughness; Adhesive force

2.1 INTRODUCTION

Development of dry powder inhaler (DPI) formulations is generally challenging due to the need for good product performance and the necessity of uniformity and quality. The active ingredients incorporated in DPI formulations are in micronized form with an aerodynamic diameter less than 5 μm which enables adequate deposition in the lung. It is well known that the high surface area to volume ratio of the micronized drug particles results in strong interactive forces(1). As a result, micronized drugs are generally highly cohesive and exhibit poor flow, which makes downstream processing, accurate dose metering, and handling of the drugs problematic. Therefore, in order to facilitate adequate powder performance, DPI formulations are frequently formulated with larger coarse "carriers" to form homogenous binary or tertiary mixtures(2). These blends are then required to be redispersed into primary particles upon inhalation by patients via the inhaler device.

α-lactose monohydrate is the most commonly used coarse carrier for DPI formulations due to its well-established safety profile, stable physico-chemical properties and compatibility with most available low molecular weight APIs(3). The particle size, size distribution(4), morphology, surface roughness(5), surface area, flowability(6), and surface energy(7) of lactose carriers all have been shown to have an influence on the DPI formulation performance. Amongst, the size and roughness of lactose carriers have been extensively investigated (2, 4, 8-10).

Several mechanisms are postulated to explain the effect of carrier size on the dispersion performance of adhesive mixtures for dry powder inhalation. Generally, to achieve good aerosolization performance, the detachment forces generated from the inspiratory flow and the interactions of the flow and formulation with the inhaler device should be large enough to overcome the adhesive force between API particle and the coarse carrier particle to efficiently redisperse the primary drug particles (11, 12). However, it has been determined previously that, in general, there are more surface asperities on the larger lactose carrier particles compared to smaller size fractions (13). These surface discontinuities, clefts and depressions, where drugs are not fully exposed to the flow stream, are proposed to prevent detachment by fluid flow mechanisms. Additionally, larger lactose particles may exhibit higher press-on forces (defined as the adhesive forces between drug and carrier particles)(14) during mixing with the micronized API due to larger mass and inertia force, resulting in a stronger adhesive force between drug and lactose carrier(15). Also, as the size of lactose carrier is increased, the amount of fine lactose (<32 μm) present in the powder tends to decrease(16). Fine lactose components have been shown to increase the redispersion of APIs, explained mainly by "active site theory", and "agglomeration theory". In the "active site theory", fine lactose particles occupy the high energy surface areas of lactose carrier particle, thus leaving the surface with lower energy binding sites for the API to occupy. It is also proposed that fine lactose facilitates the formation of agglomerate mixtures, which are more susceptible to detachment force.

As a result of these research findings, it was widely believed that carrier particles with smaller diameters were preferable to maximize aerosolization efficiency, with the

consensus that increasing diameters and surface roughness hinder efficient drug dispersion performance (4, 14, 16-20). However, it was found recently that lactose carriers with large size fraction can also improve aerosol performance, especially when combined with significantly rough surface (13). This improvement is explained by the switch of predominant detachment mechanism from turbulence flow to impaction force. Impaction force (mechanical force) arises from the abrupt momentum transfer generated from the collisions between coarse carriers and the inhaler device during inhalation. The momentum relies on particle mass, thus detachment by impaction force is proportional to the cube of the carrier particle size such that large particles will have strong detachment force(13). It was found that Aerolizer® used in previous study actively promotes particle collisions with the inhaler wall, especially, with significantly large particle diameter(21). Additionally, different from carriers with flat surface, larger carriers with significantly rough surface would shelter drugs within asperities, and drug detachment depends more on impaction force(13). Therefore, the hypothesis in this research is that larger lactose carriers can improve DPI aerosol performance as the result of the major detachment mechanism switch from turbulence flow to impaction force.

Previously, the carrier particles studied have had a particle size less than 300 μm as a result of the sizes limitations of commercially available lactose (22). In this study, the aim was to evaluate the powder and aerosol performance of lactose carrier with significantly large size ranging from 200 μm to 1000 μm. We manufactured granulated lactose, and performed the physic-chemical (e.g. solid state form, density, specific surface area and flowability) and impaction studies. To the author's knowledge, for the first time we studied the significantly large granulated lactose carriers across a wide

range of narrow sieve fractions in the size range of 200-1000 μm and correlated the physico-chemical properties of these large granulated lactose carriers with the *in vitro* aerosol dispersion from an Aerolizer® DPI.

2.2 EXPERIMENTAL

2.2.1 Materials

α-Lactose monohydrate, Pharmatose 100M, was supplied from DFE Pharma (Princeton, NJ, USA). Micronized salbutamol sulphate (Figure 2.1) was purchased from LETCO MEDICAL. Deionized water was provided by MilliQ (Millipore).

2.2.2 Manufacture of lactose granules

Wet granulation was used to manufacture lactose granules with large diameter from Pharmatose 100M (d10: 63 μm, d50: 150 μm, d90: 250 μm). Granulation is a process to generate large aggregates from small primary powders to improve the flowability of the powders (23). Wet granulation of lactose usually employs polymeric binders that are not approved for inhalation (24-27). To solve this problem, the granulation process in this research involved merely water as the binding solvent. Briefly, a batch size of 50 g starting lactose was introduced into the granulator (Robot Coupe USA. Inc.) followed by addition of 50 mL water merely as the granulating solvent. Subsequently, the granulated lactose carriers were pan dried in the oven overnight at 80 ℉.

2.2.3 Fractionation of granulated lactose carrier particles

Different size fractions of lactose granules were obtained by separation of the bulk granulated material using a sieve tower with cut off sizes as follows: 1000 μm, 850 μm, 600 μm, 425 μm, 300 μm, 250 μm, 212 μm, and a metal collection pan. A vibrating auto sieve shaker (Gilson Company Inc., OH, USA) was employed. The granulated lactose was poured on the top of the vibrating sieve shaker and sieved through the sieves for 30 min. All analysis described were performed on the sieved samples.

2.2.4 Particle size measurement

Particle size analysis of fractionized granulated lactose was evaluated by the Sympatec laser diffraction (Sympatec GmbH). The theoretical specific surface area (based on volume, assuming an ideal spherical smooth surface of the particles) was calculated by the software installed in the Sympatec. The span of the samples, which is the width of the distribution based on the 10%, 50% and 90% quintile, was calculated according to Eq. 1,

$$Span = \frac{d90 - d10}{d50}$$

(Eq. 1)

2.2.5 Scanning electron microscopy

The scanning electron microscopy (SEM; Supra 40VP, Zeiss, Germany) was used to visually assess the particle size and morphology of the granulated lactose. The coating conditions prior to SEM for all the granulated lactose was 20nm of Pd/Pt via sputter coating.

2.2.6 Differential scanning calorimetry

Differential scanning calorimetry (DSC) of the lactose granules with different size fraction was conducted with modulated temperature DSC (MTDSC), Model 2920 (TA Instruments, New Castle, DE), which was equipped with a refrigerated cooling system. The flow rate of purge gas through the DSC cell was 40 mL/min. Lactose granules of 5–10 mg were weighted in aluminum crimped pans (PerkinElmer Instruments, Norwalk, CT). An empty sample pan was used as the reference. Samples were heated at a ramp rate of 10 ℃/min from 25 to 250 ℃ with modulation temperature amplitude of 1 ℃/60s for all granule size fractions.

2.2.7 BET analysis

The specific surface area of a powder could be determined by the amount of the monomolecular layer of adorbate gas on the surface of the solid, calculated according to

Brunauer, Emmett and Teller (BET) theory. The specific surface area of the lactose populations was determined via nitrogen adsorption with a single-point BET method using a Monosorb® surface area analyzer (Quantachrome, FL, USA). All BET analysis was performed in triplicate. Surface roughness was calculated by Eq. 2.

$$\text{Roughness} = \frac{\text{BET specific surface area}}{\text{theoretical volume specific surface area}}$$

(Eq. 2)

2.2.8 True, Bulk and Tapped Density

True density of the granulated lactose and primary lactose was determined by helium pycnometry (Quantachrome, FL, USA).

The lactose samples were filled into a 10 mL gradual cylinder and the volume was recorded as the bulk volume. Then the cylinder was tapped 750 times and the new volume was recorded (tapped volume). The bulk density, tapped density and Carr's index (CI) (Eq. 3) were calculated. To measure the angle of repose, certain amount of lactose samples were passed through the tunnel with a fixed height relative to the base. The angle of repose was calculated according to Eq. 4. Carr's index and angle of repose were both used as the indicators of powder flowability. The Carr index, also called Carr's index or Carr's Compressibility Index, is an indication of the compressibility and flowability of a powder(28).

$$CI = \frac{Tapped\ density - Bulk\ Density}{Tapped\ density}\ X\ 100$$

(Eq. 3)

$$\tan(\alpha) = \frac{height}{0.5\ base}$$

(Eq. 4)

2.2.9 Preparation of salbutamol sulfate/granulated lactose binary blends

Salbutamol sulfate (SS) and fractionated granulated lactose were mixed in a ratio of 1:50 (w/w) to obtain a 500 mg 2% binary mixture. All formulations were blended at a constant speed of 46 RPM for 40 min with a Turbula® orbital mixer (Glen Mills, NJ, USA). The granules still maintained the initial shape after completion of blending. Prior to any further analysis, the blended formulations were stored in the dessicator for 5 days.

2.2.10 Drug uniformity test

Five of randomly selected samples (20 ± 1 mg) were taken for measurement of salbutamol sulfate content uniformity. The coefficient of variation (CV%) was used to determine the blending uniformity. The test was performed three times. The potency of formulations was calculated by the APIs percent amount to the nominal dose.

2.2.11 *In vitro* aerosolization study

About 20 (±1) mg mixture powders were filled into size 3 Vcaps HPMC capsules. The *in vitro* drug deposition of all formulations were assessed using Aerolizer® inhaler device (Novartis, Switzerland), of which the mixtures were loaded in the capsules pierced with four standard holes (0.6mm) (29) at each end of the capsule, referred as Capsule$4_{0.6}$ in the results and discussion part. The impaction study was performed through a Next Generation Impactor (NGI; MSP Corporation, Shoreview, MN) at a volumetric flow rate of 60 L min^{-1}, and 90 L min^{-1}, corresponding to 4 kPa pressure drop and 4 L air volume across the device.

Another 20 (±1) mg mixture powders of all formulations were filled into the same size 3 Vcaps HPMC capsules. After loading the mixtures in the capsules, one 1.2 mm hole instead was punctured at each end of the capsule, followed by *in vitro* impaction study with Aerolizer® inhaler device (Novartis, Switzerland) through the same next generation cascade at a volumetric flow rate of 90 L min^{-1} only. The dispersion method is referred as $Capsule_{1.2}$ in the results and discussion part.

A 1% (w/v) solution of silicon oil in hexane was applied to precoat the NGI stages for particle re-entrainment prevention. Amounts of salbutamol sulfate deposited on the capsule, inhaler, mouthpiece adaptor, induction port, pre-separator and NGI stages were measured and quantified. The drug content was measured by the ultraviolet visible absorption spectroscopy (Infinite M200, TECAN) at 230 nm. The parameters used to evaluate salbutamol sulfate deposition performance were emitted fraction (EF) (Eq. 5),

fine particle fraction (FPF) (Eq. 6), respirable fraction (Figure 2.7) mass median aerodynamic diameter (MMAD) and geometric standard deviation (GSD).

$$\mathrm{EF} = \frac{\text{emitted dose}}{\text{loading dose}}$$

(Eq. 5)

$$\mathrm{FPF} = \frac{\text{recovered dose of drug particles smaller than 5 μm}}{\text{emitted dose}}$$

(Eq. 6)

$$\mathrm{RF} = \frac{\text{recovered dose of drug particles smaller than 5 μm}}{\text{loading dose}}$$

(Eq.7)

2.2.12 Statistics analysis

Statistical significance between aerosol performance values was determined with one-way TTESTs between groups (* indicates $P < 0.05$).

2.3 RESULTS

2.3.1 Particle Size Distribution of Lactose Granules with Different Size Fractions

The particle size of GL fractions fell into the nominal sieve size range, as confirmed by the SEM pictures (Figure 2.2) and laser diffraction (Figure 2.3a). As expected, the size of GL particles increased progressively with increased aperture size of sieves. The volume distribution of the particles at 10% (d10%), 50% (d50%) and 90% (d90%) (Figure 2.3a) as well as the equivalent diameter from image analysis (Figure 2.3b) generally agreed with each other. Slight differences obtained using the different methods of analysis are due to the different mechanisms of size determination, which is explained in the discussion section below. The equivalent diameter of GL 650-850 μm and GL 850-1000 μm from Image Analysis (Figure 2.3a) was more accurate than the laser diffraction results for these powders and was therefore used in interpretation of other results.

Particle size distribution width (as measured by span) and the fine lactose fractions (fraction size less than 5μm) could also be determined from laser diffraction results (Figure 2.3a). The span value of all GLs was less than one, indicating relatively narrow size distributions for all samples. The fine lactose fraction was less than 1% for all sieved GL samples, indicating that sieving efficiently removed fine lactose from the granulated powders. This is important, as fine lactose has been shown to significantly improve DPI performance and is generally present in different amounts for different size lactose fractions and could confound results if not sufficiently removed from the granulated lactose (8).

2.3.2 Morphology of Lactose Carrier Particles

The particle morphology and surface roughness of pre-granulated lactose particles (commercial Pharmatose 100M) and lactose granules were visualized by SEM. As shown in Figure 2a, commercial Pharmatose 100M had a tomahawk shape, the typical morphology of alpha monohydrate lactose crystals (30). Figure 2.2b-d show the micrographs of lactose granules with different size fractions: b: GL 212-250 μm, c: 425-600 μm, and d: 850-1000 μm. Unlike the commercial Pharmatose 100M, the shape of these lactose granules were elongated aggregates comprised of the primary lactose particles. Obviously the number of primary lactose particles comprising each granule was different for the 6 size fractions. For example, less than 10 primary lactose particles were observed to be contained in each GL 212-250 μm granule compared to hundreds observed for GL 850-1000 μm.

2.3.3 Thermal Analysis

Figure 2.4 is the DSC thermographs obtained for the lactose particles. There were two endothermic peaks (220 ℃ and 150 ℃) observed for all granulated lactose, consistent with reports of commercial alpha monohydrate lactose (6). The peak at 220 ℃ is a melt endotherm; while the peak at 150 ℃ corresponded to the distinctive dehydration of crystalline hydrate water (bound water) as previously reported. The vaporization temperature of bound water (150 ℃) is significantly greater than 100 ℃, explained by

thermodynamically favorable H-bonding of the water molecules in the lactose crystal lattice (31). There was no dehydration process from unbound water, indicated by no endothermic peak at ~100 ℃. This demonstrated that there was no excessive unbound water in the lactose granules as prepared. The distinct thermographs showed that all granulated lactose fractions had similar solid-state, and was composed with alpha monohydrate lactose. This is reasonable because no special solvent other than water was used and there was no heating process above 93.5 ℃ involved in the granulation process (32).

2.3.4 Specific Surface Area

Despite different size fractions for the granulated lactose samples, all samples had similar specific surface area (~0.29 m^2/g) (mean), which was similar to the specific surface area of the primary lactose carriers (0.30 ± 0.06 m^2/g) (Figure 2.5a). These findings are explained and discussed below.

2.3.5 Density and Flowability

All granulated lactose demonstrated similar true density with commercial pharmatose 100M (1.545 g/cm^3, $P>0.05$). Thus the size of lactose granules had negligible effect on true density, which is expected and related to their similar solid state form (Figure 2.4).

The bulk and tapped densities of the lactose powders is shown in Table 2.1 According to the results, an inverse relationship was observed between bulk/tapped density and lactose size. The bulk density decreased from 0.68 g/ml to 0.44 g/ml with increasing granule size. The tapped density decreased from 0.82 g/ml to 0.48 g/ml with increasing granule size.

Carr's Index may be used as an indicator of powder flow. According to USP <1174> Powder Flow, powder with Carr's Index smaller than 16-20 % is considered to have good flow. Carr's Index results for the powders in this study are listed in Table 2.1 and show that flowability of the lactose granules (Carr's Index<= 16%) was good while that of the primary pharmatose 100M powder is only above 20%. The lactose powder and granule flow shown by the angle of repose was consistent with the data obtained from Carr's Index.

2.3.6 Aerosol Performance

2.3.6.1 In Vitro Aerosolization Performance with Capsules4$_{0.6}$ (0.6 mm, 4 holes) at 60L/min

Firstly, the aerosol performance of the 6 DPI formulations with different granular lactose size fractions was evaluated by *in vitro* impaction study at 60L/min using capsules with holes created by the standard pins used in the Aerolizer®, that is 0.6 mm

hole diameter, 4 holes at each end of the capsule (abbreviated now as Capsules$4_{0.6}$). Experimental parameters for the cascade impaction studies are tabulated in Table 2.2.

According to the results, all formulations yielded a similar aerodynamic particle size for the deposited SS in terms of the mass median aerodynamic diameter (MMAD) (1.9 ± 0.1 μm). The geometric standard deviations (GSD) (1.7 ± 0.1) for the SS aerosols were also similar between formulations. There were no significant differences for the fine particle fractions (FPF) detected between the different formulations, except for GL 850-1000 μm, which demonstrated higher dispersion efficiency (Table 2.2). An increasing trend for FPF was also noted as the size of the carrier particles increased from 425-600 μm to 850-1000 μm. However, as the 4-pin piercing mechanism employed in the commercial Aerolizer® produced piercing holes with 0.6 mm diameter, the emitted fraction (EF) of lactose carriers with larger sizes (i.e. GL 425-600 μm, GL 600-850 μm, and GL 850-1000 μm) was significantly reduced (Table 2.2), ranging only between 62.5% and 67.0%. As a result, the respirable fraction for these larger size fractions GL 425-600 μm, GL 600-850 μm, and GL 850-1000 μm was reduced, although not significantly different from smaller counterparts.

2.3.6.2 In Vitro Aerosolization Performance with Capsules$4_{0.6}$ (0.6 mm, 4 holes) at 90L/min

A greater flow rate of 90L/min was utilized under the same device and capsule design (Capsules$4_{0.6}$) for the impaction study to further investigate the detachment

mechanisms in the granulated carriers. Results are shown in Table 2.3. Similar trends were observed in this study as observed at the lower flow rates (Table 2.2), although different magnitudes for each parameter were obtained. At 90L/min compared to 60L/min, decreased MMAD value (1.7 μm) and a broader GSD (1.9 ± 0.1) (Table 2.3) were observed. Additionally, compared to flow rate at 60L/min (FPF: 19.3%-26.7%, RF: 12.6%-19.3%), the higher flow rate (90L/min) increased FPF (32.8%-41.6%), and RF (25.1%-30.4%).

2.3.6.3 In Vitro Aerosolization Performance with Capsules$_{1.2}$ (1.2 mm, 1 hole)

In order to potentially increase EF of larger size formulations, another cascade impaction study at 90L/min with larger pierced holes (1.2 mm, 1 hole) was performed. Small holes in the capsule may result in particle deaggregation by several mechanisms such as shear force break up and also higher collisions of the particles with the capsule. For example, a previous study demonstrated more efficient powder dispersion resulting from forcing powder agglomerates through the capsule holes that, in turn, induced improved powder break-up (29). As our hypothesis for these studies centers around the particle collisions with the device as a deaggregation mechanism, modified piercing holes (1.2 mm) were used in the present study. These holes were significantly greater than the size of the larger carrier formulations to eliminate confounding deaggregation mechanisms that may have contributed to the aerosol dispersion studies presented above.

According to Table 2.4, using capsules with 1.2 mm pierced holes, all formulations had EFs around or higher than 85%. The larger piercing aperture size also reduced the variability of all measured parameters of the dispersion studies, especially in the powders with larger carrier particles (Table 2.4). As expected, the larger piercing holes employed resulted in a slight decrease in FPF of GL 425-600 μm, GL 600-850 μm, and GL 850-1000 μm formulations (Table 2.3, Table 2.4), though it was not statistically significant.

Although aerosol performance of the largest lactose formulation (i.e. GL 850-1000 μm) decreased when larger piercing holes was used, the FPF was not significantly different from the smallest lactose formulations ($Capsule_{1.2,}$ $FPF_{90L/min}$: 37.8% vs. 37.1% for the largest and smallest lactose formulations respectively). Meanwhile, although not statically significantly different, a slight decreasing trend in FPF was noticed as the granular lactose size was increased from 212-250 μm to 600-850 μm.

2.4 DISCUSSION

It is well documented that the particle size, size distribution (4), morphology (33, 34), surface roughness (23, 35), surface area, flowability(6), density, and surface energy(7) of lactose carriers all have influence on the DPI formulations. The granulated lactose carrier particles produced in this study had similar solid-state, flowability, surface area and true density, but different size, morphology, roughness and bulk/tap density.

2.4.1 Particle Size Distribution

Generally, the size distributions of the lactose granules from laser diffraction (Figure 2.3a) corresponded to the data obtained from image analysis (Figure 2.3b), with the exception of GL 600-850 μm and GL 850-1000 μm due to measurement limit of laser diffraction instrument (Figure 2.3a). It is interesting to note that the particle size distribution of the sieved granulated lactose samples using laser diffraction and image analysis of SEM micrographs did not exactly match the sieve fraction value. This difference in the size of the sieved granules may be ascribed to their non-spherical elongated shape(36). The smallest cross-sectional dimensions of the particles determine their passage through the sieve mesh(37), whereas diameters obtained from laser diffraction and image analysis are different (38).

2.4.2 Specific Surface Area

Of all granulated lactose samples with different size fractions, the specific surface area remained a constant value similar to the primary lactose carriers, contradictory to theoretical surface area of smooth spherical particles in which surface area is calculated to decrease progressively with increased particle size(13). The constant surface area observed inspite of different granule sizes is related to particle roughness (Figure 2.5a), and confirmed by a linear relationship (r^2 = 0.9787) between mean diameter of lactose granules and roughness value (Figure 2.5b). Moreover, as a result of the constant surface area across the different carrier particle systems, the average drug load per unit calculated surface area (carrier surface payload) is therefore expected to be the same or most possibly slightly decrease with increasing carrier diameter (11). The slight decrease is explained by the distribution of the micronized drugs mainly on the surface of the lactose granules, instead of the both exterior and interior portions, which however also accounts for the calculation of the specific surface area of the lactose granules. In previous studies, when carriers of different sizes were compared, the findings are often confounded with surface area coverage of the carrier particle by the drug and therefore, according to the "active site theory" differences in drug adhesion may happen. In the present studies, therefore, we postulate that the difference in potential active sites could be very small between the different carrier size fractions (39).

2.4.3 Density and Flowability

The granulated lactose density measurements had a decreasing trend with size, which may be explained by the increased interparticle space as granule size is increased. As a result, compared to smaller lactose, granulated lactose powders with large sizes may have a fewer number of particle-particle contact points with neighboring particles.

Theoretically, powder flow and mean particle size is positively correlated (40). Interestingly, when the size of the lactose granules was increased from 200 μm to 850 μm, the flowability of the lactose granules did not improve significantly demonstrated by both Carr's Index and Angle of Repose (Table 2.1). Additionally, in previous study the Carr's Index of spray dried mannitol (90-125 μm) was around 13% (41), much lower than that of lactose granules (Carr's Index: 17%) even with a larger size fraction (200-250 μm). The reason of the not significantly improved flow may be the mechanical interlocking among the rough lactose particles, which prevents powder motion (42).

2.4.4 Aerosol Performance

2.4.4.1 Adhesion forces and bulk powder properties

The bulk powder properties characterized above can influence the balance between adhesion forces and separation forces for lactose granules based adhesive mixtures. It has been well studied that the size of the interactive forces between carrier particle and drug

particle significantly influence the redispersion efficiency of micronized drugs during inhalation while fixed device is used.

During powder mixing, frictional and inertial press-on are related to the adhesion of drug particles on the carrier surface (14). The differences of these forces in the different lactose size fractions, may explain the improvement of aerosol redispersion observed with the coarsest fraction of granulated lactose. In our study, larger size lactose carrier which had lower bulk density (Table 2.1) may have a fewer number of contacts with neighboring particles, resulting in smaller effective surface area involved in particle-particle collisions and thus less magnitude of triboelectrification during mixing. Furthermore, the flow properties as the function of lactose granule size didn't improve significantly (Table 2.1). As a result, it is speculated that the frequency of impacted friction and inertial press-on force of granular lactose during mixing would not increase significantly with increasing size fractions. Additionally, although at the beginning of mixing process, drugs are randomly distributed over the carrier surface, they tend to accumulate in carrier surface irregularities (steep slopes and clefts) (18, 43). Such surface cavities are not necessarily "active sites" with high adhesive forces (39). The drug particles hidden in carrier surface discontinuities are subjected to lower or fewer press-on forces than drug particles that are attached to the flat exposed carrier particle surfaces (44). As observed in Figure 2.6, most drug particles were accumulated in the surface discontinuities, likely forming weak agglomerates between the primary particles. According to a previous study (13), intensive mixing of the drug particles with relatively large lactose granules would break up hard natural drug agglomerates and render holes

for weak drug agglomerates. The weak agglomerates also were demonstrated by the relatively small aerodynamic size of the dispersed drugs (Table 2.2, Table 2.3, and Table 2.4), especially compared to the d50% of the micronized salbutamol sulfate particle size distribution (Figure 2.1). These weak drug agglomerates have higher inertial force in collision, so could be redispersed easily into primary drug particles during inhalation. Therefore, although the size of press-on forces generally will increase with increasing carrier diameter due to inertia mass, the effective surface area available for press-on effect decreases and consequently the effectiveness of the press-on force and the adhesive force decreases. Strong enough adhesive force is required such that drug preferentially adheres to the carrier during mixing, so as to achieve adequate blend homogeneity(45). So, the relatively poor blending uniformity observed with GL 850-1000 μm (Figure 2.7) partially supports the lower adhesive force in the larger lactose size fraction mixtures. Taking into account that blending uniformity is not the most efficient method, adhesive forces determined by more direct methods such as centrifugation and sieving would be investigated in the future study. The reduced adhesive forces between the carrier and drug may also be supported by the improved aerosol dispersion observed (Table 2.2, Table 2.3 and Table 2.4) for GL 850-1000 μm.

Since the granulated lactose had relatively rough surface, it is likely that press on forces would be reduced as these surface irregularities will shelter drug particles during contact between the lactose carriers. A greater quantity of drug powder would be required to fill the cavities on the surface of the granulated lactose before press-on forces would become important and limit aerosol performance. It is postulated, therefore, granulated lactose may be useful in making high drug loaded DPI formulations with acceptable

aerosol performance. In the present study 2% drug was incorporated in the blends, in which it was observed that the lactose carrier surface discontinuities were not fully occupied or saturated (Figure 2.6). Since the surface roughness of granulated lactose increased with increasing size fractions (Figure 2.5b), the larger lactose could be expected to provide a larger volume of surface pores to shelter a significantly higher amount of drugs from press-on forces during mixing (14). As a result, larger granulated lactose particles could be potential carriers for high drug loading dry powder inhalation formulations.

2.4.4.2 Separation forces and bulk powder properties

The *in vitro* cascade impaction aerosol dispersion studies of adhesive mixtures for inhalation do not solely reflect the effectiveness of the adhesion forces, but also incorportate the separation forces generated in the inhaler. Detachment by fluid flow forces and detachment by impaction/collision forces are the two major mechanisms involved in drug dispersion from large carrier particles (11, 12). Detachment by flow is preferred for carriers with relatively flat surface, such that drug particles could be exposed to the flow stream without obstructed path. Detachment by flow also facilitates the dispersion of larger drug particles, either primary drug particles or drug agglomerates, due to the increased drug surface area interacting with flow stream. Since the surface roughness of the granulated lactose increased significantly with size (Figure 2.5), according to the theory, the detachment force from flow stream would decrease with the increased granulated lactose size fractions.

Different from detachment by flow, detachment by impaction arises from the abrupt collisions between carrier particles and device walls and/or grids. Previous studies have hypothesized that there would be a transition from flow detachment to impaction detachment with larger (and significantly rough) lactose carriers. It was also shown that larger lactose particles with significantly rough surface exhibited greater aerosol performance than smaller particles (13). However, the carrier particle diameter used in previous studies was around or less than 300 μm, so it may be improper to extrapolate the improved mechanical impaction detachment force and aerosol performance for carrier particles larger than 300 μm as used in our study. In addition, as shown in previous study, even though the mechanical impaction force was still the predominant detachment force, the aerosol performance of the 250-300 μm granular lactose formulations was not significantly greater than the size fraction immediately preceding it (212-250 μm) due to relatively heavy mass of large carrier particles. It was speculated that mechanical impaction force of the granular lactose would not continuously increase with increasing carrier diameter/mass (13). Our observations in these studies of similar mass median aerodynamic diameter (MMAD) of the deposited drug (Table 2.2, 2.3 and 2.4) agreed with this assumption. In another study investigating the relationship between mechanical impaction force and particle detachment it was shown that a greater impaction force was needed for drug particles with decreasing diameter(46). It follows that the magnitude of impaction force could be similar, if similar aerodynamic diameters of deposited drugs were generated during inhalation of different formulations. As shown in Table 2.2, Table 2.3, and Table 2.4, MMAD values of the deposited drugs didn't significantly decrease with increasing granulated lactose size fractions under the same impaction parameters.

Thus, the mechanical impaction force may not significantly increase when lactose size increased from 212-250 μm to 850-1000 μm. However, previous study showed that the impaction force increases with increasing carrier size(13). Also, similar significantly low MMAD values were achieved under different carrier diameters compared to the value of d50% of micronized salbutamol sulfate (Figure 2.1), which indicates that lower impaction force was already enough to disperse down to primary size of the micronized drug particles. Thus, it is quite possible that impaction force did vary with increasing carrier diameter, but detachment due to mechanical impaction force didn't increase significantly.

Accordingly, for the separation force of the different lactose size fractions in this study, detachment by flow decreases significantly, and mechanical impaction force increases with increasing carrier diameter and surface roughness, but doesn't contribute to the increasing detachment. As a result, the detachment forces are not as effective for larger and coarser granular lactose as for smaller ones, confirmed by a decrease trend of fine particle fraction from GL 212-250 μm to GL 600-850 μm (Table 2.4). The improved aerosol performance of GL 600-850 μm is explained, on the other hand, by the reduced adhesive force as discussed in the 'adhesion forces and bulk powder properties' section.

2.5 CONCLUSION

To our knowledge, this study for the first time systemically studied the physico-chemical properties and aerosol performance of significantly large lactose carriers (>200 μm) across a wide range of narrow sieve fractions, In our study, the particle size of the lactose granules had no significant effect on solid-state, specific surface area, true density and flowability of the granulated lactose carriers. However, larger lactose granules had rougher particle surfaces and smaller bulk and tapped densities. This suggested that roughness, flowability, bulk and tapped density as well as the size of lactose could play a role together on the adhesive and removal force between drug particle and lactose particle.

In summary, the coarser size fractions of lactose (850-1000 μm) had a slight improvement of *in vitro* deposition under both 60L/min and 90L/min with and without enlarged piercing holes (Table 2.2, Table 2.3 and Table 2.4) compared to the immediately preceding size fractions (600-850 μm). A slight decreasing trend of FPF for the lactose carriers ranging from 212-250 μm to 600-850 μm was observed at 90L/min with larger piercing holes (1.2 mm) (Table 2.4). The surface roughness, size, bulk/tapped density as well as unusual powder flow are speculated to result in poor adhesion force of the largest and coarsest lactose granules, which could cause a slight increase of FPF. Meanwhile, surface roughness limits the strength of detachment by flow, which could explain a slight decreasing trend of FPF with size increasing from 212-250 μm to 600-850 μm with enlarged piercing holes, although not significantly different. Past studies, which prefer smaller carrier diameters, contribute the increased aerosol performance to increased specific surface area of smaller carriers, and increased fluid stream across drug particles

on flat carrier surface. However, the larger granulated carrier particles in this study possess different physical properties, with similar specific surface area over increasing size fractions and different predominate detachment mechanism, which is detachment by impaction force instead of fluid flow. Taken account of the different properties of the granulated lactose, poorer or enhanced aerosolization performance is not an inherent property to large size of granulated lactose carriers. The significantly large granulated lactose as the DPI carriers leads to a new way to investigate and optimize DPI formulations.

2.6 TABLE

Table 2.1 Preparation of salbutamol sulphate/granulated lactose binary blends

Formulation	GL (mg)	SBS (mg)
GLF 212-250 µm	490	10
GLF 250-300 µm	490	10
GLF 300-425 µm	490	10
GLF 425-600 µm	490	10
GLF 600-850 µm	490	10
GLF 850-1000 µm	490	10

GLF: granulated lactose formulation; GL: granulated lactose; SBS: salbutamol sulphate

Table 2.2 True density, bulk density and tapped density (mean±SD, n=3) of granulated lactose carriers GL 212-250 µm, GL 250-300 µm, GL 300-425 µm and GL 425-600 µm, GL 600-850 µm and GL 850-1000 µm .

	Pharmatose 100M	**GL 212-250 µm**	**GL 250-300 µm**	**GL 300-425 µm**	**GL 425-600 µm**	**GL 600-850 µm**	**GL 850-1000 µm**
True Density (g/ml)	1.546	1.544	1.544	1.542	1.546	1.547	1.544
Bulk Density (g/ml)	0.71 (0.02)	0.68 (0.01)	0.61 (0.01)	0.56 (0.00)	0.48±0.00	0.45±0.00	0.44±0.01
Tapped Density (g/ml)	0.94 (0.99)	0.82 (0.01)	0.71 (0.01)	0.65 (0.00)	0.58±0.00	0.53±0.03	0.48±0.01
Carr's Index (%)	23.82 (1.81)	16.66 (1.78)	14.12 (1.76)	14.23 (1.02)	15.97±0.11	14.95±3.57	9.50±3.03
Angle of Repose ( )	37.2 (1.5)	31.1 (3.0)	30.2 (1.5)	32.0 (1.5)	30.0±0.7	29.4±0.0	27.3±1.8

Table 2.3 *In Vitro* Aerosolization Performance with Capsules$4_{0.6}$ in Aerolizer at 60L/min. Emitted fraction (EF), fine particle fraction (FPF), respiratory fraction (RF), mass median aerodynamic diameter (MMAD) and geometric standard deviation (GSD) obtained from formulations containing SBS blended with granulated lactose carriers GL 212-250 μm, GL 250-300 μm, GL 300-425 μm, GL 425-600 μm, GL 600-850 μm and GL 850-1000 μm (mean ±SD, n=3).

	GL 212-250 μm	**GL 250-300 μm**	**GL 300-425 μm**	**GL 425-600 μm**	**GL 600-850 μm**	**GL 850-1000 μm**
EF (%)	87.5 (2.8)	82.3 (7.8)	71.9 (18.1)	63.3 (18.1)	62.5 (10.4)	67.0 (11.9)
FPF (%)	21.0 (2.9)	19.2 (0.4)	20.5 (5.2)	19.9 (1.8)	20.4 (4.6)	26.7 (5.7)
RF (%)	19.2 (2.8)	15.8 (1.5)	15.3 (6.8)	12.6 (2.4)	13.0 (4.6)	17.5 (2.6)
MMAD (μm)	2.04(0.13)	1.90(0.04)	2.00(0.14)	1.81(0.08)	1.93(0.13)	1.93(0.10)
GSD	1.8 (0.2)	1.7 (0.1)	1.7 (0.2)	1.7 (0.1)	1.8 (0.3)	1.7 (0.2)

.

Table 2.4 *In Vitro* Aerosolization Performance with Capsules$4_{0.6}$ in Aerolizer at 90L/min. Emitted fraction (EF), fine particle fraction (FPF), respiratory fraction (RF), mass median aerodynamic diameter (MMAD) and geometric standard deviation (GSD) obtained from formulations containing SBS blended with granulated lactose carriers GL 212-250 μm, GL 250-300 μm, GL 300-425 μm, GL 425-600 μm, GL 600-850 μm and GL 850-1000 μm (mean±SD, n=3).

	GL 212-250 μm	**GL 250-300 μm**	**GL 300-425 μm**	**GL 425-600 μm**	**GL 600-850 μm**	**GL 850-1000 μm**
EF (%)	83.2 (3.5)	83.6 (5.5)	81.1 (8.0)	76.7 (2.8)	73.2 (7.3)	69.6(11.0)
FPF (%)	36.5 (3.1)	33.8 (5.2)	35.3 (7.0)	32.8 (3.7)	36.8 (6.0)	41.6 (5.6)
RF (%)	30.4 (3.7)	28.5 (6.6)	29.0 (8.3)	25.1 (2.7)	27.1 (6.5)	29.3 (8.4)
MMAD (μm)	1.69(0.03)	1.68(0.11)	1.65(0.04)	1.67(0.03)	1.58(0.03)	1.66(0.01)
GSD	1.8 (0.1)	1.8 (0.2)	1.8 (0.2)	1.8 (0.1)	1.9 (0.0)	2.0 (0.2)

Table 2.5 *In Vitro* Aerosolization Performance with Capsules$_{1.2}$ in Aerolizer at 90L/min. Emitted fraction (EF), fine particle fraction (FPF), respiratory fraction (RF), mass median aerodynamic diameter (MMAD) and geometric standard deviation (GSD) obtained from formulations containing SBS blended with granulated lactose carriers GL 212-250 μm, GL 250-300 μm, GL 300-425 μm, GL 425-600 μm, GL 600-850 μm and GL 850-1000 μm (mean±SD, n=3).

	GL 212-250 μm	**GL 250-300 μm**	**GL 300-425 μm**	**GL 425-600 μm**	**GL 600-850 μm**	**GL 850-1000 μm**
EF (%)	89.0 (1.7)	89.2 (0.8)	89.1 (1.4)	90.0 (1.2)	88.9 (2.1)	84.6 (3.8)
FPF (%)	37.1 (4.5)	38.2 (6.1)	34.9 (3.3)	30.7 (2.6)	31.2 (2.9)	37.8 (4.2)
RF (%)	33.0 (4.3)	34.1 (5.2)	31.1 (2.8)	27.6 (2.6)	27.7 (2.6)	32.0 (4.5)
MMAD (μm)	1.73(0.02)	1.68(0.04)	1.70(0.06)	1.60(0.04)	1.62(0.07)	1.64(0.06)
GSD	1.7 (0.0)	1.7 (0.0)	1.7 (0.1)	1.7 (0.0)	1.8 (0.0)	1.8 (0.1)

2.7 FIGURE

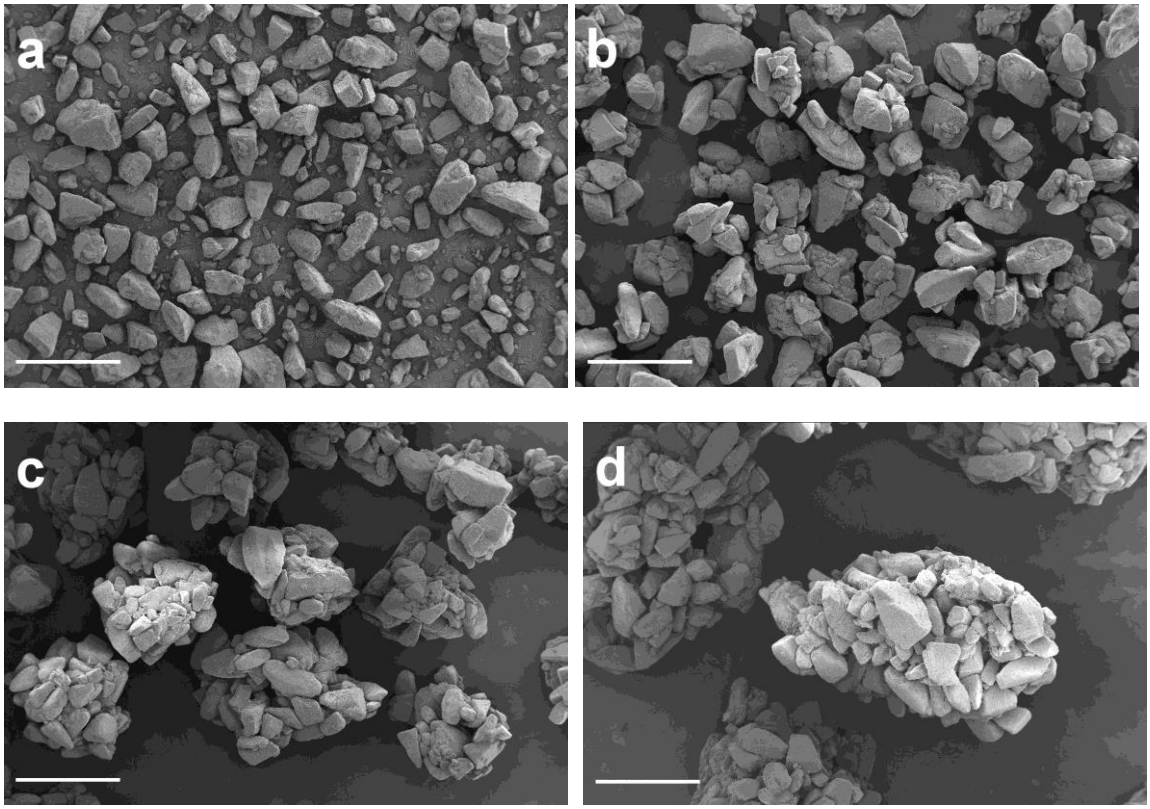

Figure 2.1 SEM micrographs of (a) Pharmatose 100M, (b) GL 212-250 μm granulated lactose, (c) GL 425-600 μm granulated lactose, (d) GL 850-1000 μm granulated lactose sieve fractions. Scale bars denote 200 μm

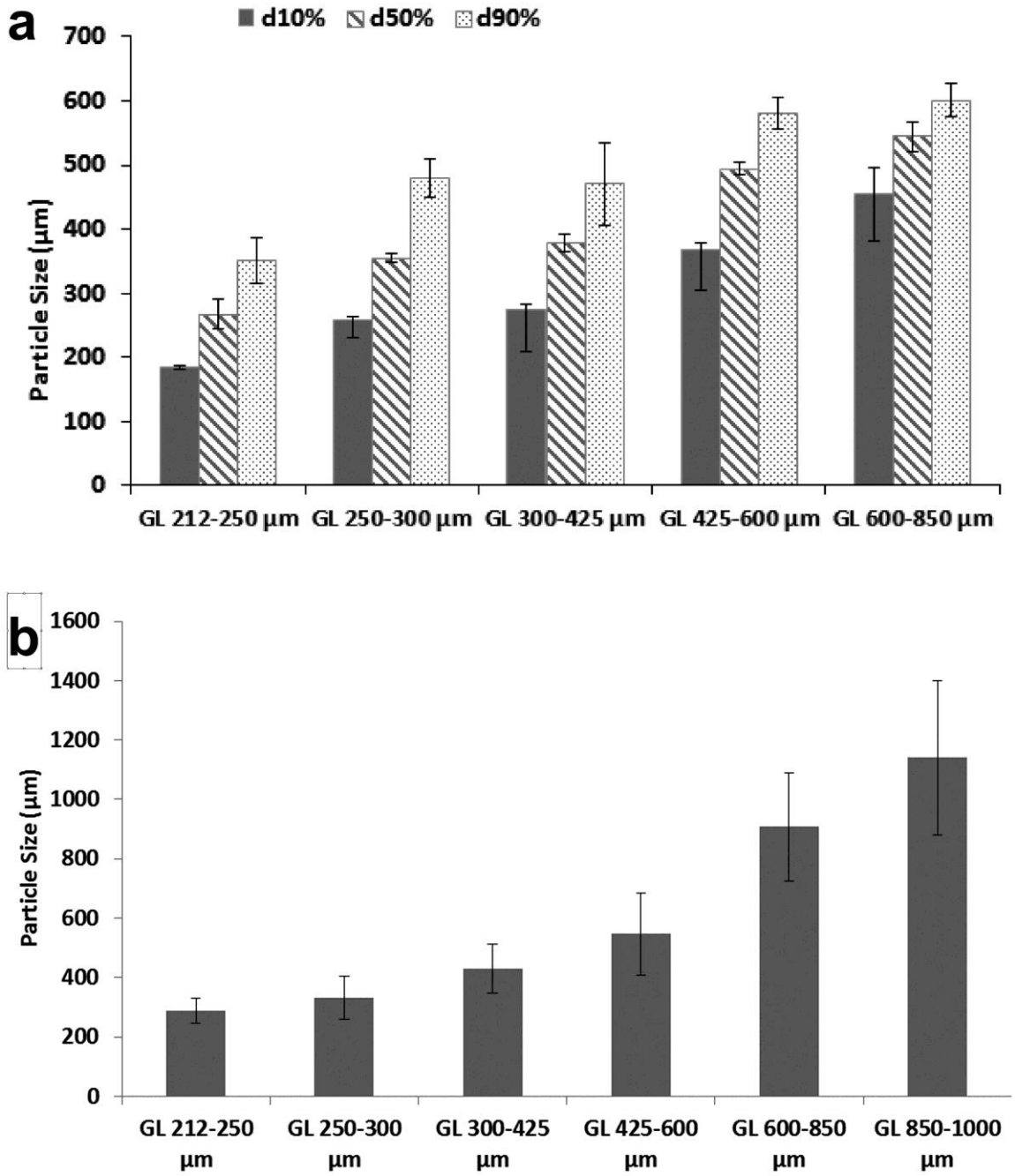

Figure 2.2 Particle size obtained by (a) laser diffraction (d10%, d50% and d90%) and (b) by image analysis SEM pictures

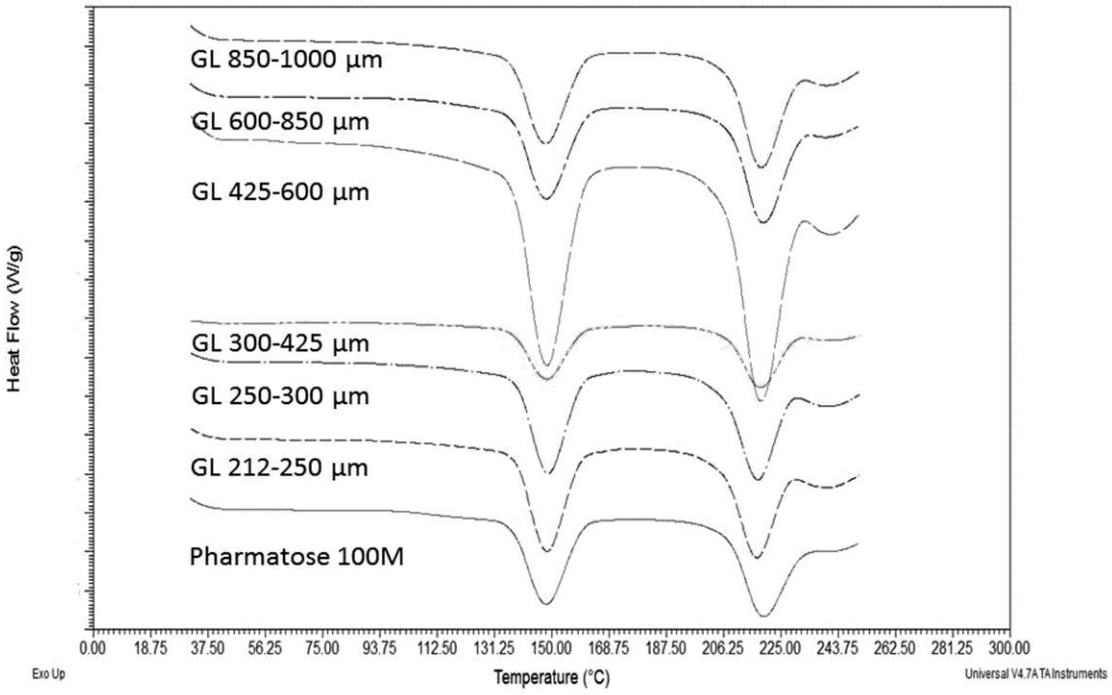

Figure 2.3 The DSC thermographs of all granulated lactose

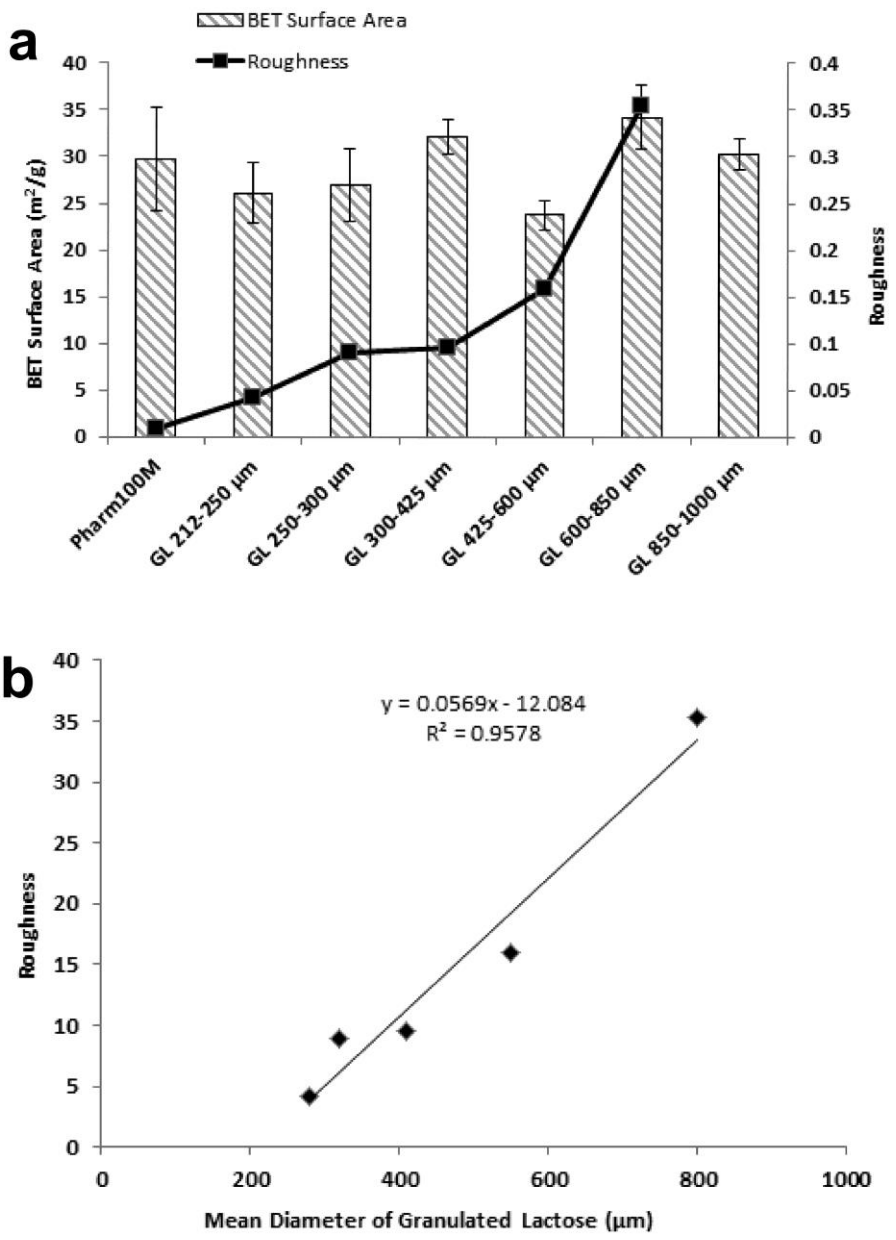

Figure 2.4 (a) BET surface area and roughness for granulated lactose carriers with different size fractions: GL 212-250 µm, GL 250-300 µm, GL 300-425 µm and GL 425-600 µm, GL 600-850 µm and GL 850-1000 µm; (b) and roughness of GL particles. All GL particles have similar specific surface area and larger GL particles have rougher surfaces.

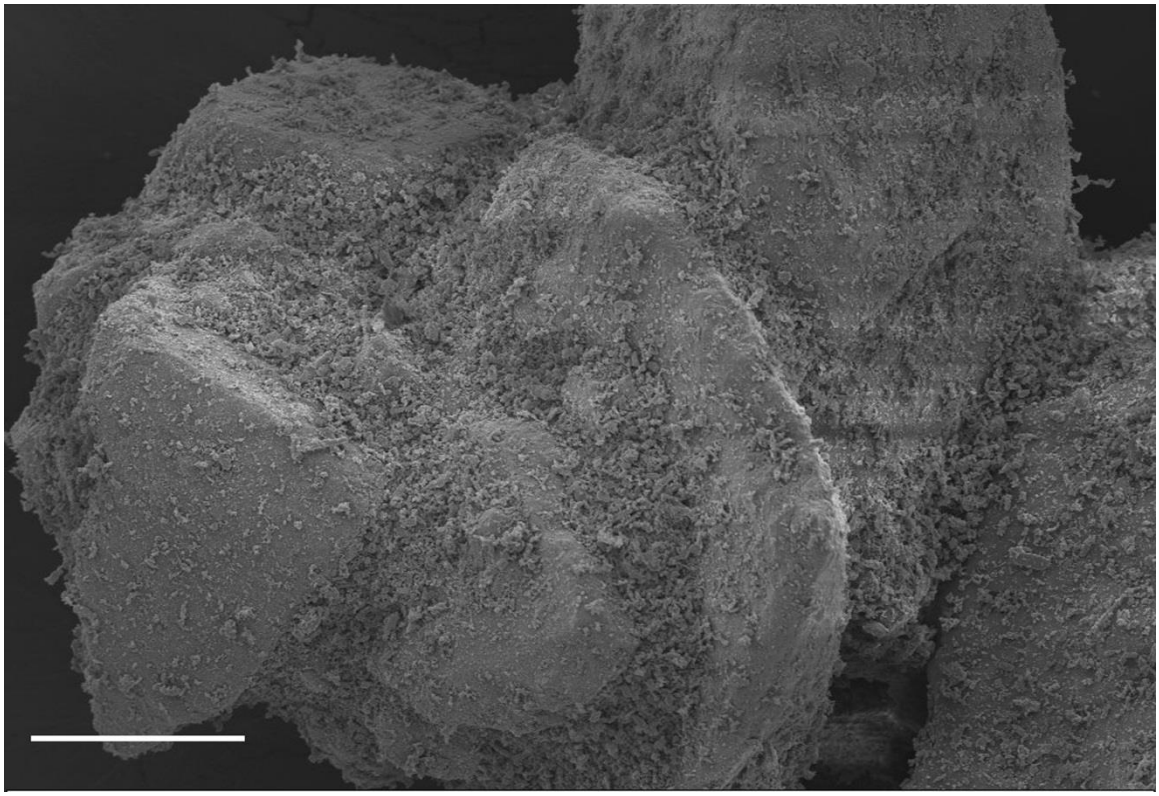

Figure 2.5 SEM pictures of granulated lactose GL 212-250 μm blended with 2% SBS.

Scale bar denotes 20 μm

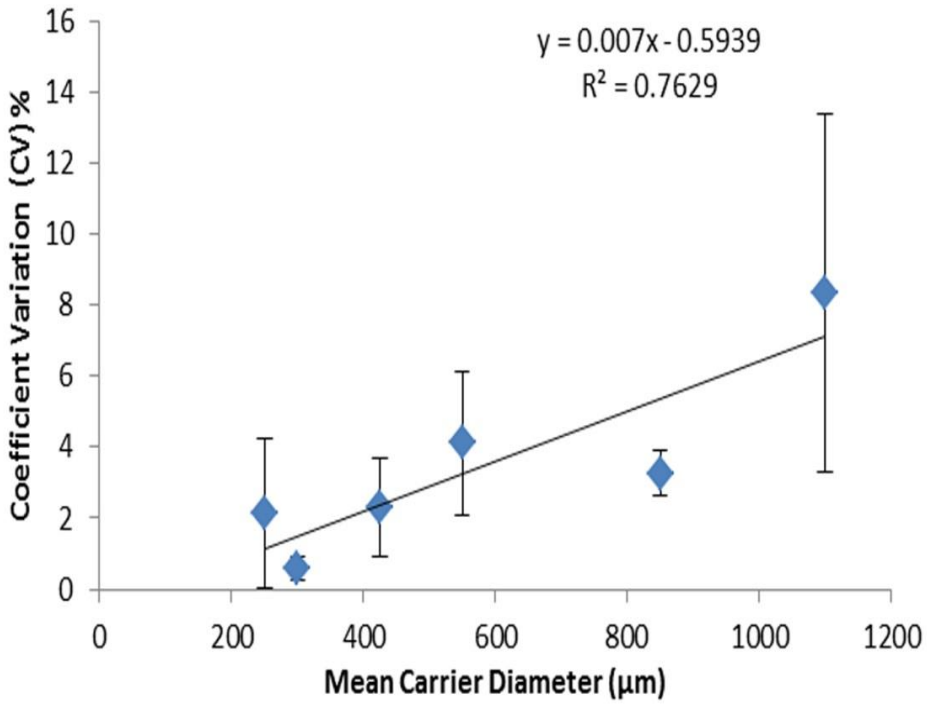

Figure 2.6 Blending uniformity of lactose granules based DPI formulations as function of the mean carrier diameter. (n = 5 x 3)

2.8 REFERENCES

1. Hickey AJ. Pharmaceutical inhalation aerosol powder dispersion - An unbalancing act. American Pharmaceutical Review. 2003;6:106-10.

2. Smyth HD, Hickey AJ. Carriers in drug powder delivery. American Journal of Drug Delivery. 2005;3:117-32.

3. Adi H, Larson I, Stewart PJ. Adhesion and redistribution of salmeterol xinafoate particles in sugar-based mixtures for inhalation. Int J Pharm. 2007;337:229-38.

4. Steckel H, Muller BW. In vitro evaluation of dry powder inhalers .2. Influence of carrier particle size and concentration on in vitro deposition. Int J Pharm. 1997;154:31-7.

5. Flament MP, Leterme P, Gayot A. The influence of carrier roughness on adhesion, content uniformity and the in vitro deposition of terbutaline sulphate from dry powder inhalers. Int J Pharm. 2004;275:201-9.

6. Pitchayajittipong C, Price R, Shur J, Kaerger JS, Edge S. Characterisation and functionality of inhalation anhydrous lactose. Int J Pharm. 2010;390:134-41.

7. Jiang RG, Zhang PW, Wang LQ, Liu H, Pan WS, Wang CL. [Effect of surface modification on surface energy of lactose and performance of dry powder inhalations]. Yao Xue Xue Bao. 2005;40:373-6.

8. Guenette E, Barrett A, Kraus D, Brody R, Harding L, Magee G. Understanding the effect of lactose particle size on the properties of DPI formulations using experimental design. Int J Pharm. 2009;380:80-8.

9. Kougoulos E, Marziano I, Miller PR. Lactose particle engineering: Influence of ultrasound and anti-solvent on crystal habit and particle size. Journal of Crystal Growth.312:3509-20.

10. Ferrari F, Cocconi D, Bettini R, Giordano F, Santi P, Tobyn M, et al. The surface roughness of lactose particles can be modulated by wet-smoothing using a high-shear mixer. AAPS PharmSciTech. 2004;5:e60.

11. de Boer AH, Hagedoorn P, Gjaltema D, Goede J, Frijlink HW. Air classifier technology (ACT) in dry powder inhalation. Part 1. Introduction of a novel force distribution concept (FDC) explaining the performance of a basic air classifier on adhesive mixtures. Int J Pharm. 2003;260:187-200.

12. Voss A, Finlay WH. Deagglomeration of dry powder pharmaceutical aerosols. Int J Pharm. 2002;248:39-50.

13. Donovan MJ, Smyth HD. Influence of size and surface roughness of large lactose carrier particles in dry powder inhaler formulations. Int J Pharm. 2010;402:1-9.

14. Dickhoff BH, de Boer AH, Lambregts D, Frijlink HW. The interaction between carrier rugosity and carrier payload, and its effect on drug particle redispersion from adhesive mixtures during inhalation. Eur J Pharm Biopharm. 2005;59:197-205.

15. Grasmeijer F, Hagedoorn P, Frijlink HW, de Boer AH. Drug content effects on the dispersion performance of adhesive mixtures for inhalation. PLoS One. 2013;8:e71339.

16. Islam N, Stewart P, Larson I, Hartley P. Lactose surface modification by decantation: are drug-fine lactose ratios the key to better dispersion of salmeterol xinafoate from lactose-interactive mixtures? Pharm Res. 2004;21:492-9.

17. Hickey AJ, Mansour HM, Telko MJ, Xu Z, Smyth HD, Mulder T, et al. Physical characterization of component particles included in dry powder inhalers. I. Strategy review and static characteristics. J Pharm Sci. 2007;96:1282-301.

18. de Boer AH, Hagedoorn P, Gjaltema D, Goede J, Kussendrager KD, Frijlink HW. Air classifier technology (ACT) in dry powder inhalation. Part 2. The effect of lactose carrier surface properties on the drug-to-carrier interaction in adhesive mixtures for inhalation. Int J Pharm. 2003;260:201-16.

19. Louey MD, Razia S, Stewart PJ. Influence of physico-chemical carrier properties on the in vitro aerosol deposition from interactive mixtures. Int J Pharm. 2003;252:87-98.

20. Cline D, Dalby R. Predicting the quality of powders for inhalation from surface energy and area. Pharm Res. 2002;19:1274-7.

21. Donovan MJ, Kim SH, Raman V, Smyth HD. Dry powder inhaler device influence on carrier particle performance. J Pharm Sci. 2012;101:1097-107.

22. Littringer EM, Mescher A, Schroettner H, Achelis L, Walzel P, Urbanetz NA. Spray dried mannitol carrier particles with tailored surface properties--the influence of carrier surface roughness and shape. Eur J Pharm Biopharm. 2012;82:194-204.

23. Kawashima Y, Serigano T, Hino T, Yamamoto H, Takeuchi H. Effect of surface morphology of carrier lactose on dry powder inhalation property of pranlukast hydrate. 1998;172:188.

24. Li J, Tao L, Buckley D, Tao J, Gao J, Hubert M. The Effect of the Physical State of Binders on High-Shear Wet Granulation and Granule Properties: A Mechanistic Approach to Understand the High-Shear Wet Granulation Process. Part IV. The Impact of Rheological State and Tip-speeds. J Pharm Sci. 2013;102:4384-94.

25. Fujiwara M, Dohi M, Otsuka T, Yamashita K, Sako K. Influence of binder droplet dimension on granulation rate during fluidized bed granulation. Chem Pharm Bull (Tokyo). 2013;61:320-5.

26. Ogawa T, Uchino T, Takahashi D, Izumi T, Otsuka M. Pharmaceutical production of tableting granules in an ultra-small-scale high-shear granulator as a pre-formulation study. Drug Dev Ind Pharm. 2012;38:1390-3.

27. Mangwandi C, Adams MJ, Hounslow MJ, Salman AD. An investigation of the influence of process and formulation variables on mechanical properties of high shear granules using design of experiment. Int J Pharm. 2012;427:328-36.

28. Singh I, Kumar P. Preformulation studies for direct compression suitability of cefuroxime axetil and paracetamol: a graphical representation using SeDeM diagram. Acta Pol Pharm. 2012;69:87-93.

29. Coates MS, Fletcher DF, Chan HK, Raper JA. The role of capsule on the performance of a dry powder inhaler using computational and experimental analyses. Pharm Res. 2005;22:923-32.

30. Zeng XM, Martin GP, Marriott C, Pritchard J. The influence of crystallization conditions on the morphology of lactose intended for use as a carrier for dry powder aerosols. J Pharm Pharmacol. 2000;52:633-43.

31. Li X, Mansour HM. Physicochemical characterization and water vapor sorption of organic solution advanced spray-dried inhalable trehalose microparticles and nanoparticles for targeted dry powder pulmonary inhalation delivery. AAPS PharmSciTech. 2011;12:1420-30.

32. Kaialy W, Ticehurst MD, Murphy J, Nokhodchi A. Improved aerosolization performance of salbutamol sulfate formulated with lactose crystallized from binary mixtures of ethanol-acetone. J Pharm Sci. 2011;100:2665-84.

33. Adi S, Adi H, Tang P, Traini D, Chan HK, Young PM. Micro-particle corrugation, adhesion and inhalation aerosol efficiency. Eur J Pharm Sci. 2008;35:12-8.

34. Adi H, Traini D, Chan HK, Young PM. The influence of drug morphology on aerosolisation efficiency of dry powder inhaler formulations. J Pharm Sci. 2008;97:2780-8.

35. Islam N, Stewart P, Larson I, Hartley P. Surface roughness contribution to the adhesion force distribution of salmeterol xinafoate on lactose carriers by atomic force microscopy. J Pharm Sci. 2005;94:1500-11.

36. Young PM, Edge S, Traini D, Jones MD, Price R, El-Sabawi D, et al. The influence of dose on the performance of dry powder inhalation systems. Int J Pharm. 2005;296:26-33.

37. Kaialy W, Martin GP, Larhrib H, Ticehurst MD, Kolosionek E, Nokhodchi A. The influence of physical properties and morphology of crystallised lactose on delivery of salbutamol sulphate from dry powder inhalers. Colloids Surf B Biointerfaces. 2012;89:29-39.

38. Sinko PJ. Martin's Physical Pharmacy and Pharmaceutical Sciences. Philadelphia, PA, USA: Lippincott Williams & Wilkins; 2005.

39. Dickhoff BH, de Boer AH, Lambregts D, Frijlink HW. The effect of carrier surface and bulk properties on drug particle detachment from crystalline lactose carrier particles during inhalation, as function of carrier payload and mixing time. Eur J Pharm Biopharm. 2003;56:291-302.

40. Liu LX, Marziano I, Bentham AC, Litster JD, White ET, Howes T. Effect of particle properties on the flowability of ibuprofen powders. Int J Pharm. 2008;362:109-17.

41. Kaialy W, Hussain T, Alhalaweh A, Nokhodchi A. Towards a More Desirable Dry Powder Inhaler Formulation: Large Spray-Dried Mannitol Microspheres Outperform Small Microspheres. Pharm Res. 2013.

42. Chew NYK, Bagster DF, Chan HK. Effect of particle size, air flow and inhaler device on the aerosolisation of disodium cromoglycate powders. Int J Pharm. 2000;206:75-83.

43. de Boer AH, Chan, H. K. and Price, R. A critical view on lactose-based drug formulation and device studies for dry powder inhalation: Which are relevant and what interactions to expect? Advanced Drug Delivery Reviews. 2012;64:257-74.

44. Podczeck F. Assessment of the mode of adherence and the deformation characteristics of micronized particles adhering to various surfaces. Int J Pharm. 1996;145:65-76.

45. Le VN, Hoang Thi TH, Robins E, Flament MP. Dry powder inhalers: study of the parameters influencing adhesion and dispersion of fluticasone propionate. AAPS PharmSciTech. 2012;13:477-84.

46. Concessio NM, VanOort MM, Knowles MR, Hickey AJ. Pharmaceutical dry powder aerosols: correlation of powder properties with dose delivery and implications for pharmacodynamic effect. Pharm Res. 1999;16:828-34.

Chapter 3: Evaluation of granulated lactose as a carrier for DPI formulations 2: Effect of Drug Loading

Abstract

The objective of this study was to investigate the effect of drug loading on aerosol performance of dry powder inhaler formulations under different flow rates. Two different micronized APIs with different shape, and surface energy were studied. Granulated lactose carriers were prepared and fractionated into three discrete narrow size fractions, GL 212-250 µm, GL 450-600 µm and GL 850-1000 µm, which were blended with salbutamol sulfate or rifampicin to formulate 10% or 30% binary mixtures respectively. The *in vitro* aerosol performance was performed on the three different size fractions of 20 mg adhesive mixtures from a commercial inhaler device (Aerolizer®) under 30 L/min and 90 L/min through NGI (Next Generation Impactor). Drug content was assessed via UV–Vis absorption spectroscopy at 230 nm or 470 nm. The selected size fractions of granulated lactose had increasing number of primary lactose particles and improved flowability with increasing granulated lactose size. There was a linear relationship (r^2 = 0.9787) between mean diameter of lactose granules and roughness value. All formulations had acceptable emitted fractions (> 70%) from impaction study. For both drug loading (10% and 30%), there was an inverse relationship between mass median aerodynamic diameters (MMAD) and size fractions. SS and Rif blended high drug loaded DPI formulations had quite different aerosol performance with each other, in terms of

granulated lactose size fraction and flow rate. Relatively large granulated lactose has improved flowability and increased surface roughness with increasing size fraction, which are promising properties for formulating high drug loaded DPI formulations. The aerosol performance of the high drug loaded DPI formulation heavily depends on the APIs and also the flow rate used in NGI study.

Keywords:

DPI formulations; Granulated lactose; Carrier size; Carrier roughness; Drug Loading

3.1 INTRODUCTION

The dry powder inhaler (DPI) has become increasingly popular in the last decade by virtue of propellant-free nature, high patient compliance and improved formulation stability[1]. In DPI formulation, active pharmaceutical ingredient (API) particles need to have aerodynamic diameters around 1-5 μm to reach therapeutic areas of the lung. However, particles with size smaller than 5 μm are very cohesive with extremely poor flowability. To facilitate powder flow, metering, dosing and downstream processing, large quantities of coarse carriers are commonly introduced to form binary or tertiary mixtures[2]. These mixtures are required to be redispersed into primary drug particles upon inhalation by patients. This is called aerosol or aerosolization performance. Nevertheless, it is challenging to develop an ideal DPI formulation, which has both good aerosol performance, and good blending uniformity. A balance is needed of interparticle forces between carrier and API particles. On one hand, adhesion force must be strong enough to ensure mixing homogeneity and stability during downstream powder handling, dosing, and transportation. On the other hand, adhesion force must be weak enough to allow efficient detachment of micronized API particles from the carrier surface upon inhalation[2].

As the major components of DPI mixtures, the physico-chemical properties of coarse carriers are key parameters in determining performance of DPI formulations[3]. α-lactose monohydrate is the commonly used coarse carrier for DPI formulation because of its well-established safety profile, stable physico-chemical properties and compatibility with most available low molecular weight APIs[4]. It was widely believed that carrier

particles with smaller diameters especially with flat surface were preferable to maximize aerosolization efficiency[5]. Nevertheless, it was found recently lactose carriers with large size fraction especially with significantly rough surface can also improve aerosol performance[6, 7]. This improvement is explained by the switch of predominant detachment mechanism from turbulence flow to impaction force[7]. It was also found that the rough surface of significantly large lactose could be used to shelter more drug particles from press-on forces much better than smooth counterparts, resulting in an improved aerosol performance[8].

A perfect blending uniformity of two types of particles is that when a group of particles are taken from any position in the mixture, the same proportions of each particle are obtained as in the whole mixture[9]. To reach acceptable blending uniformity, interactive or ordered mixing is commonly used in DPI formulations, which generally contains low drug loading (1-2%). In the ordered and interactive mixture, the fine drug particles (micronized drugs, <5um) adhere to the second coarser constituents (coarse lactose carrier). These interactive mixtures will become nearly homogenous under optimum mixing conditions[10].

Nevertheless, it is found that there is a dilemma between high aerosol performance and good blending uniformity for traditional DPI binary mixtures. As mentioned before, it is considered as a dogma in inhalation area that lactose carrier with small particle size especially with flat surface is preferred for a better aerosol performance. Thus large quantities of fine lactose particles are always added in commercial inhalation grade lactose for aerosol performance improvement. However, it is known that small size and

smooth surface of particles are detrimental to powder flow[11], and potentially would have adverse effect on blending uniformity. It has been reported by Kaialy et. al that budesonide formulated with smaller lactose carriers exhibited higher amounts of budesonide delivered to the lower stages of the impactor indicating an improved DPI aerosol performance, while lactose particles with smaller diameter had an unfavorable effect on budesonide content homogeneity[12]. Additionally, the large particle size and thus small specific surface area of the coarser carrier particles limit the loading content of fine drug particles. When the drug loading is increased further than forming the monolayer of the available space on the carrier, multiple agglomerate systems would likely to be formed, leading to formulation segregation and reduced aerosol performance[13]. This is one potential major reason that there is no high drug loaded lactose based DPI formulations right now, which however is very important for tuberculosis (TB) or other lung infections.

To solve the dilemma of poor blending uniformity or poor aerosol performance in carrier based DPI formulations, especially high drug loaded DPIs, granular lactose turns out a promising DPI carrier. Firstly, as discussed above, significantly large granulated lactose could still serve as proper DPI carriers with better aerosol performance, where inertia impaction is the major detachment mechanism. Secondly, small lactose is unfavorable in DPI blending uniformity, but when the surface of lactose carrier became rougher, an improvement in blending homogeneity could be observed for the DPI formulation powders[14]. Therefore, roughness favors blending uniformity when the particle size is fixed. Last but not least important, roughness not only is beneficial for blending uniformity but was also found important in increasing drug loading. It was

reported recently that porous carrier particles could improve drug loading during an interactive mixing process without compromising blending uniformity. For instance, compared to sugar beads and MCC granules, a new porous carrier not only improved the loading capacity to 310% to 320%, but also provided an improved content uniformity[15]. In previous study a positive relationship was found and established between surface roughness/granule cavity volumes and granular size fractions[6], thus improved blending uniformity and high drug loading could be achieved by significantly larger granular lactose for DPI formulations.

In this study, to investigate the influence of granular lactose on blending uniformity and high drug loading of dry powder formulations, three significantly large size fractions of granulated lactose and two types of pharmaceutical active ingredients (APIs) with different size, shape and density were selected. This study evaluated how different size fractions of granulated lactose and different APIs affect the aerosol performance as well as blending uniformity of the carrier based DPI formulations, over a range of flow rates.

3.2 EXPERIMENTAL

3.2.1 Materials

α-Lactose monohydrate, Pharmatose 100M, was supplied from DFE Pharma (Princeton, NJ, USA). Micronized salbutamol sulphate (D50: 1.88 μm) was purchased from LETCO MEDICAL. Deionized water was provided by MilliQ (Millipore).

3.2.2 Manufacture of lactose granules

Wet granulation was used to manufacture lactose granules with large diameter from Pharmatose 100M (d10: 63 μm, d50: 150 μm, d90: 250 μm). Granulation is a process to generate large aggregates from small primary powders to improve the flowability of the powders [16]. Wet granulation of lactose usually employs polymeric binders that are not approved for inhalation [17-20]. To solve this problem, the granulation process in this research involved merely water as the binding solvent. Briefly, a batch size of 500 g starting lactose was introduced into the granulator (Robot Coupe USA. Inc.) followed by addition of 100 mL water merely as the granulating solvent. Subsequently, the granulated lactose carriers were pan dried in the oven overnight at 75 ℃.

3.2.3 Fractionation of granulated lactose carrier particles

Different size fractions of lactose granules were obtained by separation of the bulk granulated material using a sieve tower with cut off sizes as follows: 1000 μm, 850 μm,

600 μm, 425 μm, 300 μm, 250 μm, 212 μm, and a metal collection pan. A vibrating auto sieve shaker (Gilson Company Inc., OH, USA) was employed. The granulated lactose was poured on the top of the vibrating sieve shaker and sieved through the sieves for 30 min. Three size fractions of granulated lactose (GL) were selected for future experiments: GL 212-250 μm, GL 450-600 μm and GL 850-1000 μm. All analysis described were performed on the sieved samples.

3.2.4 Fractionation of primary lactose carrier particles

A vibrating auto sieve shaker (Gilson Company Inc., OH, USA) was employed. Pharmatose 100M was poured on the top of the vibrating sieve shaker and sieved through the sieves for 30 min. Size fractions 212-250 μm of lactose was selected for future experiments.

3.2.5 Particle size measurement

Particle size analysis of fractionized granulated lactose was evaluated by the Sympatec laser diffraction (Sympatec GmbH). The theoretical specific surface area (based on volume, assuming an ideal spherical smooth surface of the particles) was calculated by the software installed in the Sympatec.

3.2.6 Scanning electron microscopy

The scanning electron microscopy (SEM; Supra 40VP, Zeiss, Germany) was used to visually assess the particle size and morphology of the granulated lactose and adhesive mixtures before and after impaction. The coating conditions prior to SEM for all the granulated lactose was 15 nm of Pd/Pt via sputter coating.

3.2.7 Inverse Gas Chromatography

The surface energetics of rifampicin particles with different size distributions were measured using a commercially available IGC system (2000, Surface Measurement Systems Ltd., London, UK). Approximately around 500 mg of each rifampicin sample was loaded into pre-silanized IGC glass columns (300mm x 3 mm i.d.) plugged with glass wool at each end of the column. Prior measurement each column was purged with dry nitrogen at 30 ℃. The retention time of both polar probes (ethyl acetate and chloroform) and nonpolar probes (n-alkanes) were measured at finite dilution conditions. Dispersive and specific surface energy under infinite dilution conditions were extrapolated from the straight lines of elution time in terms of the surface coverage by nonpolar or polar solvents[21].

3.2.8 Preparation of salbutamol sulfate or rifampicin granulated lactose binary blends

Salbutamol sulfate (SS) or rifampcin and fractionated granulated lactose were mixed to obtain 10% and 30% binary mixtures. All formulations were blended at a constant speed of 46 RPM for 10 min with a Turbula® orbital mixer (Glen Mills, NJ, USA). Prior to any further analysis, the blended formulations were stored in the dessicator for 5 days.

3.2.9 Preparation of salbutamol sulfate and lactose binary blends

Salbutamol sulfate (SS) and primary lactose with size fraction of 212-250 μm were mixed to obtain two 30% binary mixtures. One batch of formulation was blended at a constant speed of 46 RPM for 10 min and other for 60 minwith a Turbula® orbital mixer (Glen Mills, NJ, USA). Prior to any further analysis, the blended formulations were stored in the dessicator for 5 days.

3.2.10 Drug uniformity test

Five of randomly selected samples (20 ± 1 mg) were taken for measurement of salbutamol sulfate and rifampicin content uniformity. The coefficient of variation (CV%) was used to determine the blending uniformity. The test was performed three times. The potency of formulations was calculated by the APIs percent amount to the nominal dose.

3.2.11 *In vitro* aerosolisation study

About 20 (±1) mg mixture powders were filled into size 3 Vcaps HPMC capsules pierced with one enlarged holes (1.2 mm) at each end of the capsule. The *in vitro* aerosolization performance of all formulations was assessed using Aerolizer® inhaler device (Novartis, Switzerland) under 30, 60 and 90L/min with 4L air volume through the device.

A 1% (w/v) solution of silicon oil in hexane was applied to precoat the NGI stages for particle re-entrainment prevention. Amounts of salbutamol sulfate or rifampicin deposited on the capsule, inhaler, mouthpiece adaptor, induction port, pre-separator and NGI stages were measured and quantified. The content of salbutamol sulfate and rifampicin was measured by the ultraviolet visible absorption spectroscopy (Infinite M200, TECAN) at 230 nm and 474 nm respectively. The parameters used to evaluate salbutamol sulfate and rifampicin deposition performance were emitted fraction (EF) (Eq. 1), fine particle fraction (FPF) (Eq. 2), respirable fraction (Eq. 3) mass median aerodynamic diameter (MMAD) and geometric standard deviation (GSD).

$$\mathrm{EF} = \frac{\text{emitted dose}}{\text{loading dose}}$$

(Eq. 1)

$$\mathrm{FPF} = \frac{\text{recovered dose of drug particles smaller than 5 μm}}{\text{emitted dose}}$$

(Eq. 2)

$$RF = \frac{\text{recovered dose of drug particles smaller than 5 } \mu m}{\text{loading dose}}$$

(Eq.3)

3.2.10 Statistics Analysis

Statistical significance between aerosol performance values was determined with one-way TTESTs between groups (* indicates $P<0.05$; ** indicates $P<0.005$).

3.3 RESULTS

3.3.1 Laser diffraction analysis

Two different APIs (salbutamol sulfate and rifampicin) with similar particle size distribution, but different morphology, bulk density and surface energy were chosen. As shown in Figure 3.1, the particle size distribution of salbutamol sulfate was comparable to that of rifampicin. Specifically, the X_{50} of salbutamol sulfate was around 4.31 μm and that of rifampicin was around 4.17 μm.

3.3.2 SEM images of two micronized APIs

Representative images of salbutamol sulfate and rifampicin are presented in Figure 3.2. The morphology of micronized salbutamol sulfate in Figure 3.2A was flat sheets, with elongated rectangular shape and relatively smooth surface. Fine salbutamol sulfate attached on the large salbutamol sulfate particles was visible. In contrast, micronized rifampicin particles were relatively spherical, with rough surface and large amounts of fine rifampicin particles attached.

3.3.3 Inverse gas chromatography

Inverse gas chromatography was applied to study the cohesive and adhesive interactions of two different components at the molecular level. As seen in Table 3.2, salbutamol sulfate had higher surface energy and work of cohesion than rifampicin, indicating that salbutamol sulfate is more cohesive than rifampicin and tends to form agglomerates with strong interactions. Work of cohesion is the work needed to separate two cohesive particles apart. The dispersive and acid-base surface energy of salbutamol sulfate was 57.95 mJ/m^2 and 4.40 mJ/m^2, in contrast to 26.70 mJ/m^2 and 2.92 mJ/m^2 of rifampicin. Due to the higher surface energy, salbutamol sulfate had almost twice large work of cohesion than rifampicin.

3.3.4 SEM images of binary mixtures

The granulated lactose used in this study had different size fractions (GL 212-250 μm, GL 425-600 μm, and GL 850-1000 μm). Additionally, each single lactose granule was composed with aggregates formed by the primary lactose. With size increasing, the granulated lactose composed with (Figure 3.3) increasing number of primary lactose particles. Because of the aggregated primary particles, there are deep valleys and large cavities on the surface of all grades of granulated lactose, which could be obviously observed from the SEM images.

After blending with 10% or 30% SBS, respectively, the binary mixtures of granulated lactose (GL 212-250 μm, GL 425-600 μm, and GL 850-1000 μm) were characterized by scanning electron microscopy (Figure 3.4), so as to reveal the positions and distributions of SBS on the surface of lactose carriers. As shown in Figure 3.4, the SBS particles mostly were trapped inside the large valleys and cavities of granulated lactose carriers, similar to the result of granulated lactose mixed with 2% SBS in previous research.[6] Previous study in our group showed that there was a linear relationship (r^2 = 0.9787) between mean diameter of lactose granules and roughness value.[6] Thus, the three grades of lactose granules had increasing surface roughness with increasing size. Since granulated lactose with increasing size had increasing surface roughness, those granulated lactose with increasing size fractions require increasing amount of SBS to completely fill the deep valleys or the surface roughness at a macro level. In this study, with addition of 10% SBS, no obvious projections and valleys (Figure 3.4A) on the surface of GL 212-250 μm mixture could be found. 10% SBS was almost enough to cover the deep valleys and cavities on GL 212-250 μm. Nevertheless, GL 425-600 μm and GL 850-1000 μm after blended with 10% SBS (Figure 3.4B and Figure 3.4C) were still in granular shape, especially GL 850-1000 μm with deep cavity holes clearly observed. The cavity holes of GL 425-600 μm and GL 850-1000 μm could not be completely filled until SBS reached 30%. Figure 3.4D, E and F showed that with 30% SBS the surface of all lactose carriers (GL 212-250 μm, GL 425-600 μm, and GL 850-1000 μm) become relatively smooth and almost all the valleys were filled to the layer adjacent to the surface of protuberances.

Nevertheless, things are a little bit different when another APIs (rifampicin, RIF) was used. The binary mixtures of granulated lactose (GL 212-250 μm, GL 425-600 μm, and GL 850-1000 μm) with 10% RIF or 30% RIF characterized by scanning electron microscopy were shown in Figure 3.5. Contrary to 10% SBS, even if GL 212-250 μm was the carriers (Figure 3.5A), original shape of granulated lactose still could be clear observed with 10% RIF blended. Only when the amount of RIF reached 30%, the deep valleys of granulated lactose (such as GL 212-250 μm and GL 425-600 μm) could be covered and the original morphology of granulated lactose could not be easily observed. However, the 30% RIF was still not sufficient to fill all the cavities on GL 850-1000 μm and a very large hole not covered by RIF was shown in Figure 3.5F.

As mentioned in the above paragraph, with addition of 10% SBS the cavities of GL 212-250 μm could not be observed any more, but with 10% RIF the original morphology of GL 212-250 μm still could be seen obviously. To find the reason of the different phenomenon, a closer inspection of the distribution of SBS and RIF on granulated lactose was needed. Actually, (Figure 3.6B) the majority of 10% RIF merely located inside the deep cavities between two primary lactose particles. Nevertheless, the 10% SBS not only was stored in the deep valleys of GL 212-250 μm, but also spread all over the lactose granule surface.

3.3.5 Blending uniformity

One requirement of a good DPI mixture is acceptable homogeneity (low %CV or %RSD) to ensure dosing consistency and consequently uniform therapeutic effect after

aerosol delivery. Blending uniformity of the binary mixtures varied depending upon the drug loading, drug types, and size of granulated lactose (Table 3.3). Firstly, increasing drug loading from 10% to 30% led to a worse mixing homogeneity for both SBS and RIF. Secondly, RIF loaded granule mixtures had a smaller %CV or %RSD and therefore a better blending uniformity than SBS loaded granule mixtures. Last but not the least important, the mixture blending uniformity depends on the multivariate interaction between granulated lactose size fraction and drug loading. As shown from Figure 3.7, granulated lactose with different size fractions presented different blending uniformity trend with the increase of dug loading. For instance, GL 212-250 μm had the best blending uniformity of the evaluated granulated lactose carriers under 10% SBS. With the drug loading increased from 10% to 30% SBS, the blending uniformity decreased significantly. Meanwhile, granulated lactose with larger size fractions, e.g. GL 425-600 μm and GL 850-1000 μm, exhibited an improved blending uniformity with increased SBS loading. When the drug loading was at 30% SBS, GL 212-250 μm had the worst blending homogeneity among all lactose granules, with the coefficient of variation value as high as 16.26%.

3.3.6 Aerosol performance of granulated lactose based formulations

In addition to acceptable mixture homogeneity, another requirement of a good DPI mixture is that the binary mixtures (drug and carrier) should be easily separated into primary components during aerosolization. Therefore, *in vitro* aerosol performance of all mixture blends were evaluated. There are twelve formulations altogether for three grades

of lactose granules, two drug loading (10% and 30%) and two APIs (SBS and RIF). They are A) 10% SBS, GL 212-250 μm, B) 10% SBS, GL 425-600 μm, C) 10% SBS, GL 850-1000 μm, D) 30% SBS, GL 212-250 μm, E) 30% SBS, GL 425-600 μm, F) 30% SBS, GL 850-1000 μm, G) 10% RIF, GL 212-250 μm, H) 10% RIF, GL 425-600 μm, I) 10% RIF, GL 850-1000 μm, J) 30% RIF, GL 212-250 μm, K) 30% RIF, GL 425-600 μm, and M) 30% RIF, GL 850-1000 μm.

In vitro aerosol performance of the twelve formulations was evaluated under three flow rates: 90 L/min, 60 L/min and 30 L/min, respectively. The aerosol performance of these formulations was analyzed in terms of emitted fraction (EF), mass median aerodynamic diameter (MMAD), and fine particle fraction (FPF). As seen in Table 3.4, all formulations had acceptable emitted fraction (> 80%) under 90 L/min flow rate. As the flow rate decreased, the EF decreased accordingly, especially for granulated lactose mixed with 30% SBS, 10% RIF and 30% RIF. The decreased EF comes from increased amount of APIs trapped in the capsule and inhaler devices. Increasing size of lactose granules only compromised the EF under 30 L/min, particularly for GL 850-1000 μm. But whatever flow rate, drug loading and APIs used, the amount of formulation trapped in the capsule increased with increasing of lactose carrier size.

Figure 3.9 showed that MMAD of all formulations followed similar trends with different flow rate and size fraction of granulated lactose. MMAD values decreased significantly for all formulations with increasing flow rate. For instance, from 30L/min to 90L/min, the MMAD of SBS blended formulations decreased from 3.7 ± 0.3 μm to 1.9 ± 0.1 μm. Compared to SBS blended formulations, RIF formulations had an overall

relatively high MMAD. And the MMAD of RIF formulations also had a decreasing trend (30L/min: 5.4 ± 0.3 μm > 60 L/min: 4.7 ± 0.4 μm > 90 L/min: 4.3 ± 0.4 μm) with increased flow rate. Although not as significant as the influence of flow rate, with the size of granulated lactose carrier enlarged, the MMAD decreased for both APIs.

Aerosol performance of all granulated lactose based SBS formulations were flow rate and drug loading dependent. Clearly shown in Figure 3.10A, higher flow rate (90 L/min) produced a higher (1.3 ± 0.1 to 3.6 ± 1.4 fold increase) fine particle fraction of SBS (FPF: 75.4 ± 6.10% at 90 L/min versus 59.1 ± 8.7% at 60 L/min and 21.2 ± 10.0% at 30 L/min). Additionally, compared to 10% SBS loading, 30% SBS generated higher fine particle fraction for all granulated lactose size fractions with the same flow rate (30L/min: 12.6 ± 2.9% vs. 29.7 ± 6.4%, 60 L/min: 51.2 ± 3.7% vs. 67.0 ± 3.0%, and 90 L/min: 69.3 ± 3.5% vs. 81.5 ± 1.6%).

In contrast, the fine particle fraction of RIF formulations were not very flow rate and drug loading dependent. Figure 3.10 B showed that only 10%RIF, GL 425-600 μm and 10%RIF, GL 850-1000 μm had a slight increasing FPF with increasing flow rate. FPF peaked at 30 L/min or 90 L/min of the other four granulated lactose based RIF formulations. The flow rate that produced the smallest FPF was 60 L/min. In SBS formulations, high drug loading (30% SBS) produced higher fine particle fraction than low drug loading (10% SBS) with all flow rates. Unlike SBS, high drug loading of rifampicin (30% RIF) only played a role in increasing FPF than low counterparts (10%RIF) at low flow rate, such as 30 L/min (54.0 ± 6.2% vs. 28.8 ± 8.0%).

Therefore, the effect of granulated lactose size on the fine particle fraction of aerosol formulations depends on the drugs, drug loading and flow rate. With 10% SBS loading, the fine particle fraction of SBS was inversely related with carrier particle size under all the flow rates. However, fine particle fraction of 30%SBS formulations slightly increased with lactose carrier size when 90L/min or 60L/min flow rate was applied. Under the same impaction parameters (90L/min or 60L/min), although fine particle fractions of 30%RIF formulations didn't increase with increasing lactose carrier size, they also didn't decrease with lactose carrier size increasing. Thus, the detrimental influence of large lactose carrier is not an inherent property, which actually relies on APIs, drug loading and flow rate.

3.3.7 Aerosol performance comparison of granulated lactose and primary lactose based formulations under same size fractions

The aerodynamic parameters of granulated lactose were compared to primary lactose under the same size fractions to study the advantage of granulated lactose in formulating high drug loaded DPI formulations. Blended with 30% SBS, the performance of primary lactose (212-250 μm) was worse than that of granulated lactose (GL 212-250 μm). Granulated lactose (GL 212-250 μm) based formulation could be easily fluidized and emptied outside the inhaler device, leading to the highest EF (85.5%) than primary lactose (81.6% and 82.1%). Although the FPF of primary lactose (212-250 μm) and granulated lactose (GL 212-250 μm) was similar, both around 80%, when they were blended with 30% SBS for 10 min, primary lactose (212-250 μm) had a larger standard

deviation (79.0±3.5%) of the fine particle fraction than granulated lactose (80.6±1.1%). The worse dosing uniformity from primary lactose (212-250 μm) could be improved under a longer blending duration, 60 min instead, but at the price of a significantly reduced fine particle fraction (77.0±0.8%).

3.4 DISCUSSION

3.4.1 Laser diffraction analysis and SEM imaging of two micronized APIs

According to laser diffraction data (Figure 3.1), the particle size distribution of SBS was comparable to RIF, with X_{50} both around 5 μm. Although of similar geometric particle size, in fact the morphology and shape of the two APIs as shown in the SEM images (Figure 3.2) were quite different from each other. Additionally, it is interesting to note that most salbutamol sulfate particles were smaller than rifampicin particles under SEM. The discrepancy in size between SEM and laser diffraction could be ascribed to the different cohesiveness of the two drugs. SBS was more cohesive than RIF particles, as demonstrated by a higher surface energy and work of cohesion (Table 3.2). Thus, cohesive SBS particles were more difficult to disperse into single particles than RIF, rendering SBS agglomerates instead of primary particles for laser diffraction analysis. Also, the particle size measured by laser diffraction was equivalent volume diameter, which could not efficiently differentiate particles with different shape and morphology.

3.4.2 Relationship between uniformity and bulk density

It was found that blending uniformity of the high drug loaded and granulated lactose based DPI formulations may be relevant with filling extent of granule cavities by micronized drugs. GL 212-250 μm had the smallest surface roughness and smallest cavity volume to be filled by same amount of micronized drugs. Excessive micronized drugs

may result in poor blending. Same principle could also be applied to the effect of different drug loading on blending homogeneity. With the drug loading amount increasing from 10% to 30%, the blending uniformity of correspondent DPI formulations became worse. As shown in Figure 3.4 and Figure 3.5, the granule cavities (e.g. GL 425-600 μm and GL 850-1000 μm) haven't been filled completely with 10% SBS or 10% RIF, but could be filled completely with 30% SBS or 30% RIF, which potentially increase the excessive micronized drugs outside granule cavities, the tendency of segregation and thus poor blending. Another evidence of the relationship between filling cavity and blending uniformity is the density of drugs. Table 3.3 showed that RIF formulations had relatively better blending uniformity than RIF formulations. The bulk density of SBS was 0.16 ± 0 g/ml and was 0.20 ± 0.01 g/ml of RIF. Since RIF had a higher bulk density than SBS, the cavities of granulated lactose could not be completely filled by 10% RIF, compared to 10% SBS (Figure 3.5). As displayed in Figure 3.6, with same amount of micronized drugs added, RIF particles mostly accumulated in the deep valleys of granulated lactose, but same amount of SBS spread all over the valleys.

GL 850-1000 μm was an exception. In the experiment, only around 35 particles of GL 850-1000 μm mixtures (~20mg) were weighed out for uniformity analysis. As result of small number of particles used, the uniformity test may not qualify statistical analysis.

3.4.3 Aerosol performance

3.4.3.1 Effect of Press-on Forces on Aerosol Performance of High Drug Loaded DPI Formulations

Reduced effectiveness of press-on forces with increasing lactose size fractions could be used to explain the improvement of aerosol redispersion observed with 30% SBS loaded coarsest fraction of granulated lactose at 90L/min. As studied previously, the frequency of impacted friction and inertial press-on force of granular lactose during mixing would not increase significantly with increased granule size, owing to reduced bulk density and not significantly improved flowability[6]. In addition, drugs, including both SBS and RIF, tend to accumulate in cavities of granular lactose, which serve as shelters to prevent effective press-on force from heavy granular lactose during mixing. Nevertheless, with more drugs get filled into the cavities and become contingent with the granular surface, the protective effect of granule cavity from press-on force will not continue indefinitely. Since the roughness of granular lactose increases with increasing size, the cavity volume required to be filled also increases. According to Figure 3.5 and Figure 3.6, higher amount of SBS or RIF were required to completely fill the cavities of granular lactose with larger size fractions (e.g. GL 850-1000 μm), demonstrated also by increased blending uniformity results (Table 3.3). Therefore, with increasing granular size, not only the effective surface area available for press-on effect decreases as discussed in previous research, but effective press-on force also decreases for extremely high drug loaded granular based formulation. Reduced effectiveness of press-on force potentially results in reduced adhesive forces between micronized drugs and lactose carrier surface. It is known that weak adhesive force favors better detachment of micronized drugs from carrier surface and thus an improved aerosol performance. So, the

improved aerosol performance of 30% SBS GL 850-1000 μm (FPF: 82.8±0.7%) at 90 L/min, compared to 30% SBS GL 425-600 μm (FPF: 81.0±2.2%) and especially 30% SBS GL 212-250 μm (FPF: 80.6±1.1%), could be explained to some extent by reduced effectiveness of press-on force. The increased aerosol performance however is not that significant because the increased press-on force for smaller lactose size fraction may not be that significant. For instance with GL 212-250 μm, when the drug loading is extremely large to fill completely the granule valleys, the excessive drugs could be pushed into the valleys to increase the press-on and adhesive forces, but could also be separated from the granule valley due to no more space, which is also confirmed by the reduced blending uniformity of 30% SBS GL 212-250 μm compared to larger lactose counterparts. The increased press-on force with smooth lactose surface could also be confirmed by Table 3.5.

As discussed above, the protective shelter effect of granule cavities from press-on force could be reduced by increased drug amount, so the reduced shelter effect or thus increased press-on force is drug loading dependent. This explained why 10% SBS GL 850-1000 μm generally didn't work as well as 10% SBS GL 212-250 μm. Same reason could also be applied to 10% RIF GL 850-1000 μm and 30% RIF GL 850-1000 μm, since RIF has a higher bulk density than SBS and more RIF would be required to result in increased press-on force for GL 212-250 μm. Additionally, adhesive force is about the interaction between drug particles and lactose valley surface. In the granule valleys, there will be large amount of drug agglomerates not directly contacted with valley surface. Thus, aerosol performance evaluated under high flow rate is more relevant with the different adhesive force.

3.4.3.2 Surface energy

Aerosol performance of traditional lactose based dry powder inhalation formulations has also been predicted by interparticulate interaction analysis using inverse gas chromatography[22]. Higher surface energy of micronized APIs has been correlated with poor aerosol performance, due to a stronger particle interaction between drug and lactose carrier particles, in conventional lactose DPI formulations. In this study, SBS with higher surface energy than RIF led to higher SBS still attached on granulated lactose carriers during impaction studies and thus higher amounts of SBS trapped in the pre-seperator (Table 3.4). Nevertheless, the higher surface energy of SBS didn't correlate to a low aerosol performance anymore in the high drug loaded lactose based formulation, because aerosol performance herein not only is relevant with detachment of micronized drugs from lactose carrier but also with induction port deposition and primary drug particle redispersion.

3.4.3.3 Rifampicin vs. Salbutamol sulfate

Aerosol performance of the high drug loaded granular lactose based dry powder inhalation formulation is drug substance dependent. In this study the fine particle fraction generated from RIF based DPI formulations is much smaller than that from SBS based DPI formulations. The difference came from different particle size, shape and also bulk density of micronized drugs used.

Firstly, different from SBS based formulations, RIF based formulations generated a large amount of drugs deposited in the induction port. Micronized RIF had a higher bulk density, and larger particle size, than micronized SBS particles, which resulted in potential higher particle inertia force. As the drug particles become larger, their response to change in the fluid flow is slower[23]. Consequently, larger particles tend to hit the induction port neck and get trapped inside the induction port. Additionally, as shown in Table 3.4, the aerosol performance (fine particle fraction) of RIB based DPI formulation is less flow rate dependent than SBS based formulation. According to Table 4C and 4D, the amount of micronized RIF trapped in induction port was correlated with flow rate. A higher flow rate resulted in more micronized RIF trapped in induction port. A higher flow rate generally is known to improve fine particle fraction. Therefore, the increased detachment ability at a higher flow rate was counterbalanced by the increased induction trap micronized RIF. Secondly, there is a positive relationship between MMAD and drug particle size. Micronized RIF had a larger particle size and the MMAD was around 4-6 μm. On the other hand, smaller micronized SBS had a MMAD around 2-4 μm. Thus, even if micronized RIF could be detached from granular lactose carrier the same extent as micronized SBS, there will be less micronized RIF be able to deliver to the lung.

3.5 CONCLUSION

Relatively large granulated lactose was evaluated to produce a high drug loading dry powder formulations, which could generate a significant improved fraction of fine particles for inhalation. The aerosol performance of high drug loaded granulated lactose based formulation depends on the lactose size fraction, drug loading and also APIs. More efficient fine particle fraction (FPF) was observed with small size fractions (GL 212-250 μm) at 10% SBS. However, when the drug loading was increased to 30%, the large size fraction (GL 850-1000 μm) had a better aerosol performance. The roughness of the granulated lactose was found to increase with increasing lactose size. Therefore, the driving mechanism behind these findings perhaps is because larger lactose carriers with relatively rougher surface could 'shelter' more SBS drug particles from press-on forces than smooth counterparts. Nevertheless, RIF based high drug loaded formulation didn't follow the same rules as SBS. RIF had a less flow rate and lactose size fraction dependent performance than SBS, due to a different drug particle shape, and bulk density.

3.6 TABLES

Table 3.1 Particle size distributions of the APIs (n >3)

APIs	X_{10} (µm)	X_{50} (µm)	X_{90} (µm)
Salbutamol sulfate (SBS)	1.21 (0.08)	4.31 (0.24)	13.28 (2.21)
Rifampicin (RIF)	1.09 (0.05)	4.17 (0.13)	8.63 (0.54)

Table 3.2 Surface energy parameters of micronized salbutamol sulfate and micronized rifampicin measured by inverse gas chromatography

	γ_d (mJ/m^2)	γ_{ab} (mJ/m^2)	γ_t (mJ/m^2)	W_{coh} (Dispersive)	W_{coh} (Specific)	W_{coh} (Total)
Salbutamol sulfate	57.95	4.40	62.35	115.91	8.80	124.70
Rifampicin	26.70	2.92	29.62	53.40	5.85	59.25

Table 3.3 Content uniformity of salbutamol sulfate/rifampicin blended with different granulated lactose carriers

(A) Average content in salbutamol sulfate (% w/w) for the different blends.

Lactose Grade	Drug in the blend (% w/w)	CV (%)
10% Salbutamol sulfate		
GL 212-250 μm	8.12 (0.34)	4.19
GL 425-600 μm	7.56 (0.17)	2.30
GL 850-1000 μm	7.13 (0.33)	4.61
30% Salbutamol sulfate		
GL 212-250 μm	38.68 (6.29)	16.26
GL 425-600 μm	25.53 (0.59)	2.33
GL 850-1000 μm	26.82 (2.34)	8.70

(B) Average content in rifampicin (% w/w) for the different blends.

Lactose Grade	Drug in the blend (% w/w)	CV (%)
10% Rifampicin		
GL 212-250 μm	6.90 (0.46)	6.61
GL 425-600 μm	7.50 (0.10)	1.27
GL 850-1000 μm	7.42 (0.24)	3.20
30% Rifampicin		
GL 212-250 μm	25.46 (1.02)	4.02
GL 425-600 μm	25.34 (0.99)	3.90
GL 850-1000 μm	22.39 (1.17)	5.22

Table 3.4 Effect of APIs, drug loading, carrier size, and flow rate on the aerosolization of adhesive mixture dry powder formulations: (A) 10% salbutamol sulfate, (B) 30% salbutamol sulfate, (C) 10% rifampicin, (D) 30% rifampicin (values are means ± SD, n = 3).

(A)	Cap (%)	Device (%)	EF (%)	FPF (%)	RF (%)	MMAD (μm)	PRE (%)	Port (%)
90 L/min, 10% SBS								
GL 212-250 μm	1.3 (0.2)	16.7 (1.4)	82.1 (1.5)	73.3 (1.0)	60.1 (0.5)	1.9 (0.1)	17.3 (1.2)	6.3 (0.3)
GL 425-600 μm	1.7 (0.6)	16.1 (2.8)	82.2 (3.4)	67.9 (2.8)	55.9 (4.5)	1.8 (0.0)	22.8 (0.8)	5.8 (0.4)
GL 850-1000 μm	2.0 (0.6)	11.9 (2.0)	86.1 (1.9)	66.9 (2.1)	57.6 (1.5)	1.7 (0.0)	23.2 (1.7)	7.1 (0.7)
60 L/min, 10% SBS								
GL 212-250 μm	1.1 (0.2)	23.0 (0.7)	75.9 (0.9)	51.9 (1.6)	39.4 (1.6)	2.1 (0.1)	34.6 (1.1)	6.5 (0.4)
GL 425-600 μm	1.0 (0.0)	20.0 (1.3)	79.0 (1.3)	47.0 (1.3)	37.1 (0.4)	2.0 (0.1)	42.0 (1.8)	5.4 (0.8)
GL 850-1000 μm	2.2 (0.4)	17.5 (1.3)	80.3 (1.0)	54.7 (2.2)	43.9 (1.8)	2.0 (0.0)	37.2 (1.4)	5.5 (0.5)
30 L/min, 10% SBS								
GL 212-250 μm	0.6 (0.1)	17.7 (4.6)	81.7 (4.5)	14.1 (3.7)	11.4 (2.5)	3.4 (0.1)	75.3 (5.2)	6.7 (0.7)
GL 425-600 μm	0.5 (0.2)	12.6 (0.2)	86.8 (0.4)	12.1 (3.7)	10.5 (3.2)	3.6 (0.3)	77.7 (4.6)	5.5 (0.8)
GL 850-1000 μm	6.6 (5.5)	18.8 (3.3)	74.6 (8.3)	11.7 (1.2)	8.7 (0.4)	3.4 (0.1)	80.5 (2.2)	4.6 (0.6)

Table 3.4 Effect of APIs, drug loading, carrier size, and flow rate on the aerosolization of adhesive mixture dry powder formulations: (A) 10% salbutamol sulfate, (B) 30% salbutamol sulfate, (C) 10% rifampicin, (D) 30% rifampicin (values are means ± SD, n = 3). (Continued)

(B)	Cap (%)	Device (%)	EF (%)	FPF (%)	RF (%)	MMAD (μm)	PRE (%)	Port (%)
90 L/min, 30% SBS								
GL 212-250 μm	0.9 (0.2)	13.6 (2.1)	85.5 (2.2)	80.6 (1.1)	68.9 (1.0)	2.1 (0.1)	8.7 (0.3)	7.1 (0.9)
GL 425-600 μm	0.7 (0.2)	17.2 (0.7)	82.1 (0.5)	81.0 (2.2)	66.5 (2.2)	2.0 (0.1)	7.9 (0.8)	7.6 (1.0)
GL 850-1000 μm	1.0 (0.2)	18.4 (1.4)	80.6 (1.6)	82.8 (0.7)	66.8 (1.8)	1.9 (0.0)	7.3 (0.1)	6.6 (0.5)
60 L/min, 30% SBS								
GL 212-250 μm	1.1 (0.4)	28.7 (11.3)	70.2 (11.3)	66.0 (4.2)	46.3 (7.6)	2.3 (0.1)	15.6 (1.2)	7.5 (1.6)
GL 425-600 μm	1.5 (0.2)	29.2 (3.5)	69.3 (3.4)	65.7 (2.4)	45.6 (3.9)	2.2 (0.0)	16.6 (0.1)	7.5 (0.1)
GL 850-1000 μm	2.1 (1.2)	24.2 (6.0)	73.8 (6.4)	69.2 (1.1)	51.0 (3.6)	2.1 (0.1)	14.1 (1.2)	7.2 (0.1)
30 L/min, 30% SBS								
GL 212-250 μm	0.9 (0.0)	30.9 (4.1)	68.2 (4.1)	35.9 (3.0)	24.5 (3.3)	4.0 (0.2)	40.3 (0.5)	10.7 (0.3)
GL 425-600 μm	0.4 (0.1)	28.3 (1.2)	71.3 (1.3)	22.2 (1.7)	15.8 (1.3)	3.9 (0.1)	55.4 (2.9)	12.1 (1.6)
GL 850-1000 μm	24.1 (17.8)	29.0 (2.4)	46.8 (15.8)	31.2 (2.0)	14.7 (5.7)	4.0 (0.1)	42.9 (1.8)	8.3 (1.8)

Table 3.4 Effect of APIs, drug loading, carrier size, and flow rate on the aerosolization of adhesive mixture dry powder formulations: (A) 10% salbutamol sulfate, (B) 30% salbutamol sulfate, (C) 10% rifampicin, (D) 30% rifampicin (values are means ± SD, n = 3). (Continued)

(C)	**Cap (%)**	**Device (%)**	**EF (%)**	**FPF (%)**	**RF (%)**	**MMAD (μm)**	**PRE (%)**	**Port (%)**
90 L/min, 10% RIF								
GL 212-250 μm	2.3 (0.6)	12.5 (0.9)	85.3 (1.5)	44.6 (2.4)	38.0 (2.3)	4.4 (0.2)	10.7 (1.3)	24.8 (1.2)
GL 425-600 μm	2.1 (0.4)	12.1 (0.9)	85.8 (1.2)	41.2 (0.9)	35.3 (0.9)	3.9 (0.2)	15.3 (0.1)	26.7 (1.0)
GL 850-1000 μm	2.4 (0.6)	13.0 (1.6)	84.6 (1.6)	43.2 (1.6)	36.6 (1.9)	3.9 (0.1)	13.9 (2.1)	26.4 (0.6)
60 L/min, 10% RIF								
GL 212-250 μm	3.6 (0.1)	15.6 (1.4)	80.8 (1.4)	33.5 (1.2)	27.1 (1.2)	5.0 (0.4)	14.5 (0.8)	16.4 (0.5)
GL 425-600 μm	3.2 (1.0)	15.1 (3.1)	81.7 (2.5)	31.5 (1.5)	25.7 (0.4)	4.4 (0.1)	24.5 (2.1)	15.0 (0.3)
GL 850-1000 μm	3.8 (0.1)	19.9 (2.3)	76.3 (2.3)	33.2 (2.0)	25.3 (1.5)	4.2 (0.2)	22.6 (4.0)	14.1 (0.7)
30 L/min, 10% RIF								
GL 212-250 μm	7.4 (2.2)	19.0 (5.2)	73.7 (3.3)	37.7 (3.1)	27.7 (1.1)	5.5 (0.4)	38.5 (3.5)	4.3 (0.9)
GL 425-600 μm	4.9 (1.0)	15.4 (2.2)	79.7 (2.4)	25.7 (3.8)	20.4 (2.4)	5.1 (0.2)	59.7 (5.5)	3.4 (0.3)
GL 850-1000 μm	10.8 (0.3)	19.8 (3.2)	69.4 (2.9)	23.0 (6.9)	15.8 (4.1)	5.2 (0.1)	62.1 (9.3)	3.6 (0.5)

Table 3.4 Effect of APIs, drug loading, carrier size, and flow rate on the aerosolization of adhesive mixture dry powder formulations: (A) 10% salbutamol sulfate, (B) 30% salbutamol sulfate, (C) 10% rifampicin, (D) 30% rifampicin (values are means ± SD, n = 3). (Continued)

(D)	**Cap (%)**	**Device (%)**	**EF (%)**	**FPF (%)**	**RF (%)**	**MMAD (μm)**	**PRE (%)**	**Port (%)**
90 L/min, 30% RIF								
GL 212-250 μm	0.4 (0.1)	9.3 (2.0)	90.3 (1.9)	42.8 (4.8)	38.6 (4.6)	4.9 (0.2)	6.4 (0.1)	31.8 (4.4)
GL 425-600 μm	0.4 (0.1)	13.7 (8.2)	86.0 (8.2)	42.8 (2.3)	36.9 (5.3)	4.4 (0.2)	5.7 (0.0)	31.5 (2.0)
GL 850-1000 μm	0.5 (0.1)	9.5 (0.9)	90.0 (0.9)	42.3 (1.5)	38.1 (1.6)	4.2 (0.1)	6.9 (0.9)	33.2 (0.8)
60 L/min, 30% RIF								
GL 212-250 μm	0.6 (0.1)	17.8 (2.0)	81.6 (2.0)	37.4 (3.4)	30.5 (3.5)	4.9 (0.3)	5.6 (0.4)	17.8 (0.7)
GL 425-600 μm	0.7 (0.3)	16.0 (0.8)	83.3 (0.5)	37.5 (1.1)	31.3 (1.0)	4.8 (0.4)	5.7 (0.5)	19.3 (3.1)
GL 850-1000 μm	0.7 (0.2)	16.7 (1.5)	82.6 (1.3)	37.6 (1.0)	31.0 (1.1)	4.6 (0.2)	6.0 (0.3)	20.4 (2.1)
30 L/min, 30% RIF								
GL 212-250 μm	1.1 (0.4)	21.2 (0.8)	77.6 (1.1)	59.2 (0.9)	46.0 (1.1)	5.6 (0.1)	6.8 (0.5)	7.4 (0.7)
GL 425-600 μm	1.0 (0.1)	24.6 (2.0)	74.4 (1.9)	54.7 (7.8)	40.7 (6.5)	5.6 (0.1)	13.7 (8.8)	7.0 (0.7)
GL 850-1000 μm	5.4 (5.3)	26.1 (1.6)	68.6 (5.9)	48.2 (1.2)	33.1 (3.6)	5.7 (0.1)	20.7 (0.7)	7.1 (0.5)

Table 3.5 Aerodynamic parameters between primary lactose and granulated lactose at same size fractions.

	Time (min)	**EF (%)**	**FPF (%)**	**RF (%)**	**MMAD (μm)**	**PRE (%)**
90 L/min, 30% SBS						
GL 212-250 μm	10 min	85.5 (2.2)	80.6 (1.1)	68.9 (1.0)	2.1 (0.1)	8.7 (0.3)
P 212-250 μm	10 min	81.6 (2.8)	79.0 (3.5)	64.5 (4.1)	2.0 (0.1)	10.1 (1.8)
P 212-250 μm	60 min	82.1 (2.4)	77.0 (0.8)	63.2 (1.9)	2.1 (0.1)	11.3 (0.8)

3.7 FIGURES

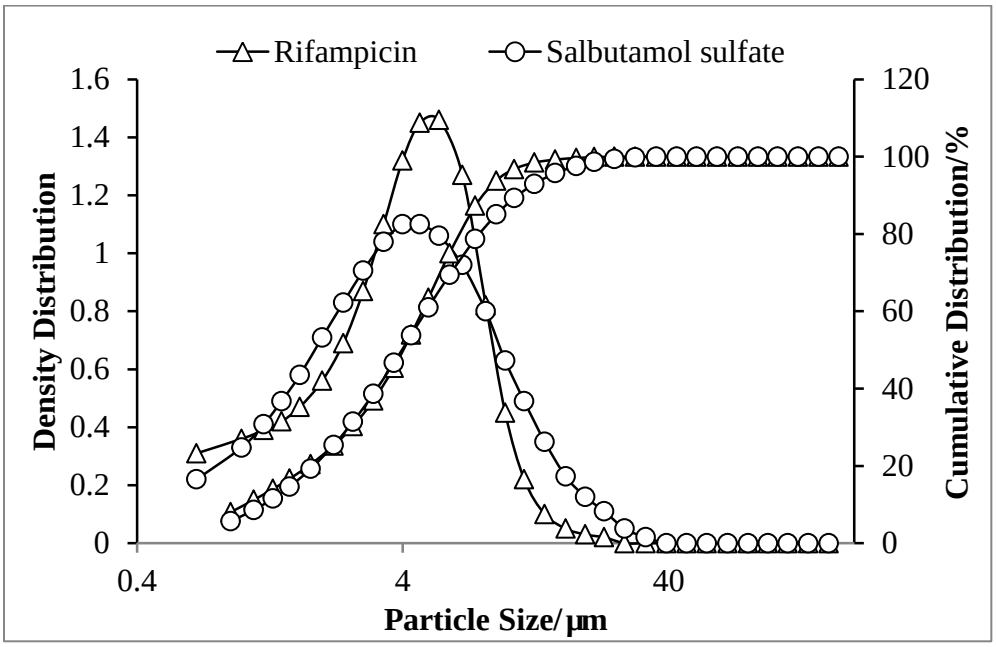

Figure 3.1 Particle size distribution of micronized salbutamol sulfate and micronized rifampicin

(A)

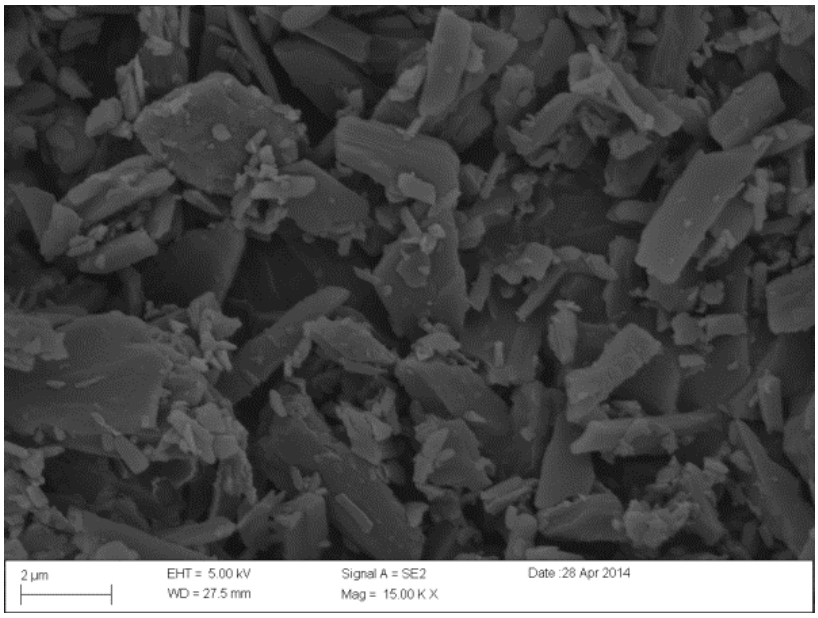

(B)

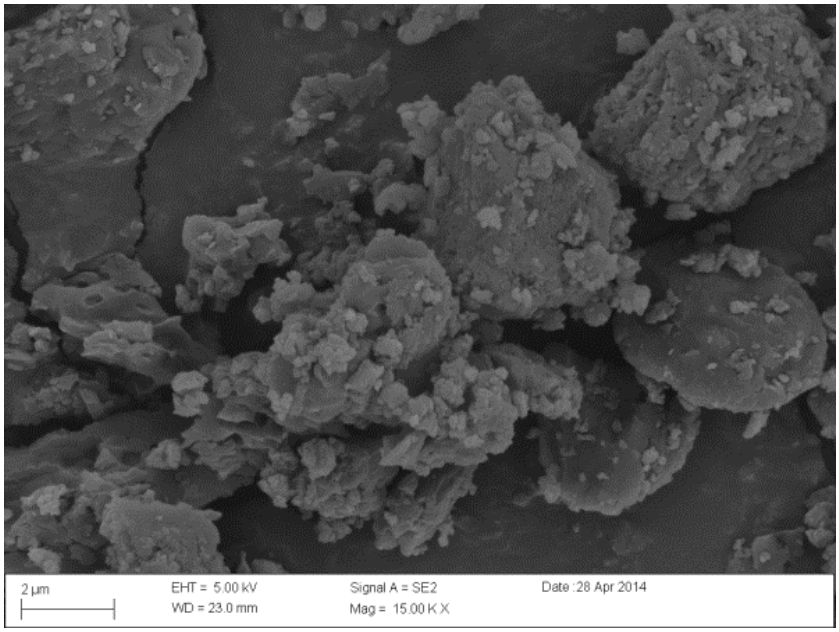

Figure 3.2 SEM of (A) micronized salbutamol sulfate and (B) micronized rifampicin

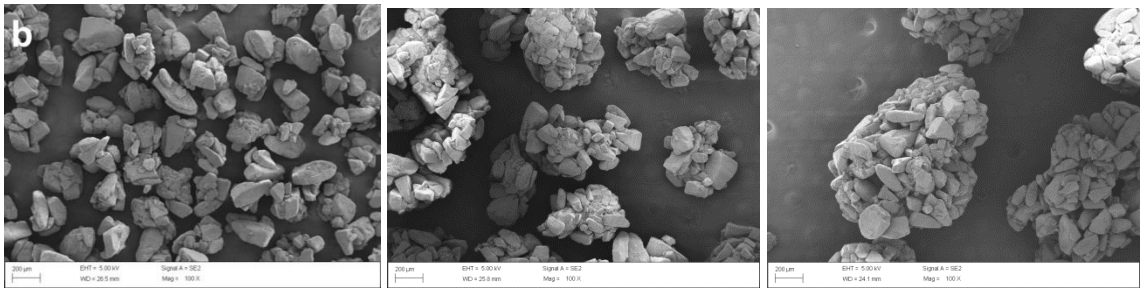

Figure 3.3 SEM micrographs of (a) Pharmatose 100M, (b) GL 212-250 µm granulated lactose, (c) GL 425-600 µm granulated lactose, (d) GL 850-1000 µm granulated lactose sieve fractions. Scale bars denote 200 µm.

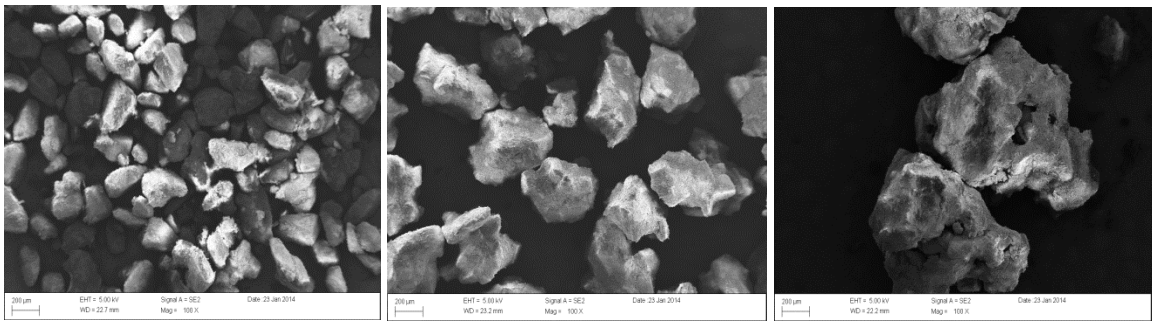

(A) **(B)** **(C)**

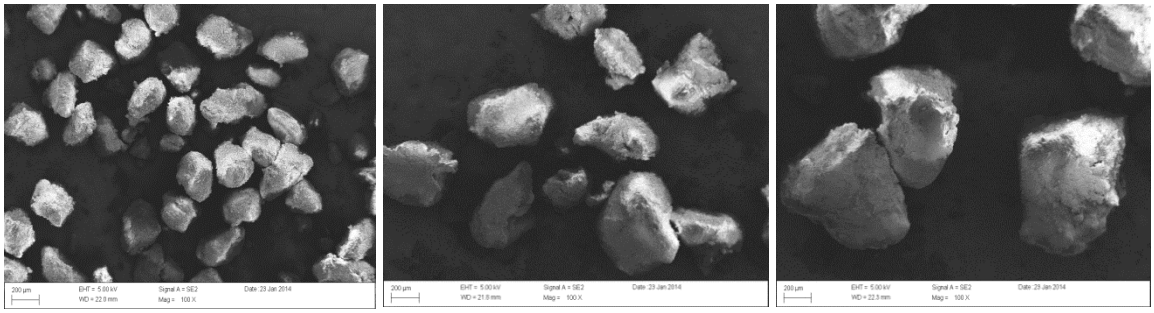

(D) **(E)** **(F)**

Figure 3.4 SEM micrographs of micronized salbutamol sulfate (SBS) and granulated lactose mixtures: A) 10% SBS, GL 212-250 μm, B) 10% SBS, GL 425-600 μm, C) 10% SBS, GL 850-1000 μm, D) 30% SBS, GL 212-250 μm, E) 30% SBS, GL 425-600 μm, F) 30% SBS, GL 850-1000 μm.

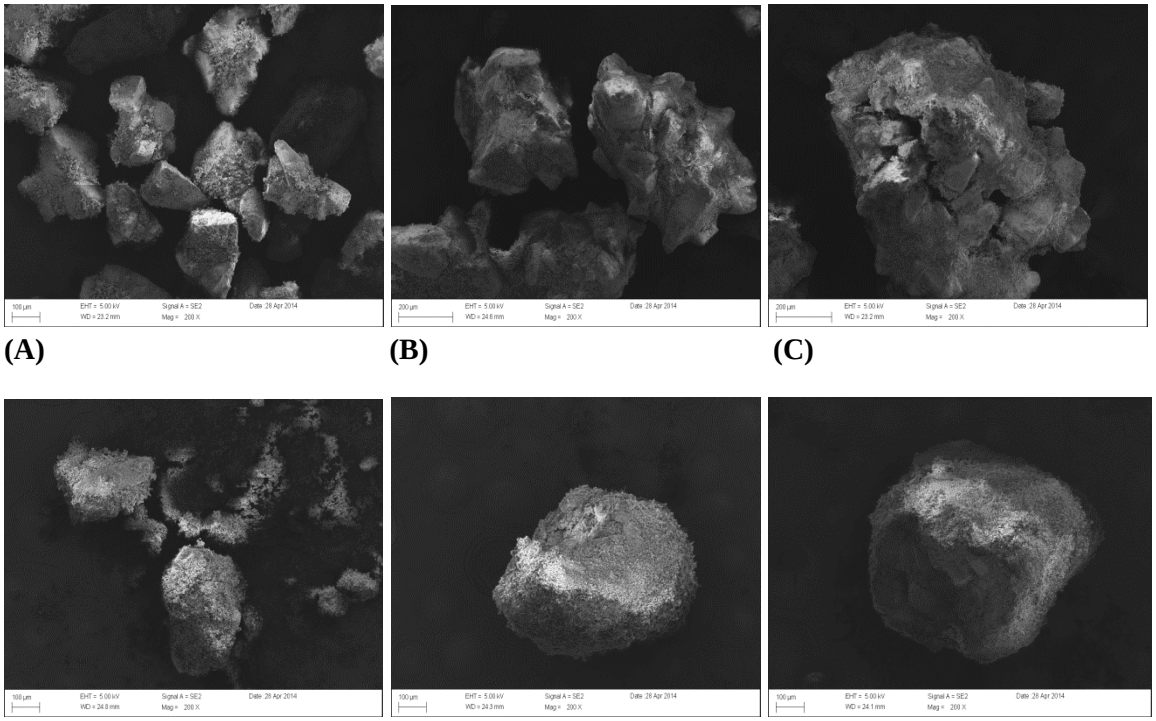

Figure 3.5 SEM micrographs of micronized rifampicin and granulated lactose mixtures: A) 10% RIF GL 212-250 μm, B) 10% RIF, GL 425-600 μm, C) 10% RIF, GL 850-1000 μm, D) 30% RIF, GL 212-250 μm, E) 30% RIF, GL 425-600 μm, F) 30% RIF, GL 850-1000 μm.

(A)

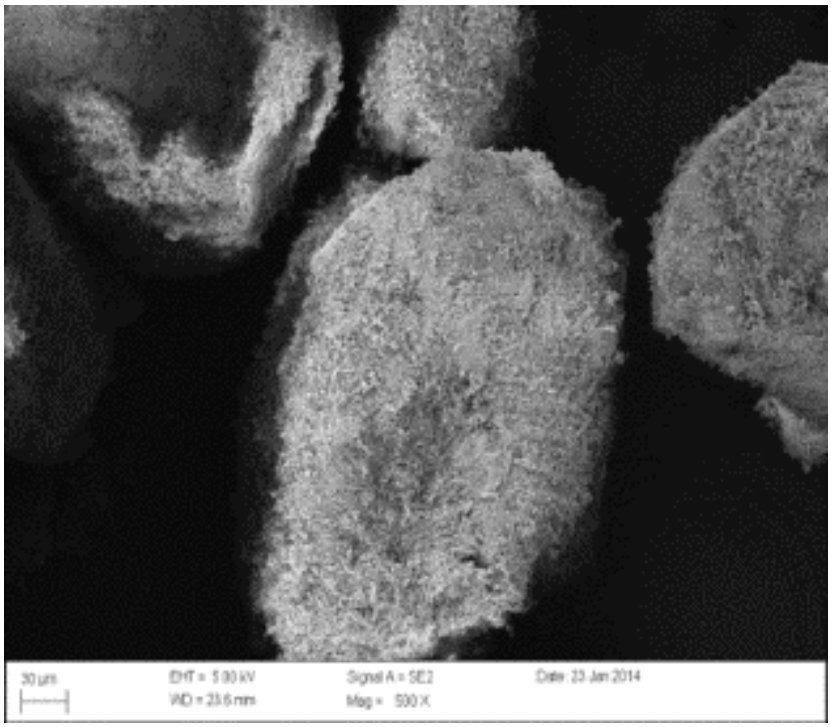

(B)

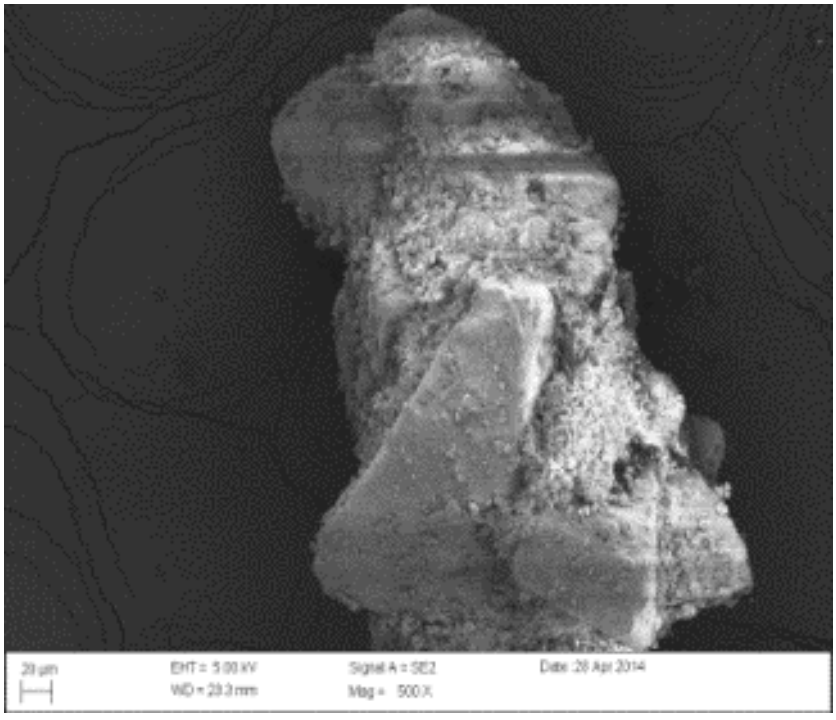

Figure 3.6 (A) 10% SBS, G100M 212-250, (B) 10% RIF, G100M 212-250

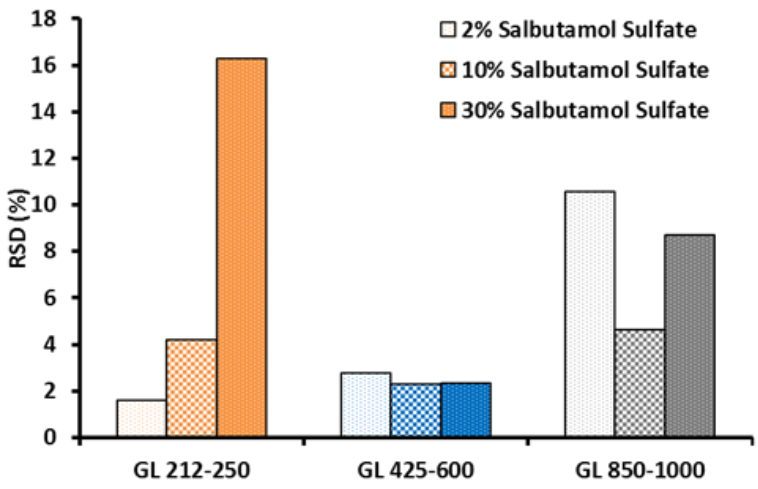

Figure 3.7 Content uniformity of 2%, 10% and 30% Salbutamol Sulfate and granulated lactose with different size fractions.

(A)

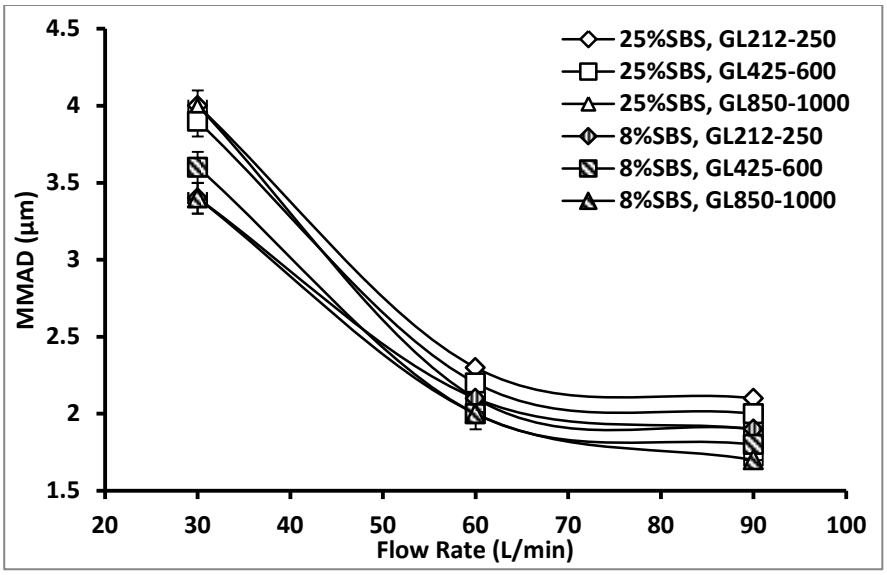

(B)

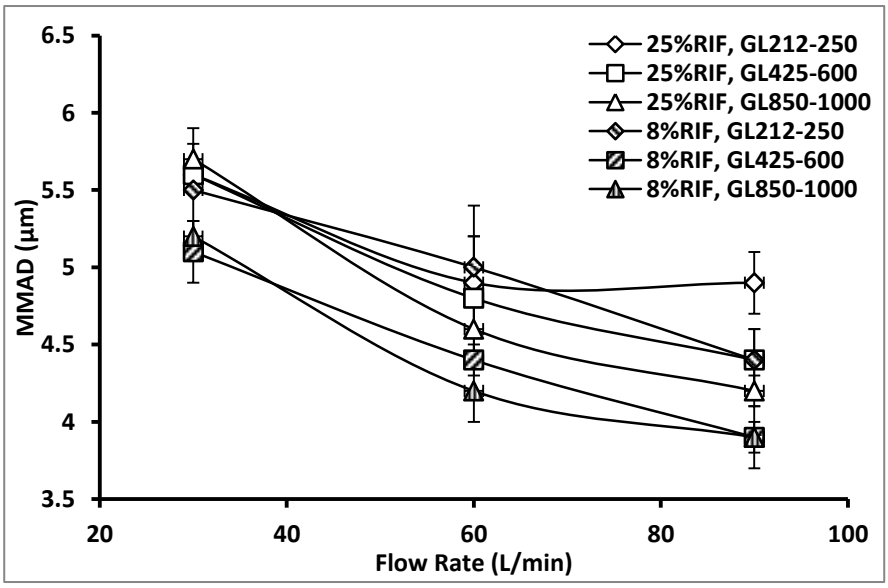

Figure 3.8 MMAD of A) SBS formulations; and B) RIF formulations under different flow rate and lactose granule size fractions.

(A)

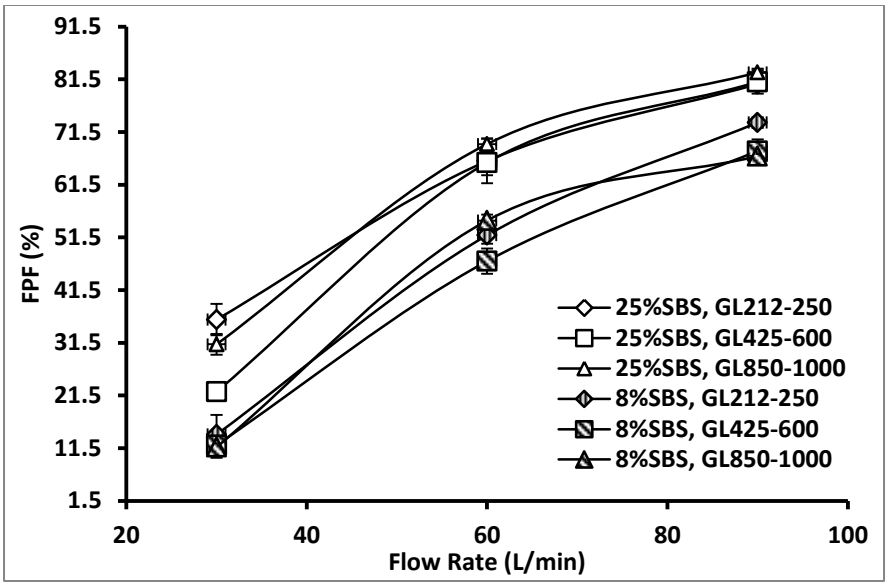

(B)

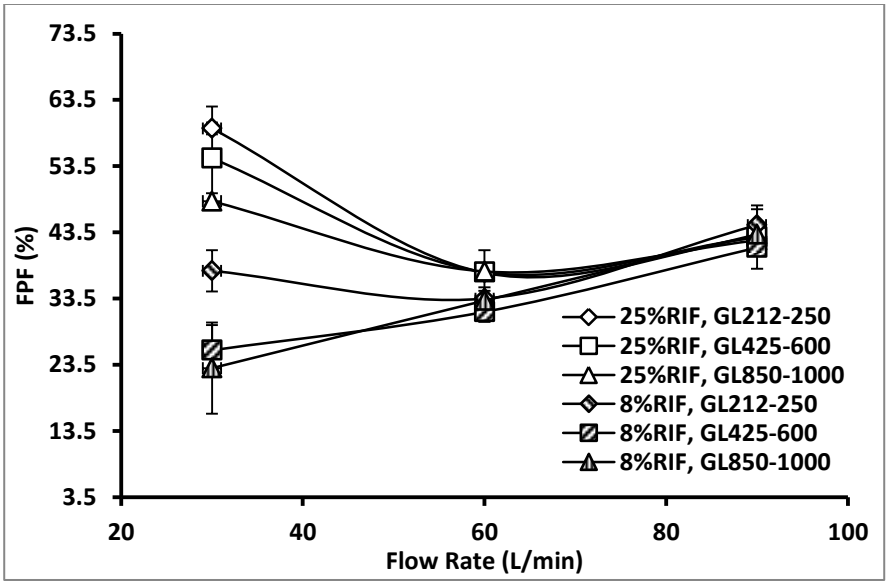

Figure 3.9 Fine particle fraction (FPF) of A) SBS formulations; and B) RIF formulations versus flow rate.

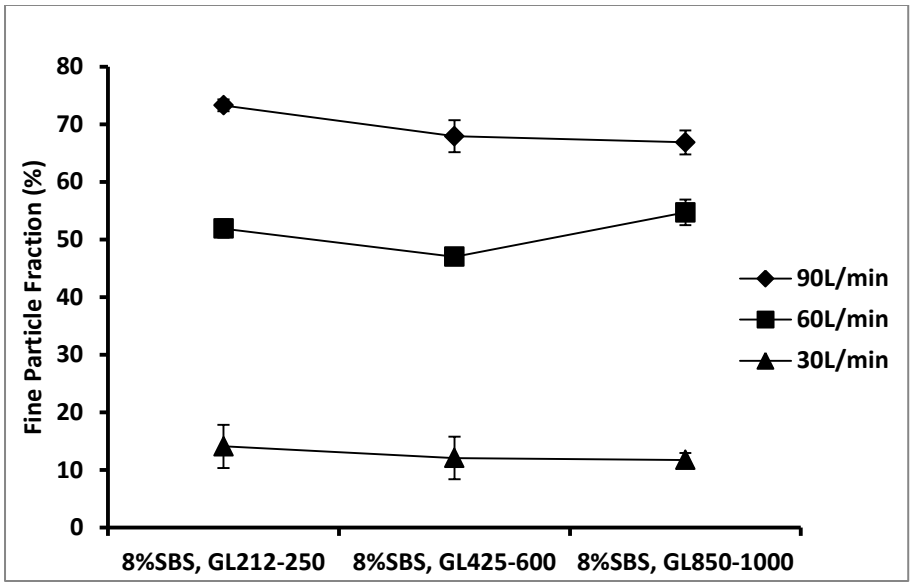

(A)

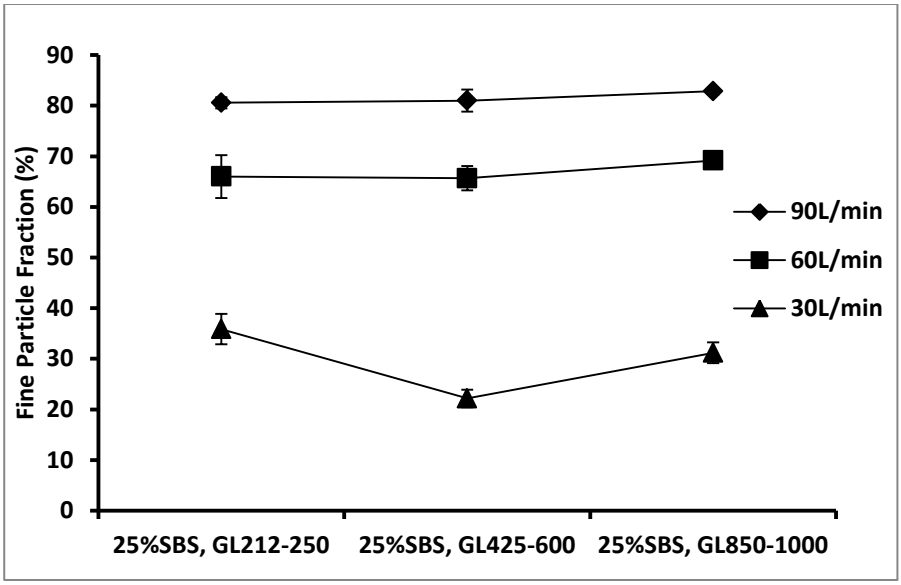

(B)

Figure 3.10 Fine particle fraction (FPF) of (A) 10% salbutamol sulfate, B) 30% salbutamol sulfate, (C) 10% rifampicin, (D) 30% rifampicin formulations versus lactose granule size fractions.

(C)

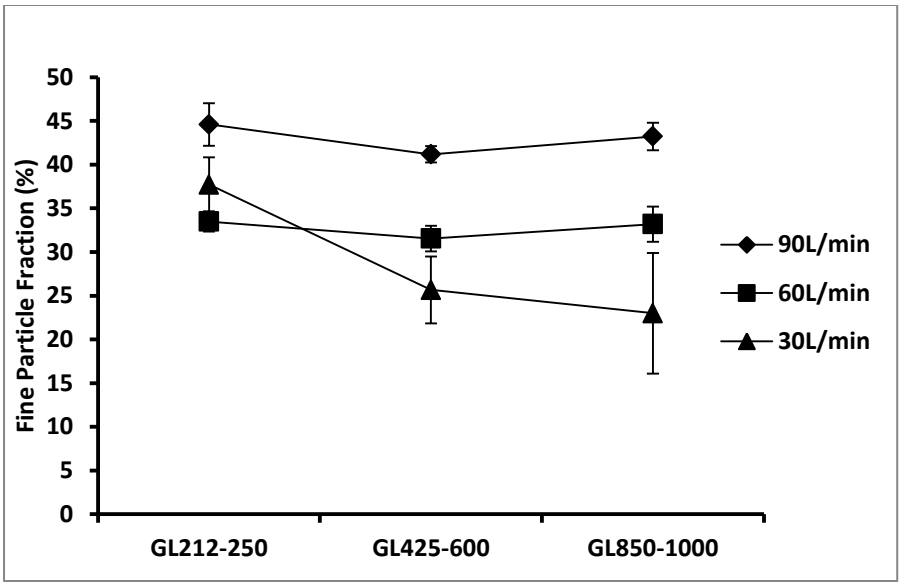

(D)

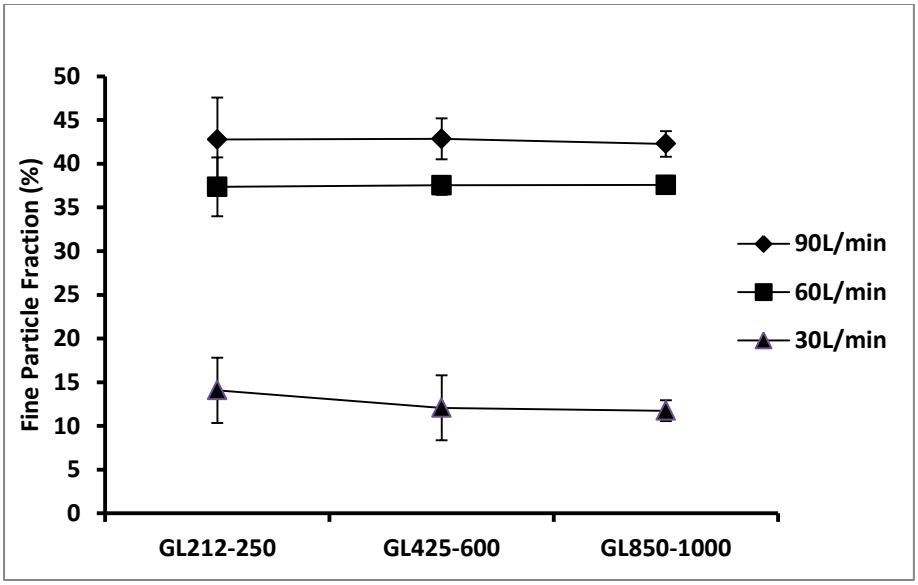

Figure 3.10 Fine particle fraction (FPF) of (A) 10% salbutamol sulfate, B) 30% salbutamol sulfate, (C) 10% rifampicin, (D) 30% rifampicin formulations versus lactose granule size fractions. (Continued)

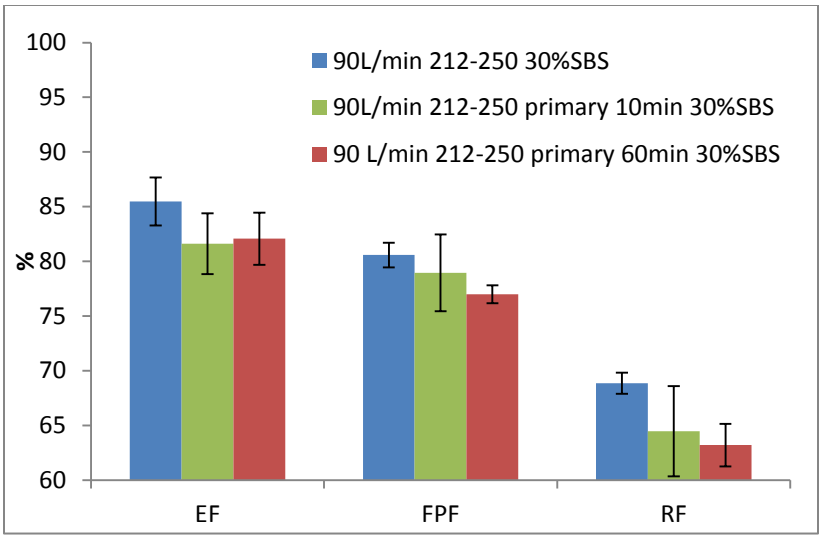

Figure 3.11 Aerodynamic parameters between primary lactose and granulated lactose at same size fractions.

3.8 REFERENCES

1. Son YJ, Longest PW, Tian G, Hindle M. 2013. Evaluation and modification of commercial dry powder inhalers for the aerosolization of a submicrometer excipient enhanced growth (EEG) formulation. Eur J Pharm Sci. 49:390-9.

2. Littringer EM, Mescher A, Schroettner H, Achelis L, Walzel P, Urbanetz NA. 2012. Spray dried mannitol carrier particles with tailored surface properties--the influence of carrier surface roughness and shape. Eur J Pharm Biopharm. 82:194-204.

3. Pilcer G, Wauthoz N, Amighi K. 2012. Lactose characteristics and the generation of the aerosol. Adv Drug Deliv Rev. 64:233-56.

4. Adi H, Larson I, Stewart PJ. 2007. Adhesion and redistribution of salmeterol xinafoate particles in sugar-based mixtures for inhalation. Int J Pharm. 337:229-38.

5. Steckel H, Muller BW. 1997. In vitro evaluation of dry powder inhalers .2. Influence of carrier particle size and concentration on in vitro deposition. Int J Pharm. 154:31-7.

6. Du P, Du J, Smyth HD. 2014. Evaluation of Granulated Lactose as a Carrier for DPI Formulations 1: Effect of Granule Size. AAPS PharmSciTech.

7. Donovan MJ, Smyth HD. 2010. Influence of size and surface roughness of large lactose carrier particles in dry powder inhaler formulations. Int J Pharm. 402:1-9.

8. Podczeck F. 1996. Assessment of the mode of adherence and the deformation characteristics of micronized particles adhering to various surfaces. Int J Pharm. 145:65-76.

9. Rhodes M. Introduction to Particle Technology. New York, NY: John Wiley & Sons Ltd, ; 1998.

10. Le VN, Hoang Thi TH, Robins E, Flament MP. 2012. Dry powder inhalers: study of the parameters influencing adhesion and dispersion of fluticasone propionate. AAPS PharmSciTech. 13:477-84.

11. Schulze D. Powders and Bulk Solids. Behavior, Characterization, Storage and Flow: Springer; 2007.

12. Kaialy W, Alhalaweh A, Velaga SP, Nokhodchi A. 2012. Influence of lactose carrier particle size on the aerosol performance of budesonide from a dry powder inhaler. Powder Technology. 227:74-85.

13. Young PM, Wood O, Ooi J, Traini D. 2011. The influence of drug loading on formulation structure and aerosol performance in carrier based dry powder inhalers. Int J Pharm. 416:129-35.

14. Kaialy W, Ticehurst M, Nokhodchi A. 2012. Dry powder inhalers: mechanistic evaluation of lactose formulations containing salbutamol sulphate. Int J Pharm. 423:184-94.

15. Song M, Li N, Tiedt LR, Degennaro MD, de Villiers MM. 2010. Preparation and characterization of highly porous direct compression carrier particles with improved drug loading during an interactive mixing process. AAPS PharmSciTech. 11:698-707.

16. Kawashima Y, Serigano T, Hino T, Yamamoto H, Takeuchi H. 1998. Effect of surface morphology of carrier lactose on dry powder inhalation property of pranlukast hydrate. 172:188.

17. Li J, Tao L, Buckley D, Tao J, Gao J, Hubert M. 2013. The Effect of the Physical State of Binders on High-Shear Wet Granulation and Granule Properties: A Mechanistic Approach to Understand the High-Shear Wet Granulation Process. Part IV. The Impact of Rheological State and Tip-speeds. J Pharm Sci. 102:4384-94.

18. Fujiwara M, Dohi M, Otsuka T, Yamashita K, Sako K. 2013. Influence of binder droplet dimension on granulation rate during fluidized bed granulation. Chem Pharm Bull (Tokyo). 61:320-5.

19. Ogawa T, Uchino T, Takahashi D, Izumi T, Otsuka M. 2012. Pharmaceutical production of tableting granules in an ultra-small-scale high-shear granulator as a pre-formulation study. Drug Dev Ind Pharm. 38:1390-3.

20. Mangwandi C, Adams MJ, Hounslow MJ, Salman AD. 2012. An investigation of the influence of process and formulation variables on mechanical properties of high shear granules using design of experiment. Int J Pharm. 427:328-36.

21. Tay T, Das S, Stewart P. 2010. Magnesium stearate increases salbutamol sulphate dispersion: what is the mechanism? Int J Pharm. 383:62-9.

22. Tong HH, Shekunov BY, York P, Chow AH. 2006. Predicting the aerosol performance of dry powder inhalation formulations by interparticulate interaction analysis using inverse gas chromatography. J Pharm Sci. 95:228-33.

23. Donovan MJ, Kim SH, Raman V, Smyth HD. 2012. Dry powder inhaler device influence on carrier particle performance. J Pharm Sci. 101:1097-107.

Chapter 4: Effect of Device Design on Dispersion Performance of Granulated Lactose Based DPI formulations

Abstract

Purpose: The aim of this study was to evaluate and modify commercial dry powder inhalers (DPIs) Aerolizer® for significantly large granulated lactose based DPI formulations. Methods: Granulated lactose (GL) with size fraction of 300-450 µm was selected to blend with micronized salbutamol sulfate (SS) to obtain a 2% binary mixtures. Firstly, the effect of capsule and capsule piercing size was evaluated. Three different capsule piercing sizes were used, A), four holes (0.6 mm): $Cap_{4,0.6\ mm}$, B), one piercing hole (1.2 mm): $Cap_{1,1.2\ mm}$ and C), one piercing hole (1.5 mm): $Cap_{1,1.5\ mm}$ at each end of the VCaps HPMC capsule. The commercial Aerolizer® was then modified in terms of tube length, tube width, tube geometry, inlet airway and grid size of the mesh. These devices were designed by Autodesk Inventor and manufactured by W M Keck Center for 3D Innovation. The *in vitro* aerosol performance of all the modified inhaler devices was investigated through NGI (Next Generation Impactor), with flow rates corresponding to 4 kPa pressure drop and 4 L air volume. EF (Emitted Fraction), FPF (Fine Particle Fraction) of the impaction studies with different modified devices were calculated and compared. Drug content deposited on the NGI system was assessed via UV–vis absorption spectroscopy at 230 nm. Results: The smallest capsule piercing ($Cap_{4,0.6\ mm}$) had the worst EF and FPF compared to larger ones ($Cap_{1,1.2}$, $Cap_{1,1.5}$), while $Cap_{1,1.2}$ provided the

smallest standard deviation of the aerosol performance. The modification of the commercial Aerolizer geometry, except for 2/3 inner tube width and 1/3 inlet air, merely slightly altered the in vitro aerosol performance of the granulated lactose based formulation. 2/3 inner tube width had a significantly lower aerosol performance (FPF) compared to all the other modified devices. 1/3 inlet air, however, increased the aerosol performance (FPF) significantly among all the modified devices. Reduced air inlet and bent inhaler tube have synergy effect and could improve the aerosol performance of the model formulation further. Conclusion: Modification of commercial available devices could potentially maximize granulated lactose based DPI formulations.

Keywords

DPI formulations; Granulated lactose; Device, Aperture Size, Device Geometry

4.1 INTRODUCTION

Dry powder inhaler (DPI) has become extensively popular in the last decade, serving as an efficient vehicle to deliver therapeutic agents to the lung.[1] This has led to a rapid growth in dry powder aerosol delivery systems with defined characteristics to produce optimal respirable particles.[2-5] DPIs have many advantages over pMDIs and nebulizers. DPIs are very stable, very portable, patient friendly and easy to use. Different from pMDIs, DPIs avoid propellant gas and the need for coordination with inhalation and actuation.[6] An ideal DPI should be cost effective, simple to use, easy to carry, accurate with uniform dose delivery, delivery high respirable fraction with optimal aerodynamic size, and low flow rate dependency.[7] In fact, DPI is a much complex system, and the performance of DPI depends on many variables including the physicochemical properties of the powder formulation, device design and the patient's inspiratory effort.[8, 9]

Right now, DPIs are frequently formulated into binary mixtures of micronized drugs with a large population of coarse lactose carriers. As the key component of DPI formulations, extensive research has been performed to study the physico-chemical properties of lactose carriers, on the aerosolization of DPIs.[10-15] It was agreed on by most literatures that lactose with small size (size around 60-90 μm with addition of fine lactose, smaller than 5 μm) especially with smooth surface is preferred to maximize aerosol performance. [16-20] Although lactose with small size favors aerosol performance, the addition of fine lactose particles is detrimental to the flowability, blending uniformity and dosing consistency of the whole formulation.[21] Our lab recently found that poor aerosolization performance is not an inherent property to large size (>200 μm) of lactose

carriers.[12, 22] This is because of the interplay between DPI formulation and inhaler device, which causes the major detachment mechanism switched from flow-based detachment (lift and drag) for carrier particles with small size and minimal surface roughness, to impaction-based detachment as carrier particle size and roughness increase (inertial separation forces).[8, 23] Our previous work have already developed several granulated lactose based DPI formulations with improved aerosol performance, without adversely influencing flowability and dosing consistency.[22]

Another potential way to enhance dispersion performance is optimizing the device design, which is critical to the redispersion of the DPI formulations. Merely small modifications in Aerolizer® device design cause significant variation in deagglomeration and aerosolization.[24-28] Nevertheless, to the best knowledge of the author, there is no study performed to evaluate the impact of modifications of Aerolizer® device on the aerosol performance of granulated lactose based DPI formulations. It is hypothesized that the aerodynamic behavior of granulated lactose carrier particles can vary significantly based on the different design of the inhaler device (Aerolizer®). Accordingly, in this study, we have built on previous work and assess the effect of presence of capsule, capsule piercing size, device geometry, grid structure and air inlet passage on aerosol performance of a standard granulated lactose based formulation. The drug used in this study is salbutamol sulfate. Salbutamol sulfate, belonging to short acting beta receptor agonist, alleviates symptom of asthma and COPD by relaxing airway muscle. Additionally, most of previous studies evaluating different devices didn't cater the pressure drop across the device to patients or USP, which however is not the standard method to compare different devices.[24-28] Herein, we also consider device airflow

resistance and pressure drop across the device. *In vitro* drug deposition studies of all different devices were all performed under 4kpa, which is the maximum inhalation effort that could be achieved from patients, and the flow rate applied to devices varies between 42 and 95 L min^{-1} depending on their airflow resistance.

4.2 EXPERIMENTAL

4.2.1 Materials

α-Lactose monohydrate, Pharmatose 100M, was supplied from DFE Pharma (Princeton, NJ, USA). Micronized salbutamol sulphate was purchased from LETCO MEDICAL. Deionized water was provided by MilliQ (Millipore).

4.2.2 Manufacture of lactose granules

Wet granulation was used to manufacture lactose granules with large diameter from Pharmatose 100M (d10: 63 μm, d50: 150 μm, d90: 250 μm). Granulation is a process to generate large aggregates from small primary powders to improve the flowability of the powders [29]. Wet granulation of lactose usually employs polymeric binders that are not approved for inhalation [30-33]. To solve this problem, the granulation process in this research involved merely water as the binding solvent. Briefly, a batch size of 500 g starting lactose was introduced into the granulator (Robot Coupe USA. Inc.) followed by addition of 100 mL water merely as the granulating solvent. Subsequently, the granulated lactose carriers were pan dried in the oven overnight at 75 ℃.

4.2.3 Fractionation of granulated lactose carrier particles

Different size fractions of lactose granules were obtained by separation of the bulk granulated material using a sieve tower with cut off sizes as follows: 1000 μm, 850 μm, 600 μm, 425 μm, 300 μm, 250 μm, 212 μm, and a metal collection pan. A vibrating auto sieve shaker (Gilson Company Inc., OH, USA) was employed. The granulated lactose was poured on the top of the vibrating sieve shaker and sieved through the sieves for 30 min. One size fractions of granulated lactose (GL) was selected for future experiments: GL 300-450 μm. All analysis described were performed on the sieved samples.

4.2.4 Preparation of salbutamol sulfate/granulated lactose binary blends

Salbutamol sulfate (SS) and fractionated granulated lactose were mixed to obtain 2% binary mixtures. All formulations were blended at a constant speed of 46 RPM for 10 min with a Turbula® orbital mixer (Glen Mills, NJ, USA). Prior to any further analysis, the blended formulations were stored in the dessicator for 5 days.

4.2.5 Drug uniformity test

Five of randomly selected samples (20 ± 1 mg) were taken for measurement of salbutamol sulfate content uniformity. The coefficient of variation (CV%) was used to

determine the blending uniformity. The test was performed three times. The potency of formulations was calculated by the APIs percent amount to the nominal dose.

4.2.6 *In vitro* aerosolisation study

About 20 (±1) mg mixture powders were filled into size 3 Vcaps HPMC capsules pierced with one enlarged holes (1.2 mm) at each end of the capsule. The *in vitro* aerosolization performance of all formulations was assessed using Aerolizer® (Novartis, Switzerland) and different modified counterparts corresponding to 4kPa pressure drop and 4L air volume through the device.

A 1% (w/v) solution of silicon oil in hexane was applied to precoat the NGI stages for particle re-entrainment prevention. Amounts of salbutamol sulfate deposited on the capsule, inhaler, mouthpiece adaptor, induction port, pre-separator and NGI stages were measured and quantified. The drug content was measured by the ultraviolet visible absorption spectroscopy (Infinite M200, TECAN) at 230 nm. The parameters used to evaluate salbutamol sulfate deposition performance were emitted fraction (EF) (Eq. 1), fine particle fraction (FPF) (Eq. 2), respirable fraction (Eq. 3) mass median aerodynamic diameter (MMAD) and geometric standard deviation (GSD).

$$\mathrm{EF} = \frac{\text{emitted dose}}{\text{loading dose}}$$

(Eq. 1)

$$\text{FPF} = \frac{\text{recovered dose of drug particles smaller than 5 μm}}{\text{emitted dose}}$$

(Eq. 2)

$$\text{RF} = \frac{\text{recovered dose of drug particles smaller than 5 μm}}{\text{loading dose}}$$

(Eq.3)

4.2.7 Capsule Aperture Size Optimization with the Aerolizer

The effect of capsule aperture size on the granulated lactose based dry powder formulations was firstly investigated using the commercial device (Aerolizer®) at 90L/min, corresponding to a 4 kPa pressure drop. Aerolizer® was previously used to evaluate the aerosolization performance of a series of granulated lactose based salbutamol sulphate formulations.[22] As shown in Table 4.1, three aperture sizes 0.6 mm, 1.2 mm and 1.5 mm were chosen to optimize the EF, FPF and MMAD. Aperture size of 0.6 mm was pierced with the 4-pin piercing mechanism of currently available Aerolizer®, represented by $PIC4_{0.6}$. The other two aperture sizes were pierced by hand along the major axis of the capsules, with respectively a single 1.2 mm ($PIC1_{1.2}$) and a single 1.5 mm piercing hole ($PIC1_{1.5}$) at each capsule end.

4.2.8 Inhaler Engineering and Geometries

The commercial Aerolizer® was modified in terms of tube length, tube width, tube geometry, inlet airway and grid size of the mesh (Figure 4.1, Figure 4.2, Figure 4.3 and Figure 4.4). These devices were designed by Autodesk Inventor and manufactured by W M Keck Center for 3D Innovation. Device resistance of all modified inhalers was measured by Manometer and maximum flow rate was calculated respectively based on 4kPa pressure drop.

4.2.9 Statistics Analysis

Statistical significance between aerosol performance values was determined with one-way TTESTs between groups (* indicates $P<0.05$; ** indicates $P<0.005$).

4.3 RESULTS

4.3.1 Capsule Aperture Size Optimization with the Aerolizer

As explained in the method section, two additional piercing capsules ($PIC1_{1.2}$ and $PIC1_{1.5}$) were chosen to maximize EF originally. Original piercing capsule has four 600 μm holes at each end of the capsule, represented by $PIC4_{0.6}$, while $PIC1_{1.2}$ and $PIC1_{1.5}$ only have one piercing hole of 1.2 mm and 1.5 mm respectively at each end of the capsule. (Table 4.2) Increasing the capsule-end aperture led to increase in the FPF, from 48.1% for $PIC4_{0.6}$ to 53.9% and 53.1% for $PIC1_{1.2}$ and $PIC1_{1.5}$ respectively. Capsule retention and inhaler mouthpiece retention of $PIC4_{0.6}$ was 7.8% and 5.3%. With the piercing holes increased, reduced capsule retention ($PIC1_{1.2}$: 3.0%, $p^* < 0.05$; $PIC1_{1.5}$: 2.3%, $p^{**} < 0.005$) but increased inhaler mouthpiece retention ($PIC1_{1.2}$: 6.3%; $PIC1_{1.5}$: 7.2%, $p<0.05$) were observed. As expected, EFs were statistically and significantly improved with $PIC1_{1.2}$ (85.8%) and $PIC1_{1.5}$ (84.5%) compared to $PIC4_{0.6}$ (81.9%). $PIC1_{1.2}$ even had a much more significantly increased EF compared to $PIC1_{1.5}$. Also, a decreasing trend of induction port retention was correlated with increasing capsule aperture size. Amongst, $PIC1_{1.5}$ had the lowest induction port retention. Specifically, the amount of powder retained in the induction port was reduced from 4.7% for $PIC4_{0.6}$ to 4.1% and 3.7% for $PIC1_{1.2}$ and $PIC1_{1.5}$. Because of the highest EF, $PIC_{1.2}$ also had a higher RF (46.3%) than $PIC1_{1.5}$ (44.9%) and $PIC4_{0.6}$ (39.4%).

4.3.2 Capsule Presence Effects

The optimal capsule aperture size is 1.2 mm to achieve a high FPF (53.9%) with minimal capsule and device retention under a 4kpa pressure drop. Based on the effects of different piercing holes on aerosol performance obtained from described studies, $PIC1_{1.2}$ was selected for further experiments and used as the control group. When powders were loaded directly into the device with the presence of an empty capsule (POC), significant difference in the inhaler performance was observed (Table 4.3). Compared to $PIC1_{1.2}$, value of the FPF generated by POC was found reduced to 48.6% ($p^*<0.05$) from 53.9% and EF increased to 89.5% from 85.8%. When powders were loaded into the device without capsule (PONC), the EF remained similar as $PIC1_{1.2}$. Although FPF from PONC decreased to 50.9%, it was still slightly higher than FPF (48.6%) from POC. Statistically increase in the amount of powders retained in device base chamber was observed for both POC (5.2%) and especially PONC (8.7%), compared to $PIC1_{1.2}$ (4.9%).

4.3.3 Length of the mouthpiece

When the length of the mouthpiece was varied, (Table 4.4) no statistically significant difference in both FPF and RF was observed for the three mouthpiece cases. Furthermore, there was no significant trend observed between the lengths of mouthpiece and the amount of powders deposited in the induction port of cascade impactor.

4.3.4 Geometry of the mouthpiece

Three mouthpieces were designed with different geometry, bent, tapered and narrow inner mouthpiece cases (Figure 4.2). Horizontal position was chosen to compare the performance of the bent mouthpiece in this section. As shown in Table 4.5, mouthpiece geometry significantly influenced the device resistance and aerosol performance. A significant inverse relationship between device resistance and FPF performed under 4 kPa pressure drop was observed ($R^2 = 0.9997$). It is clear that FPF initially increased significantly with decreasing device resistance and then reached a plateau at around 0.071 (cm of $H_2O)^{0.5}L^{-1}$min. The narrow inner mouthpiece with device resistance of 0.154 (cm of $H_2O)^{0.5}L^{-1}$min had the lowest FPF of 37.8%, while the horizontal bent mouthpiece with small device resistance (0.067 (cm of $H_2O)^{0.5}L^{-1}$min) had the highest FPF of around 54.8%. Additionally, as a result of the bent tube which prevented exit of powders from device, the EF of horizontal bent mouthpiece was statistically smaller than the other two cases.

4.3.5 Spatial Positions of the mouthpiece

Of the bent mouthpiece inhaler, there are multiple (360 ºrotations) spatial positions available for the impaction studies. The device resistance is the inherent property of the mouthpiece and doesn't change with different positions, so same flow rate (96 L/min) was used for the study corresponding to 4 kpa pressure drop. Three representative rotation degrees (horizontal 0 º, upward 90 º, downward 270 º) were selected to investigate

the effect of spatial positions of mouthpiece on the aerosolization performance. As shown in Table 4.6, the fine aerosol fraction (around 54.7%) generated didn't change significantly with the bent mouthpiece rotating from 0 º (horizontal) to 90 º (upward), while the bent mouthpiece with (270 º) downward position produced a significant low FPF (46.9%). Of the three positions of the mouthpiece, upward position had the highest EF (88%). Also, there was a decreasing relationship between the amounts of powders collected from mouthpiece with the positions of mouthpiece rotated from downside to upward. But increasing amount of powders deposited in the induction port was noticed with the same rotation order.

4.3.6 Grid effect study

As the voidage of the grid was increased, there was a statistically significant influence in the aerosol performance. Specifically, (Table 4.7) the FPF decreased from 53.9% for the complete grid case to 50.5% for the modified grid. And the EF increased from 85.8% for the complete grid case to 88.4% for the modified grid. Although increasing the grid voidage led to a slight increase in the powders retained in the induction port, powder retention decreased slightly in the device mouthpiece.

4.3.7 Inhaler air passage effect

Reducing air inlet size significantly increased the performance of the inhaler. As shown in Table 4.8, the FPF and RF increased to 57.8% and 50.3% from 53.9% and 46.3%

respectively, when the air inlet size reduced to one third of the original device. The improvement of the FPF partially may come from a better deagglomeration effect, resulting in the inhaler with reduced air inlet size having a lower MMAD value (1.7 μm). But reduced air inlet resulted in a slight decrease of EF from 85.8% to 84.9%. And increased deposition of powders in the induction port from 4.1% to 6.2% was observed with the reduction of inlet air pathway.

4.3.8 Synergistic effect of reduced inlet air and bent mouthpiece tube

Due to the improved performance of reduced inlet air passage and bent up mouthpiece in terms of FPF and EF respectively, these two modified device pieces were selected for a combined study to further improve powder redispersion. Both the original device and combined pieces were tested for aerosol performance and results are presented in Table 4.9. The combination of two modified device pieces improved the FPF to 57.8% from 53.9% without decreasing EF compared to original device. Similar to the effect of single reduce inlet air piece, combined pieces provided a much lower MMAD value (1.7 μm). Additionally, in the *in vitro* compactor studies, the cut-off diameter of the combined device and commercial device was 5.45 μm and 6.48 μm, respectively. Therefore, the FPFs listed in Table 4.9 were not compared under the same parameters. And the increased FPF from the combined pieces should be far more than what was listed in the table.

4.4 DISCUSSION

The purpose in this study was (1) to better understand different modified device pieces on the detachment mechanism and performance of previously developed granulated lactose based DPI formulations; (2) to optimize current commercial device-Aerolizer® to further improve the aerosolization performance.

Currently, four mechanisms have been proposed to redisperse lactose binary drug mixtures to form a fine respirable aerosol: (1) Particle-capsule interaction, (2) Particle interaction with flow stream and shear turbulence, (3) Particle impaction with device, (4) Particle-particle interaction.[26, 28] Donovan et. al. suggested that the predominant detachment mechanism for significantly large particles is impaction-based detachment, which is demonstrated by increased collision frequency of the relatively large model particles with inhaler mouthpiece.[23] Du et. al. exhibited that particle-device impaction may be the major detachment force for significantly large granulated lactose based DPI formulation, but the effect of shear flow and turbulence in the redispersion also should not be overlooked. [22]

4.4.1 Capsule Aperture Size Optimization with the Aerolizer

For the particle-capsule interaction, Coates et. al[26], and Chew et. al[34] demonstrated that capsule played a significant role in improving FPF by deagglomeration of mannitol powder from within the capsule and this effect depends on the size of capsule hole. A

significant increase in FPF of mannitol powder was observed in the order of $PIC4_{0.6}$ > $PIC1_{1.2}$ > POC. It is found in this study that capsule and aperture size also had a significant effect, but in a different way, on the overall performance of the inhaler. The deagglomeration didn't increase the fine drug fraction (FPF) as discussed in Coates et. al's study (Table 4.2 and Table 4.3), with the FPF of granulated lactose based DPI formulation in the order of $PIC1_{1.2} \approx PIC1_{1.5}$ > PONC > POC > $PIC4_{0.6}$ dispersion method. This discrepancy could be explained by different formulations used and different redispersion mechanism. Unlike spray dried mannitol powder agglomerates, formulation used in this study is significantly large aggregated lactose granules (300-450 μm) with micronized APIs attached on the surface. With larger capsule aperture size, e.g. $PIC1_{1.2}$ and $PIC1_{1.5}$, intact granulated carriers could be efficiently removed from the capsules. The break-up mechanism through capsule holes of $PIC4_{0.6}$, which deagglomerated spray dried mannitol powders into primary drug particles to generate inhalable aerosols[26], deaggregated granulated lactose mixtures into primary lactose particles still with micronized drugs on the surface, confirmed by a decreasing mouthpiece retention ($PIC4_{0.6}$: 5.3% < $PIC1_{1.2}$: 6.3% < $PIC1_{1.5}$: 7.2%). This decreasing retention is because that deaggregated primary lactose particles are less likely to be trapped by the grid mesh, compared to large and intact granulated lactose. Although not directly measured, it was assumed that lactose carrier particles flying out from capsule holes in $PIC1_{1.2}$ and $PIC1_{1.5}$ are larger than from $PIC4_{0.6}$. Since the major detachment force for granulated lactose mixtures, inertial impaction force, is proportional to the particle diameter,[12] FPF was higher with larger capsule hole size in dispersion method $PIC1_{1.2}$ (53.9%) and $PIC1_{1.5}$ (53.1%) than with smaller capsule hole size $PIC4_{0.6}$ (48.1%), indicating that the break-up

mechanism by forcing granulated lactose mixtures through the capsule holes prevents dispersing of micronized drugs from the surface of significantly large granulated lactose carrier surface.

4.4.2 Capsule Presence Effects

Without the presence of capsule (PONC), higher turbulence level (~65% more) could be generated,[26] which increases the aerosol dispersion of spray dried mannitol powders via detachment by flow mechanism. Nevertheless, PONC with increased turbulence level still produced a slightly lower FPF (50.9%) than $PIC1_{1.2}$ (53.9%) for granulated lactose mixtures, which indicated that the high turbulence level was not that effective in generating respirable drug particles from lactose carrier surface and further confirmed that the major detachment mechanism of significantly large granulated lactose mixture is detachment by inertial collision and impaction.

4.4.3 Length of the mouthpiece

There are two types of particle-device interaction, particle interacted with the mouthpiece wall or with the inhaler mesh grid. As shown in this study (Table 4.4), the mouthpiece length had no significant influence on the aerosolization of granulated lactose carrier-based DPI formulations. Although with varied mouthpiece length, identical flow patterns and turbulence were generated[35]. To produce similar aerosolization performance as noticed, similar or identical collision force should also be generated in the inhaler

device with different mouthpiece length. Therefore it is speculated that the lactose particles mainly impacted with the lower region of the mouthpiece.

4.4.4 Geometry of the mouthpiece

The geometry of the mouthpiece significantly affected the device resistance and the aerosolization performance. Different geometry widely varied the internal diameters and dimension of mouthpieces, causing the device resistance ranging from 0.067 to 0.154 (cm of $H_2O)^{0.5}$ L^{-1} min. Higher resistance is known to generate higher turbulence level, leading to a higher FPF under a given air flow through devices.[36] But as shown in our study (Table 4.5), when air flow rate varied based on similar pressure drop (4kpa), the device with high resistance didn't perform better than smaller counterparts.[36]

4.4.5 Spatial Positions of the mouthpiece

Spatial positions of the bent mouthpiece significantly influenced the aerosolization performance of granulated lactose mixtures. On one hand, bent mouthpiece with (270) downward position produced a much lower FPF (46.9%) than the other two positions (54.7%). The explanation for the FPF decline is the adverse effect of gravitational forces acting on the lactose carriers. Although high aerosol performance can be produced with significantly large lactose carriers, the improvement imparted by large carrier particles will not continue with opposite gravitational and drag forces acting upon them for the mouthpiece with downward position (Figure 4.5). The benefit of momentum transfer

from inertial collision with device will be countered by a reduced particle velocity. This finding further indicated the importance of inertial impaction of granulated lactose with device in improving aerosol performance. On the other hand, gravitational forces acted on the large lactose particles with (90) upward bent mouthpiece increased the particle velocity and facilitated the particle emptying from inhaler with an increased EF to 88.0% from 86.1%. The increased particle velocity was confirmed by increased induction port retention from 3.7% to 4.7%, which balanced the increased impaction intensity with device in improving aerosol performance.

4.4.6 Grid effect study

An alternative way to investigate the detachment mechanism for large lactose particles is to study the interaction with device mesh grid. Significantly low FPF (50.5% vs. 53.9%) was produced with the grid voidage increased, explained by a reduced impaction frequency and force magnitude with device.

4.4.7 Inhaler air passage effect

This study showed that smaller inlet size improved the aerosol performance significantly. Although FPF of granulated lactose based formulation improved from 53.9% to 57.8%, there was significant impaction loss with modified inlet size. Smaller inlet size increased the particle velocity,[25] leading to a higher induction port retention to 6.2% from 4.1%. A higher air velocity tends to increase impaction magnitude between large lactose

particles with device, which resulted in increased capsule chamber, mouthpiece retention and thus reduced emitted fraction.

4.4.8 Synergistic effect of reduced inlet air and bent mouthpiece tube

Although reduced inlet size among all modified inhaler cases improved the FPF, adverse performance of reduced EF and improved induction port retention was produced. Induction port retention is associated with systemic toxicity. To reconcile the higher FPF, increased induction port retention and reduced EF achieved by reduced inlet, combined modified inhaler pieces were evaluated. Bent mouthpiece at upward position compared to other devices had the highest EF, and also smaller induction port retention than device with reduced inlet size. As expected, from the modified mouthpieces and inhaler bases, the optimum device is the upward bent mouthpiece with reduced inlet air.

Limitations of the current investigation include the evaluation of a single granulated lactose based formulation, single size fraction of granulated lactose carrier, single drug loading, and single flow rate used for each modified device case. The aerosol performance is the interplay of formulation, device and patient inspiratory effort. The optimum device or combination should be different with another formulation.

4.4.9 Dispersion of drug particle agglomerates with modified inhalers

Varying MMAD was produced with different kinds of modified inhaler pieces. This is explained by different turbulence levels generated through device. Impaction and collision force is responsible for detaching micronized drug particle agglomerates from the granulated lactose carrier surface. Higher velocity generates high turbulence levels, which facilitates redispersion of agglomerates into primary particles and improvement of aerosol dispersion.

4.5 CONCLUSION

The preferred device is one device that is simple, cheap, easy to use, generates high turbulence at a low flow-rate to give a high and consistent FPF of the drug, but retain the lactose carrier only in the upper airway.[36] Granulated lactose based DPI formulation was developed in previous study which had acceptable aerosol performance, good flowability, blending uniformity and consistent dosing. Aerolizer® as the commercial off the shelf device is portable, simple to use and cost effective. With the modification of capsule aperture, mouthpiece geometry, grid structure, inlet size and spatial position of mouthpiece, both aerosol performance and aerodynamic parameters were optimized with different levels of impaction intensity and turbulence flow generated. Also, the combined pieces of the modified inhalers synergistically improve the performance of the granulated lactose based formulation.

4.6 TABLES

Table 4.1 Pressure drop and cut off diameter table

	Description
$PIC4_{0.6}$	Powder loaded in the size 3 capsule pierced with the 4-pin mechanism by Aerolizer®
$PIC1_{1.2}$	Powder loaded in the size 3 capsule with a single 1.2 mm hole at each end
$PIC1_{1.5}$	Powder loaded in the size 3 capsule with a single 1.5 mm hole at each end
POC	Powder loaded directly in the chamber with the presence of the empty capsule
PONC	Powder loaded in the size 3 capsule without the presence of the empty capsule

Table 4.2 Capsule-end Aperture Effects

Description	**$PIC4_{0.6}$**	**$PIC1_{1.2}$**	**$PIC1_{1.5}$**
Capsule Aperture (mm)	0.6	1.2	1.5
Total Number of Holes	8	2	2
Aperture Area/Hole (cm^2)	0.06π	0.36π	0.56π
Total Aperture Area (cm^2)	0.36π	0.36π	0.56π
Device Resistance	0.071	0.071	0.071
Air Flow Rate ($L \cdot min^{-1}$)	90	90	90
Cut off Diameter (μm)	6.48	6.48	6.48
Emitted Fraction (%)	81.9 (4.5)	85.8 (3.6)*	84.5 (1.5)
Capsule Retention (%)	7.8 (1.3)	3.0 (0.3)*	2.3 (0.1) **
Capsule Chamber Retention (%)	5.1 (2.6)	4.9 (1.7)	6.0 (1.0)
Inhaler Mouthpiece Retention (%)	5.3 (1.1)	6.3 (2.2)	7.2 (0.4)*
Induction Port (%)	4.7 (0.4)	4.1 (0.4)	3.7 (0.2) *
FPF (%)	48.1 (1.1)	53.9 (0.4)**	53.1 (1.7)*
RF (%)	39.4 (3.0)	46.3 (2.1)**	44.9 (1.5)
MMAD(μm)	1.9 (0.3)	2.0 (0.0)	1.9 (0.1)

Table 4.3 Capsule Presence Effects

Description	**PIC1$_{1,2}$**	**POC**	**PONC**
Capsule Aperture (mm)	1.2	N/A	N/A
Device Resistance	0.071	0.071	0.083
Air Flow Rate (L/min)	90	90	77
Cut off Diameter (μm)	6.48	6.48	6.48
Emitted Fraction (%)	85.8 (3.6)	89.5 (3.7)	85.8 (1.6) *
Capsule retention (%)	3.0 (0.3)	0 **	0 **
Inhaler Base retention (%)	4.9 (1.7)	5.2 (1.9)	8.7 (1.8) *
Inhaler Mouthpiece retention (%)	6.3 (2.2)	5.3 (1.8)	5.5 (0.4)
Induction Port (%)	4.1 (0.4)	4.0 (1.0)	4.1 (1.0) *
FPF (%)	53.9 (0.4)	48.6 (3.0) *	50.9 (1.9)
RF (%)	46.3 (2.1)	43.5 (4.4)	43.7 (1.7)
MMAD(μm)	2.0 (0.0)	2.3 (3.0)	1.9 (0.1)

Table 4.4 Length of the mouthpiece

Description	Full Mouthpiece	Long mouthpiece	Short mouthpiece
Capsule Aperture (mm)	1.2	1.2	1.2
Device Resistance	0.070	0.071	0.071
Air Flow Rate (L/min)	90	90	90
Cut off Diameter (µm)	6.48	6.48	6.48
Emitted Fraction (%)	85.8 (3.6)	86.0 (0.5)	86.2 (1.8)
Capsule retention (%)	3.0 (0.3)	3.3 (0.2)	4.3 (1.2)
Capsule chamber retention (%)	4.9 (1.7)	5.6 (0.8)	6.1 (0.5)
Inhaler Mouthpiece retention (%)	6.3 (2.2)	5.0 (1.6)	3.4 (0.6)
Induction Port (%)	4.1 (0.4)	4.1 (0.2)	4.6 (0.7)
FPF (%)	53.9 (0.4)	54.6 (3.7)	55.9 (1.2)
RF (%)	46.3 (2.1)	47.0 (3.4)	48.2 (1.2)
MMAD(µm)	2.0 (0.0)	2.0 (0.1)	2.0 (0.1)

Table 4.5 Geometry of the mouthpiece

Description	Horizontal Bent	Tapered	Narrow Inner
Capsule Aperture (mm)	1.2	1.2	1.2
Device Resistance	0.067	0.077	0.147
Air Flow Rate (L/min)	96	84	43
Cut off Diameter (μm)	6.25	6.72	5.3
Emitted Fraction (%)	86.1 (1.4)	88.6 (1.8)	88.6 (1.5)
Capsule retention (%)	2.1 (1.9)	2.9 (0.4)	2.7 (0.3)
Capsule chamber retention (%)	5.8 (0.7)	4.6 (0.6)	4.0 (0.3)
Inhaler Mouthpiece retention (%)	5.9 (0.6)	3.9 (1.1)	4.7 (1.5)
Induction Port (%)	3.7 (0.5)	6.8 (0.5)	3.8 (0.3)
FPF (%)	54.7 (1.7)	52.9 (2.2)	37.8 (3.3)
RF (%)	47.2 (1.4)	46.9 (2.8)	33.5 (3.1)
MMAD(μm)	2.0 (0.1)	2.0 (0.1)	1.9 (0.1)

Table 4.6 Spatial Positions of the mouthpiece

Description	Horizontal Bent	Downward Bent	Upward Bent
Capsule Aperture (mm)	1.2	1.2	1.2
Device Resistance	0.067	0.067	0.067
Air Flow Rate (L/min)	96	96	96
Cut off Diameter (μm)	6.25	6.25	6.25
Emitted Fraction (%)	86.1 (1.4)	87.0 (2.7)	88.0 (0.8)
Capsule retention (%)	2.1 (1.9)	2.0 (1.7)	2.9 (0.4)
Capsule chamber retention (%)	5.8 (0.7)	4.8 (1.3)	4.4 (0.4)
Inhaler Mouthpiece retention (%)	5.9 (0.6)	6.2 (0.6)	4.7 (0.6)
Induction Port (%)	3.7 (0.5)	3.2 (0.0)	4.7 (0.6)
FPF (%)	54.7 (1.7)	46.9 (2.5)	54.7 (0.4)
RF (%)	47.2 (1.4)	40.8 (3.0)	48.1 (0.2)
MMAD(μm)	2.0 (0.1)	2.2 (0.1)	2.0 (0.1)

Table 4.7 Grid effect study

Description	Full Grid	Modified Grid
Capsule Aperture (mm)	1.2	1.2
Device Resistance	0.071	0.058
Air Flow Rate (L/min)	90	96
Cut off Diameter (μm)	6.48	6.25
Emitted Fraction (%)	85.8 (3.6)	88.4 (1.3)*
Capsule retention (%)	3.0 (0.3)	3.2 (0.1)
Capsule chamber retention (%)	4.9 (1.7)	4.1 (1.0)
Inhaler Mouthpiece retention (%)	6.3 (2.2)	4.3 (0.7)
Induction Port (%)	4.1 (0.4)	5.1 (0.4)
FPF (%)	53.9 (0.4)	50.5 (2.5)*
RF (%)	46.3 (2.1)	44.6 (1.6)
MMAD(μm)	2.0 (0.0)	2.0 (0.3)

Table 4.8 Inhaler air passage effect

Description	Full Inlet Air	Reduced Inlet
Capsule Aperture (mm)	1.2	1.2
Device Resistance	0.071	0.154
Air Flow Rate (L/min)	90	42
Cut off Diameter (μm)	6.48	5.37
Emitted Fraction (%)	85.8 (3.6)	83.4 (2.6)
Capsule retention (%)	3.0 (0.3)	2.9 (1.0)
Capsule chamber retention (%)	4.9 (1.7)	6.7 (3.1)
Inhaler Mouthpiece retention (%)	6.3 (2.2)	7.0 (0.6)
Induction Port (%)	4.1 (0.4)	6.2 (1.2)
FPF (%)	53.9 (0.4)	57.8 (1.3)*
RF (%)	46.3 (2.1)	48.2 (2.2)
MMAD(μm)	2.0 (0.0)	1.7 (0.0) (turbulence level)

Table 4.9 Synergistic effect of reduced inlet air and bent mouthpiece tube

Description	Original Device	Combined Devices
Capsule Aperture (mm)	1.2	1.2
Device Resistance	0.071	
Air Flow Rate (L/min)	90	44
Cut off Diameter (μm)	6.48	5.45
Emitted Fraction (%)	85.8 (3.6)	85.5 (1.8)
Capsule retention (%)	3.0 (0.3)	3.0 (0.8)
Capsule chamber retention (%)	4.9 (1.7)	4.5 (0.4)
Inhaler Mouthpiece retention (%)	6.3 (2.2)	6.9 (1.2)
Induction Port (%)	4.1 (0.4)	4.5 (0.2)
FPF (%)	53.9 (0.4)	57.8 (0.8)*
RF (%)	46.3 (2.1)	49.4 (1.4)
MMAD(μm)	2.0 (0.0)	1.7 (0.0)

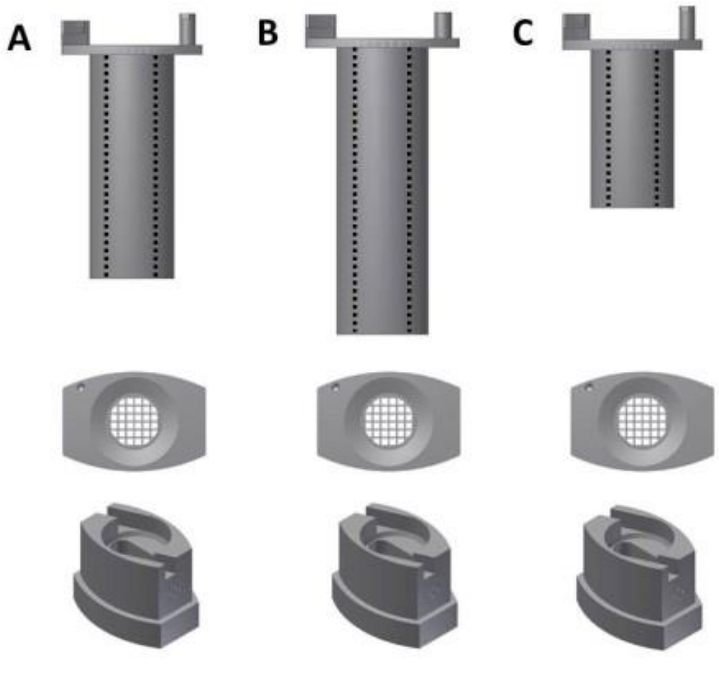

Figure 4.1 A) Original; B) 4/3 Mouthpiece Length; C) 2/3 Mouthpiece Length

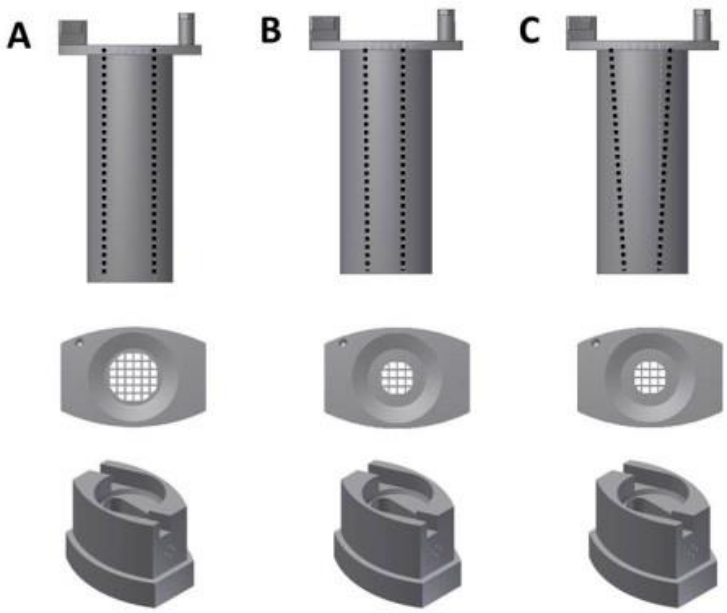

Figure 4.2 A) Original; B) 2/3 Inner Tube Width; C) Tapered Tube

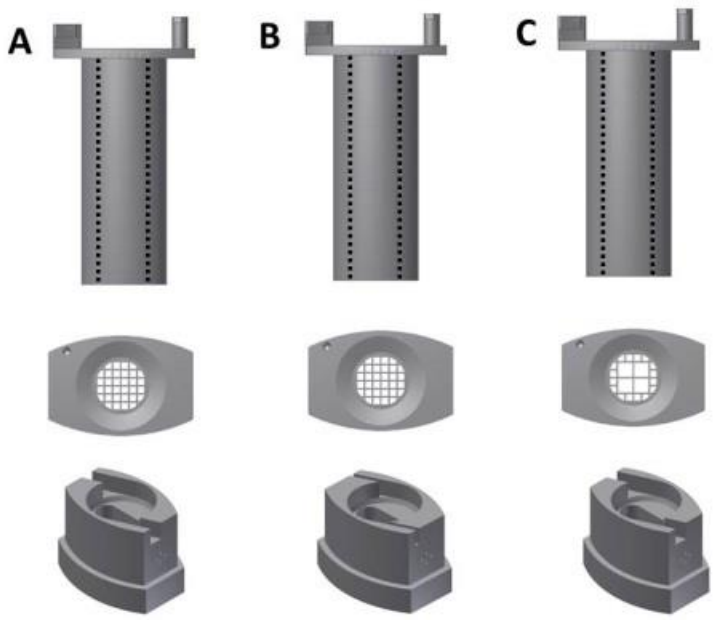

Figure 4.3 A) Original; B) 1/3 Inlet size; C) Cross Grid

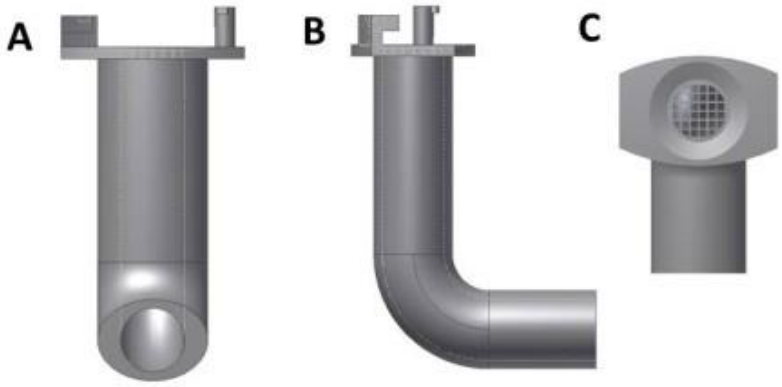

Figure 4.4 A) Bent Tube; B) Side View of Bent Tube; C) Top View of Bent Tube

4.7 REFERENCES

1. Telko MJ, Hickey AJ. 2005. Dry powder inhaler formulation. Respiratory care. 50:1209-27.

2. Ungaro F, d'Angelo I, Coletta C, d'Emmanuele di Villa Bianca R, Sorrentino R, Perfetto B, et al. 2012. Dry powders based on PLGA nanoparticles for pulmonary delivery of antibiotics: modulation of encapsulation efficiency, release rate and lung deposition pattern by hydrophilic polymers. J Control Release. 157:149-59.

3. Traini D, Adi H, Valet OK, Young PM. 2012. Preparation and evaluation of single and co-engineered combination inhalation carrier formulations for the treatment of asthma. J Pharm Sci. 101:4267-76.

4. Behara SR, Longest PW, Farkas DR, Hindle M. 2014. Development and comparison of new high-efficiency dry powder inhalers for carrier-free formulations. J Pharm Sci. 103:465-77.

5. Kaialy W, Hussain T, Alhalaweh A, Nokhodchi A. 2013. Towards a More Desirable Dry Powder Inhaler Formulation: Large Spray-Dried Mannitol Microspheres Outperform Small Microspheres. Pharm Res.

6. Behara SR, Farkas DR, Hindle M, Longest PW. 2014. Development of a high efficiency dry powder inhaler: effects of capsule chamber design and inhaler surface modifications. Pharm Res. 31:360-72.

7. Selvam P, McNair D, Truman R, Smyth HD. 2010. A novel dry powder inhaler: Effect of device design on dispersion performance. Int J Pharm. 401:1-6.

8. de Boer AH, Chan HK, Price R. 2012. A critical view on lactose-based drug formulation and device studies for dry powder inhalation: which are relevant and what interactions to expect? Adv Drug Deliv Rev. 64:257-74.

9. Zhou QT, Tang P, Leung SS, Chan JG, Chan HK. 2014. Emerging inhalation aerosol devices and strategies: where are we headed? Adv Drug Deliv Rev. 75:3-17.

10. Kou X, Chan LW, Steckel H, Heng PW. 2012. Physico-chemical aspects of lactose for inhalation. Adv Drug Deliv Rev. 64:220-32.

11. Kaialy W, Martin GP, Larhrib H, Ticehurst MD, Kolosionek E, Nokhodchi A. 2012. The influence of physical properties and morphology of crystallised lactose on delivery of salbutamol sulphate from dry powder inhalers. Colloids Surf B Biointerfaces. 89:29-39.

12. Donovan MJ, Smyth HD. 2010. Influence of size and surface roughness of large lactose carrier particles in dry powder inhaler formulations. Int J Pharm. 402:1-9.

13. Guenette E, Barrett A, Kraus D, Brody R, Harding L, Magee G. 2009. Understanding the effect of lactose particle size on the properties of DPI formulations using experimental design. Int J Pharm. 380:80-8.

14. Guchardi R, Frei M, John E, Kaerger JS. 2008. Influence of fine lactose and magnesium stearate on low dose dry powder inhaler formulations. Int J Pharm. 348:10-7.

15. Young PM, Chan HK, Chiou H, Edge S, Tee TH, Traini D. 2007. The influence of mechanical processing of dry powder inhaler carriers on drug aerosolization performance. J Pharm Sci. 96:1331-41.

16. Islam N, Stewart P, Larson I, Hartley P. 2004. Lactose surface modification by decantation: are drug-fine lactose ratios the key to better dispersion of salmeterol xinafoate from lactose-interactive mixtures? Pharm Res. 21:492-9.

17. Hickey AJ, Mansour HM, Telko MJ, Xu Z, Smyth HD, Mulder T, et al. 2007. Physical characterization of component particles included in dry powder inhalers. I. Strategy review and static characteristics. J Pharm Sci. 96:1282-301.

18. de Boer AH, Hagedoorn P, Gjaltema D, Goede J, Kussendrager KD, Frijlink HW. 2003. Air classifier technology (ACT) in dry powder inhalation. Part 2. The effect of lactose carrier surface properties on the drug-to-carrier interaction in adhesive mixtures for inhalation. Int J Pharm. 260:201-16.

19. Louey MD, Razia S, Stewart PJ. 2003. Influence of physico-chemical carrier properties on the in vitro aerosol deposition from interactive mixtures. Int J Pharm. 252:87-98.

20. Cline D, Dalby R. 2002. Predicting the quality of powders for inhalation from surface energy and area. Pharm Res. 19:1274-7.

21. Kaialy W, Alhalaweh A, Velaga SP, Nokhodchi A. 2012. Influence of lactose carrier particle size on the aerosol performance of budesonide from a dry powder inhaler. Powder Technology. 227:74-85.

22. Du P, Du J, Smyth HD. 2014. Evaluation of Granulated Lactose as a Carrier for DPI Formulations 1: Effect of Granule Size. AAPS PharmSciTech. 15:1417-28.

23. Donovan MJ, Kim SH, Raman V, Smyth HD. 2012. Dry powder inhaler device influence on carrier particle performance. J Pharm Sci. 101:1097-107.

24. Coates MS, Chan HK, Fletcher DF, Chiou H. 2007. Influence of mouthpiece geometry on the aerosol delivery performance of a dry powder inhaler. Pharm Res. 24:1450-6.

25. Coates MS, Chan HK, Fletcher DF, Raper JA. 2006. Effect of design on the performance of a dry powder inhaler using computational fluid dynamics. Part 2: Air inlet size. J Pharm Sci. 95:1382-92.

26. Coates MS, Fletcher DF, Chan HK, Raper JA. 2005. The role of capsule on the performance of a dry powder inhaler using computational and experimental analyses. Pharm Res. 22:923-32.

27. Coates MS, Chan HK, Fletcher DF, Raper JA. 2005. Influence of air flow on the performance of a dry powder inhaler using computational and experimental analyses. Pharm Res. 22:1445-53.

28. Coates MS, Fletcher DF, Chan HK, Raper JA. 2004. Effect of design on the performance of a dry powder inhaler using computational fluid dynamics. Part 1: Grid structure and mouthpiece length. J Pharm Sci. 93:2863-76.

29. Kawashima Y, Serigano T, Hino T, Yamamoto H, Takeuchi H. 1998. Effect of surface morphology of carrier lactose on dry powder inhalation property of pranlukast hydrate. 172:188.

30. Li J, Tao L, Buckley D, Tao J, Gao J, Hubert M. 2013. The Effect of the Physical State of Binders on High-Shear Wet Granulation and Granule Properties: A Mechanistic Approach to Understand the High-Shear Wet Granulation Process. Part IV. The Impact of Rheological State and Tip-speeds. J Pharm Sci. 102:4384-94.

31. Fujiwara M, Dohi M, Otsuka T, Yamashita K, Sako K. 2013. Influence of binder droplet dimension on granulation rate during fluidized bed granulation. Chem Pharm Bull (Tokyo). 61:320-5.

32. Ogawa T, Uchino T, Takahashi D, Izumi T, Otsuka M. 2012. Pharmaceutical production of tableting granules in an ultra-small-scale high-shear granulator as a pre-formulation study. Drug Dev Ind Pharm. 38:1390-3.

33. Mangwandi C, Adams MJ, Hounslow MJ, Salman AD. 2012. An investigation of the influence of process and formulation variables on mechanical properties of high shear granules using design of experiment. Int J Pharm. 427:328-36.

34. Chew NYK, Chan HK, Bagster DF, Mukhraiya J. 2002. Characterization of pharmaceutical powder inhalers: estimation of energy input for powder dispersion and effect of capsule device conFigureuration. Journal of Aerosol Science. 33:999-1008.

35. Zhou QT, Tong Z, Tang P, Citterio M, Yang R, Chan HK. 2013. Effect of Device Design on the Aerosolization of a Carrier-Based Dry Powder Inhaler-a Case Study on Aerolizer((R)) Foradile ((R)). AAPS J.

36. Srichana T, Martin GP, Marriott C. 1998. Dry powder inhalers: the influence of device resistance and powder formulation on drug and lactose deposition in vitro. Eur J Pharm Sci. 7:73-80.

Chapter 5: Development of a high rifampicin loaded dry powder inhalation formulation

Abstract

The aim of this research was to investigate a novel dry powder formulation of rifampicin (RF) that presents an improved lung deposition profile by using granulated lactose carrier and rifampicin particles. Rifampicin in micro (RFMS) and nano size (RFNS) was prepared by jet milling process. Granulated lactose was manufactured by wet granulation and two different size fractions were selected for further study. The physicochemical properties of RFMS and RFNS were characterized. Aerosol performance of RFMS and RFNS formulated with different lactose carriers were investigated with two dry powder inhalers (DPIs), a commercial Aerolizer and a modified Aerolizer, with a Next Geneartion Impactor (NGI). The dry powder formulation formulated with granulated lactose carrier had a significant improved aerosol performance than inhalation grade lactose. The RFNS had a smaller particle size distribution and a lower bulk density. This physical property of RFNS improved aerosolization properties than RFMS with a decreased induction port deposition. Induction port deposition could also be alleviated by using modified Aerozlier device. With this modified Aerolizer inhaler, the maximum fine particle fraction (FPF) of 70.6% was achieved by formulating RFNS with granulated lactose at 212-250 μm size fractions. The granulated lactose based high loaded RFNS dry powder formulation offers the

benefits of delivering a maximum potency formulation of rifampicin directly to the site of infected lung.

Keywords:

DPI formulations; Granulated lactose; Uniformity; Dissolution; Rifampicin; Drug Loading

5.1 INTRODUCTION

Tuberculosis (TB), caused by *Mycobacterium tuberculosis*, is second only to HIV/AIDS as the greatest killer worldwide. Infection rate of TB is one per second and one third of world population is infected with TB right now. The WHO reports that, in 2012, 8.6 million people fell ill with TB and 1.3 million died from TB[1]. Most of these deaths (>95%) occur in low- and middle-income countries where access barriers pose a significant hurdle in healthcare management[2]. Recent emergency of drug-resistant strains of *Mycobacterium tuberculosis* makes the situation even worse[3, 4], and the increased death incidence from anti-drug strains is threatening the control of TB contamination.

One possible reason for the resistance is the exposure of mycobacteria to suboptimal levels of one or more anti-TB drugs[5, 6]. Pulmonary tuberculosis is the most common form of tuberculosis[7], with alveolar macrophages containing large numbers of tuberculosis bacilli[8]. Conventional therapy for respiratory tract infections, including TB, is oral or parenteral administration of high doses of single or combined antibiotics. While oral administration is the most common treatment of TB, high systemic exposure of antibiotics causes unwanted side-effects[9]. The lung lesions hosting large numbers of bacteria are poorly vascularized and fortified by thick fibrous tissue, resulting in the inability of antibiotic drug to achieve high enough target concentration level at these highly sequestered organisms. Due to the poor pulmonary distribution, only small amount of drugs would reach the site of infection after systemically administration.

Delivering drugs through inhalation directly to the lungs allows higher drug concentrations in the vicinity of these lesions than that by either oral or parenteral administration[10, 11]. For the pulmonary delivery route, Dry Powder Inhalers (DPIs) enable a wide range of therapeutic agents and are portable, convenient, and have the critical advantage of ensuring long-term drug stability and also potential for rapid delivery of high doses, compared to pMDIs and nebulizers. Collectively these attributes make DPI systems an attractive solution to several global and developing country respiratory diseases, including Tuberculosis (TB).

The formulations of commercial DPIs are frequently composed of active ingredients and large lactose coarse carriers (50-200 μm) to form homogenous, binary, or tertiary mixtures. The active ingredients in DPI formulations are in micronized form, usually with an aerodynamic diameter around 1-5 μm, which enables adequate deposition in the lung. On inhalation, dry powder formulations are required to be redispersed into primary drug particles for patients to use. In most DPI formulation, drug particles present low concentration in the mixture, and a typical drug to carrier ratio is 1:67.5 (w/w)[12]. This is mainly because asthma and COPD drugs are potent and active in the microgram range. In fact, most antibiotics are low potent drugs and consequently a larger dose is commonly required for oral administration (e.g. 300 mg ciprofloxacin b. i. d. and 500 mg azithromycin q. d.)[13, 14]. Although administration of antibiotics by pulmonary delivery is likely to achieve therapeutic efficacy with smaller amount of drug doses compared to oral delivery route, traditional lactose carrier based dry powder formulation is unable to deliver a high enough dose and is not the ideal vehicle for antibiotics.

It has been reported that high drug loading compromised delivery efficiency and dose uniformity of drugs into the lung when using traditional lactose carrier systems[15], due to limited drug loading capacity of lactose carrier. Current researches into high drug loaded DPI formulations have mainly focused on expensive and complex particle engineering techniques, such as spray drying or solvent evaporation processes[14, 16], which would never be feasible for use in low income countries where therapies are needed most. Despite technological advancement, spray drying can often lead to processing problems[14]. For example, the amorphous form of microencapsulated or spray dried antibiotics, which often undergo recrystallization or chemical degradation, may not provide required long-term stability[16-18]. Moreover, the number of excipients approved by FDA for pulmonary delivery is very restricted and scarce. Most excipients used in spray dried aerosols are under research only[19] and safety issue is still a concern[16, 19, 20]. Thus, it is urgently desired to develop an effective delivery system with high drug loading that will slow down or prevent development and spread of TB. Such a delivery system should also be safe, economical, and suitable for industrial processing.

An attractive way to solve the problem may be achieved by developing carrier system with optimized physico-chemical properties. Lactose is the frequently used carrier approved by FDA in commercial DPI formulation[19], with safety profile clearly documented. As the major composite of dry powder formulation, the physico-chemical property of lactose carrier is the key to the aerosol performance, which determines the interaction force between drug particle and carrier particles[21]. Granulated lactose with significantly large particle size and rough surface was previously developed in our lab as the carrier for dry powder inhalation formulations, which proved to provide a better

blending uniformity, proper aerosol performance and also showed promise for high drug loading due to increased specific surface area than smooth counterparts under similar size fractions[22]. Additionally, granulation is a common approach adopted in industry. It is a process to improve the flowability of powders by generating large aggregates from small primary powders[23].

It is the goal of this research to demonstrate that granulated lactose can serve as improved carrier system than inhalation grade lactose for rifampicin, one of the first line anti-tuberculosis (TB) drugs active both *in vitro* and *in vivo* against Mycobacterium tuberculosis[8]. This study also describes how the physico-chemical properties of rifampicin, e.g. particle size, influence the aerosol performance. The aim of this study is to develop a cost effective lactose based high drug loaded dry powder inhalation (DPI) formulation that has improved aerodynamic properties as well as a good dose delivery uniformity. The aerodynamic properties of formulated rifampicin dry powders are evaluated with two dry powder inhalers (DPIs), the Aerolizer® and mouthpiece modified Aerolizer®.

5.2 EXPERIMENTAL

5.2.1 Materials

α-Lactose monohydrate, Pharmatose 100M, was obtained from DFE Pharma (Princeton, NJ, USA). Rifampicin was purchased from LETCO MEDICAL. Deionized water was supplied by MilliQ (Millipore).

5.2.2 Manufacture of lactose granules

Lactose granules with large diameter were manufactured by wet granulation from Pharmatose 100M (d10: 63 μm, d50: 150 μm, d90: 250 μm). Wet granulation of lactose usually employs polymeric binders that are not approved by FDA for inhalation[24-27]. To solve this problem, the binding solvent used in the granulation process of this research involved merely water. Briefly, after a batch size of 500 g starting lactose was introduced into the granulator (Robot Coupe USA. Inc.), 100 mL water was added merely as the granulating solvent. Subsequently, in the oven overnight at 75 ℃, the granulated lactose carriers were pan dried.

5.2.3 Fractionation of granulated lactose carrier particles

A vibrating auto sieve shaker (Gilson Company Inc., OH, USA) and meshes with successive cut off size were employed to separate bulk granules into different size fractions. The granulated lactose was poured on the top of the vibrating sieve shaker and sieved through the sieves for 30 min. Two size fractions, GL 212-250 μm, and GL 450-600 μm, of granulated lactose (GL) were selected for future experiments. All analysis described afterwards were performed on the sieved samples.

5.2.4 Particle size reduction via jet milling

Jet-milling is the most common milling technique that employs extreme turbulence force to reduce particle size. The turbulence generated from high pressure and velocities and the orbital nature of grinding chamber ensure intensive particle-particle and particle-wall collisions at a high frequency and speed[28]. In this study, rifampicin drug particles were reduced into micro range or nanosize range with jet mill (Glen Mills, Inc.) installed with a vibrating feeder. Samples with different size distributions were collected at chamber surface or collection bag for further analysis by laser diffraction and SEM.

5.2.5 BET analysis

The specific surface area of jet-milled rifampicin was determined by BET analysis. According to Brunauer, Emmett and Teller (BET) theory, the specific surface area of bulk solids could be calculated by the amount of monomolecular layer of adsorbate gas on the surface of the solid. Before performing the surface area analysis, the processed rifampicin powders were firstly degassed under 80 ℃ for 18 hrs to remove contaminants, residues and moistures. Then, a single-point BET method using a Monosorb® surface area analyzer (Quantachrome, FL, USA) via nitrogen adsorption was applied to determine the specific surface area of degassed rifampicin powders. All BET analysis was performed in triplicate.

5.2.6 Scanning electron microscopy

The scanning electron microscopy (SEM; Supra 40VP, Zeiss, Germany) was used to visually assess the particle size and morphology of the granulated lactose and adhesive mixtures before and after impaction. The coating conditions prior to SEM for all the granulated lactose was 15 nm of Pd/Pt via sputter coating.

5.2.7 X-Ray powder diffraction (XRPD)

The crystallinity of the micronized rifampicin and nanosized rifampicin was examined with wide angle XRD. A Philips 1710 X-ray diffractometer with a copper

target (Cu Ka1, k = 1.54056 Å) and nickel filter (Philips Electronic Instruments Inc., Mahwah, NJ) was used to measure the XRD profiles. Samples were analyzed in the 2-theta range from 10 ºto 50 ºunder a step size of 0.05 2-theta degree and a dwell time of 2 s.

5.2.8 Inverse Gas Chromatography

The surface energetics of rifampicin particles with different size distributions were measured using a commercially available IGC system (2000, Surface Measurement Systems Ltd., London, UK). Approximately around 500 mg of each rifampicin sample was loaded into pre-silanized IGC glass columns (300mm x 3 mm i.d.) plugged with glass wool at each end of the column. Prior measurement each column was purged with dry nitrogen at 30 ℃. The retention time of both polar probes (ethyl acetate and chloroform) and nonpolar probes (n-alkanes) were measured at finite dilution conditions. Dispersive and specific surface energy under infinite dilution conditions were extrapolated from the straight lines of elution time in terms of the surface coverage by nonpolar or polar solvents[29].

5.2.9 Preparation of rifampicin/granulated lactose binary blends

Rifampicin (RF) and fractionated granulated lactose were mixed to obtain 30% binary mixtures. All formulations were blended at a constant speed of 46 RPM for 10 min

with a Turbula® orbital mixer (Glen Mills, NJ, USA). Prior to any further analysis, the blended formulations were stored in the dessicator for 5 days.

5.2.10 Drug uniformity test

Five of randomly selected samples (20 ± 1 mg) were taken for measurement of rifampicin content uniformity. The coefficient of variation (CV%) was used to determine the blending uniformity. The test was performed three times. The potency of formulations was calculated by the APIs percent amount to the nominal dose.

5.2.11 *In vitro* aerosolisation study

About 50 (±1) mg mixture powders were filled into size 3 Vcaps HPMC capsules pierced with one enlarged holes (1.2 mm) at each end of the capsule. The *in vitro* aerosolization performance of all formulations was assessed using modified Aerolizer® inhaler device (bent inhaler tube coupled with narrow inlet air passage, Fig) under 44L/min, corresponding to 4kpa pressure drop and 4L air volume.

A 1% (w/v) solution of silicon oil in hexane was applied to precoat the NGI stages for particle re-entrainment prevention. Amounts of rifampicin deposited on the capsule, inhaler, mouthpiece adaptor, induction port, pre-separator and NGI stages were measured and quantified. The drug content was measured by the ultraviolet visible absorption spectroscopy (Infinite M200, TECAN) at 474 nm. The parameters used to evaluate

rifampicin deposition performance were emitted fraction (EF) (Eq. 1), fine particle fraction (FPF) (Eq. 2), respirable fraction (Eq. 3) mass median aerodynamic diameter (MMAD) and geometric standard deviation (GSD).

$$\mathrm{EF} = \frac{\text{emitted dose}}{\text{loading dose}}$$

(Eq. 1)

$$\mathrm{FPF} = \frac{\text{recovered dose of drug particles smaller than 5 μm}}{\text{emitted dose}}$$

(Eq. 2)

$$\mathrm{RF} = \frac{\text{recovered dose of drug particles smaller than 5 μm}}{\text{loading dose}}$$

(Eq.3)

5.2.12 Statistics Analysis

Statistical significance of aerosol performance values was calculated with one-way TTESTs between groups (* indicates $P<0.05$; ** indicates $P<0.005$).

5.3 RESULTS

5.3.1 Particle size distribution and morphology

Three kinds of rifampicin with different particle size distributions are shown in Fig. 1. The original rifampicin crystals (RF form I) (Figure 5.1A) had a rod-like and elongated shape. These columnar rifampicin particles possessed relatively smooth surface with slight surface crevices. During the applied jet milling process, the rods degraded in length and fractured into scattered particles. Depending on the collected positions, the degraded rifampicin crystals were defined as micronized rifampicin (RFMS) and nano-sized rifampicin (RFNS), respectively. Specifically, RFMS were collected at the chamber surface of jet-milling instrument and RFNS were collected from the collection bag. These grinded RFMS and RFNS didn't show similarity to the external form of the original rifampicin particles. Apparently, RFMS and RFNS were composed with aggregated rifampicin particles, especially RFNS. The RFMS powders consisted with larger spherical particles in micron range with relatively small particles attached on the surface. The surface of RFMS was very rough and corrugated (Figure 5.1D) which may come from the intense jet milling process. In contrast, RFNS were made with spherical particles at nano-size range (Figure 5.1C). And the surface of RFNS was smoother than RFMS (Figure 5.1E), perhaps due to a smaller size.

5.3.2 Specific Surface Area

Specific surface area, a property of bulk solids, is the total surface area of a material per unit of mass. Powder materials with smaller size generally have larger specific surface area than larger counterparts. Therefore, the nanosized rifampicin should have larger BET value than micronized rifampicin. As shown in Figure 5.3, the BET value for nanosized rifampicin was 15.15 ± 0.62 m^2/g and the value for micronized rifampicin was only 8.67 ± 0.64 m^2/g.

5.3.3 X-Ray powder diffraction

The crystalline structure of prepared rifampicin samples was analyzed using XRPD. According to the literature, the characteristic peaks of the RF form I exhibited at 13.65 and 14.35 ° 2θ[30]. As shown in Figure 5.4, both RFMS and RFNS showed identical characteristic peaks at 13.65 and 14.35 ° 2θ, although the intensity peaks of milled rifampicin (RFMS and RFNS) were slightly lower than that of the pure RF form I. Also, the intensity peaks of RFNS were a little lower than RFMS, but not significantly different. Thereby, the two processed rifampicin had same polymorphic form with RF form I. Despite not significant, the amorphous content of the three rifampicin powders was in the order of: RFNS > RFMS > original rifampicin crystals.

5.3.4 Inverse gas chromatography

Inverse gas chromatography is an objective analytical technique to measure surface properties of bulk solids. Based on the retention volume and elution time of a series of polar and non-polar organic solvent probes on the surface of the powder materials, the dispersive surface energy (γ_d) and acid-base surface energy (γ_{ab}) can be determined. In Table 5.1, the surface energy of RFNS were slightly higher than RFMS, in terms of dispersive surface energy (28.27 mJ/m^2 vs 27.41 mJ/m^2), acid-base surface energy (8.50 mJ/m^2 vs 6.07 mJ/m^2), total surface energy (36.76 mJ/m^2 vs 33.48 mJ/m^2) as well as the work of cohesion. The higher surface energy values may be contributed by the amorphous content on the surface of RFNS. [31]

5.3.5 Blending uniformity

The blending uniformity of dry powder mixtures depends on the properties of both rifampicin and lactose particles. When the size fraction of granulated lactose was fixed, blending uniformity reduced with a decreased rifampicin particle size. The blending uniformity with 30% RFNS was generally larger than that with 30% RFMS. And among them, granulated lactose with larger size fractions had a better blending uniformity than smaller counterparts. Although ML006 is commercial available inhalation grade lactose, the blending uniformity of the two kinds of rifampicin in this study with ML006 was not better than granulated lactose. Nevertheless, the effect of rifampicin particle size on blending uniformity with ML 006 was different from granulated lactose. While 30%

RFMS had a better mixture homogeneity than 30% RFNS with granulated lactose, 30% RFMS (RSD%: 13.51%) blended with ML006 provided a much worse uniformity than 30% RFMS (RSD%: 32.52%).

5.3.6 *In Vitro* Aerosol Characterization

5.3.6.1 Effect of device design on aerosol performance

With the combined modified inhaler pieces (Figure 5.5B), the amount of micronized rifampicin trapped in the induction port decreased from 31.8% to 12.4% and FPF increased from 42.8% to 48.0%. The downside of the combined inhaler is a higher loss of drugs in the device, leading to a reduced EF to 73.7% from 90.3%.

5.3.6.2 Effect of rifampicin size on aerosol performance

Evaluation of the formulations containing RFMS or RFNS blended with granulated lactose indicated RFNS had better aerosol performance than RFMS (Figure 5.5). The FPF of RFNS was 70.7 ± 3.9 % when formulated with GL 212-250 μm, compared with merely 48.0 ± 1.6 % from RFMS formulation. RFNS formulated with GL 212-250 μm also had a higher EF (82.6 ± 1.7 %) than RFMS equivalents (73.7 ± 1.9 %). As shown in Fig. 5b, both formulations had good enough flowability, to be fluidized by inhalation effort and exit freely out of the capsule. Actually, the improved EF of 30%RFNS+

GL212-250μm mainly resulted from significantly decreased deposition in the device tube, although device chamber trapped slightly higher amount of rifampicin. Although RFNS detached from GL212-250μm was less than RFMS, there was less RFNS trapped in the induction port and along with that the overall rifampicin deposited in the stages shifted to lower cut off size. Specifically, the MMAD of 30%RFNS+GL212-250μm was 2.46 ± 0.28 μm and the MMAD of 30%RFMS+GL212-250μm was 4.04 ± 0.12 μm. Consequently, there are two factors, fewer drugs deposited in the induction port and smaller MMAD, contributing to higher FPF of 30%RFNS+GL212-250μm than 30%RFMS+GL212-250μm. RFNS and RFMS blended with ML006 as mentioned had similar trend with GL212-250um. The reason for high FPF and high EF of RFNS mixed with ML006 was also similar as above: as shown in Figure 5.6b, fewer rifampicin deposited in the device tube, induction port with a smaller MMAD value. Even if RFNS and RFMS were mixed with ML006 (Figure 5.6), the inhalation grade lactose, a similar trend was still observed, where RFNS (47.5 ± 2.0 %) had a higher FPF value than RFMS (28.2 ± 3.1 %) and the EF of RFNS and RFMS was 78.2 ± 1.6 % and 68.9 ± 5.1 %, respectively (Fig. 6a).

5.3.6.3 Comparison of granulated lactose with traditional inhalation grade lactose

Rifampicin with a smaller particle size (RFNS) was superior to rifampicin with larger size (RFMS) in achieving a much better aerosol performance. Thus RFNS was blended with different lactose carriers, GL212-250 μm and Respitose ML006, respectively for further study. Respitose ML006 is a typical inhalation grade lactose for

maximizing aerosolization performance, but the aerosol performance of 30% RFNS mixed with ML006 was much worse than with GL212-250 μm. Figure 5.7a showed that 30%RFNS+GL212-250μm had both better EF (82.6 ± 1.7 % vs. 78.2 ± 1.6 %) and FPF (70.7 ± 3.9 % vs. 47.5 ± 2.0 %) than 30%RFMS+ML006. Reduced deposition in device tube resulted in increased EF. And reduced deposition in induction port and increased deposition in latter stages of NGI were the reasons of higher FPF.

5.3.6.4 Effect of different size fractions of granulated lactose on aerosol performance

Although 30%RFNS+GL212-250μm had the highest aerosol performance among the four evaluated formulations, the blending uniformity of 30% RFNS with GL212-250μm was not good enough, similar to the uniformity of 30%RFNS mixed with ML006. According to Table 5.2, GL425-600μm was better than GL212-250μm in improving the blending uniformity. Thus, the aerosol performance of GL425-600μm mixed with 30%RFNS was investigated. From Figure 5.8a, it was found that the fine particle fraction (FPF) generated from 30%RFNS+GL425-600μm was comparable to 30%RFNS+GL212-250μm. Nevertheless, the emitted fraction (EF) of 30%RFNS+GL425-600μm was much smaller, merely 76.0 ± 4.1%, owing to higher amount of RFNS trapped in the capsule (Figure 5.8b).

5.4 DISCUSSION

5.4.1 Particle size distribution and morphology

Bulky micronized rifampicin (RFMS) and nano-sized rifampicin (RFNS) powders were both obtained by jet-milling under the same process parameters. But, RFMS and RFNS were collected at different positions from jet-milling instrument. RFMS was recovered from chamber surface, while RFNS was collected from collection bag. The place where milled particles deposit depends on the drag force from flow stream and particle weight. Theoretically, particles collected from bag (e.g. RFNS) should be smaller than from chamber (e.g. RFMS). All rifampicin were processed under the same parameters and collected from the same batch, so drug force in the jet-milling instrument was the same for all milled particles. The weight of milled particle is the only factor determining the final deposition position. Consequently, the smaller the milled particle, the longer distance it will travel through jet milling instrument and more possible it will be deposited in the collection bag.

As displayed in Figure 5.1 and Figure 5.2, both RFMS and RFNS have achieved size small enough via jet milling for pulmonary delivery, and as presumed, RFNS had much smaller size than RFMS. Specific surface area is the total surface area of powders per unit of mass. Particles with small geometric size tend to have a large specific surface area. According to the BET data, RFNS had a significantly larger specific surface area than RFMS (Figure 5.3), which is consistent with the laser diffraction results of RFNS and RFMS.

Nevertheless, particle size observed from SEM and particle size distribution measured by Sympatec didn't match each other very well, especially for RFNS. The size observed for RFNS was much smaller than what was measured from Sympatec. This is because RFNS tended to form relatively strong agglomerates and could not be dispersed into primary particles efficiently prior Sympatec measurement. There are two reasons for the cohesiveness of RFNS in forming strong agglomerates. Firstly, RFNS particles had a relatively high surface energy (Table 5.1) as a result of more amorphous content (Figure 5.4) generated on the surface after jet-milling. Secondly, RFNS was smaller than RFMS, so the weight force of RFNS is smaller than RFMS. The weight force of RFNS therefore contributed less than that of RFMS in breaking the RFNS particle-particle interaction, resulting in a higher tendency in forming agglomerates.

5.4.2 Physicochemical characteristics

One objective of this study is to evaluate the influence of drug size on the aerosol performance of DPI formulations. To study the effect of size, it is necessary to keep other physicochemical properties of the two milled rifampicin particles similar. Jet-milling used in this study is a milling process that employs extreme turbulence force from high pressure and air flow velocities to induce particle fracture and size reduction.[28] There is no solvent used in jet milling process, crystallization or significant structural change won't happen. Consistent with this technique, after jet milling, both RFMS and RFNS still kept same characteristic peaks (13.65 and 14.35 ° 2θ) as the RF form I.

If enough energy is imparted during milling process, total/partial crystallinity loss, or local amorphous domains may be generated.[32, 33] Therefore, although milling didn't induce polymorphic conversion of rifampicin particles, the milled samples lost partial crystallinity or obtained amorphous domains on particle surface to some extent (Figure 5.4), ultimately leading to slightly increase in surface energy, particularly RFNS particles (Figure 5.3).

5.4.3 Blending uniformity

Blending uniformity is the potential factor critical to dosing consistency of drug product, such as DPI formulations. It was found in previous research that the blending uniformity of drugs with granulated lactose is relevant with the filling extent of the granule valleys, which is determined further by drug loading and bulk density[34]. The bulk and tapped density of RFMS in this study was 0.20±0.01 mg/ml and 0.33±0.01 mg/ml, respectively. As a result of high surface electrostatic charge, RFNS had a smaller bulk (0.14±0.01 mg/ml) and tapped density (0.22±0.01 mg/ml). Also, it was known before 30% RFMS was already enough to fill the granule valleys of the granules used in this study. Consequently, when 30% RFMS and 30% RFNS were loaded into granules with same size fraction to completely fill the volume of granule valleys, there would be much more excessive RFNS outside the valley and tend to separate from granules, resulting in poorer blending uniformity than RFMS. It is not surprisingly to notice that when ML006 is used as the lactose carrier, the blending uniformity, no matter mixed with 30% RFMS or 30%

RFNS, was very poor. The small size, cohesive nature of ML006 leads to poor flow, poor dispersion, and subsequently poor blending uniformity.[35]

5.4.4 Dry powder formulation and the aerodynamic properties

5.4.4.1 Effect of device design on aerosol performance

Chapter 4 studied the effect of different high loaded APIs on granulated lactose based DPI formulations. It was found that 30% micronized rifampicin (RFMS) had much smaller aerosol performance (lower FPF) than 30% micronized salbutamol sulfate when both formulated with granulated lactose carrier under same size fractions. The reduced aerosol performance of micronized rifampicin was explained by large amount of deposition loss in the induction port. Similar induction deposition phenomenon has also been observed with pressurized metered dose inhalers (pMDI), a propellant driven device which generates a high aerosol velocity and needs coordination between patients and device. To reduce oropharyngeal deposition and increase lung deposition of pMDI, distance has been placed by auxiliary spacer between the point of aerosol generation and the patient's mouth[36]. The bent mouthpiece of modified inhaler acted as the spacer similar to the effect on pMDI, resulting in reduced deposition in the induction port and thus improved aerosol performance.

5.4.4.2 Inhalation grade lactose versus granulated lactose

To reconcile the different effect of inhalation grade lactose and granulated lactose carrier on aerosol performance, it is proposed that significant large granulated particles are better than small and smooth carriers to break up and prevent formation of agglomerates. Two types of drug agglomerates are present in the DPI formulations: A) natural agglomerates in pure drugs and B) mixing drug agglomerates when drug and carrier particles are blended[37]. Larger carriers have the potential to break up natural drug agglomerates due to the greater mass and better flowability. While larger carrier particles with smooth surface and small specific surface area can induce mixing agglomerates and strong drug particle interactions, the significantly large granulated lactose with greater specific surface area inhibits formation of strong blending agglomerates.

5.5 CONCLUSION

A high drug loaded (30%) rifampicin DPI formulation was developed, which is a simple binary mixture of significantly large granulated lactose carrier with nanosize rifampicin particles (RFNS). DPI is very complicated and the performance is the interplay of formulation, device and patient inspiratory effort. To maximize the aerosol performance, a previously developed combined device was used to evaluate the formulation in this study. The maximum FPF achieved for this formulation with modified Aerolizer device was 70.7%. Upon inhalation, these rifampicin aerosols could deposit predominately in the central and peripheral regions with a minimal amount in the oropharyngeal area. Additionally, the developed rifampicin formulation has better flowability than commercial inhalation grade lactose based rifampicin formulation.

5.6 TABLES

Table 5.1 Surface energy parameters of RFMS and RFNS measured by inverse gas chromatography

	γ_d (mJ/m^2)	γ_{ab} (mJ/m^2)	γ_t (mJ/m^2)	W_{coh} (Dispersive)	W_{coh} (Specific)	W_{coh} (Total)
RFMS	27.41	6.07	33.48	54.82	12.13	66.95
RFNS	28.27	8.50	36.76	56.53	16.99	73.52

Table 5.2 Blending uniformity of rifampicin with granulated lactose or inhalation grade lactose

	ML006	GL 212-250 μm	GL 425-600 μm
30% RFMS	32.52%	4.02%	3.90%
30% RFNS	13.51%	15.24%	9.30%

5.7 FIGURES

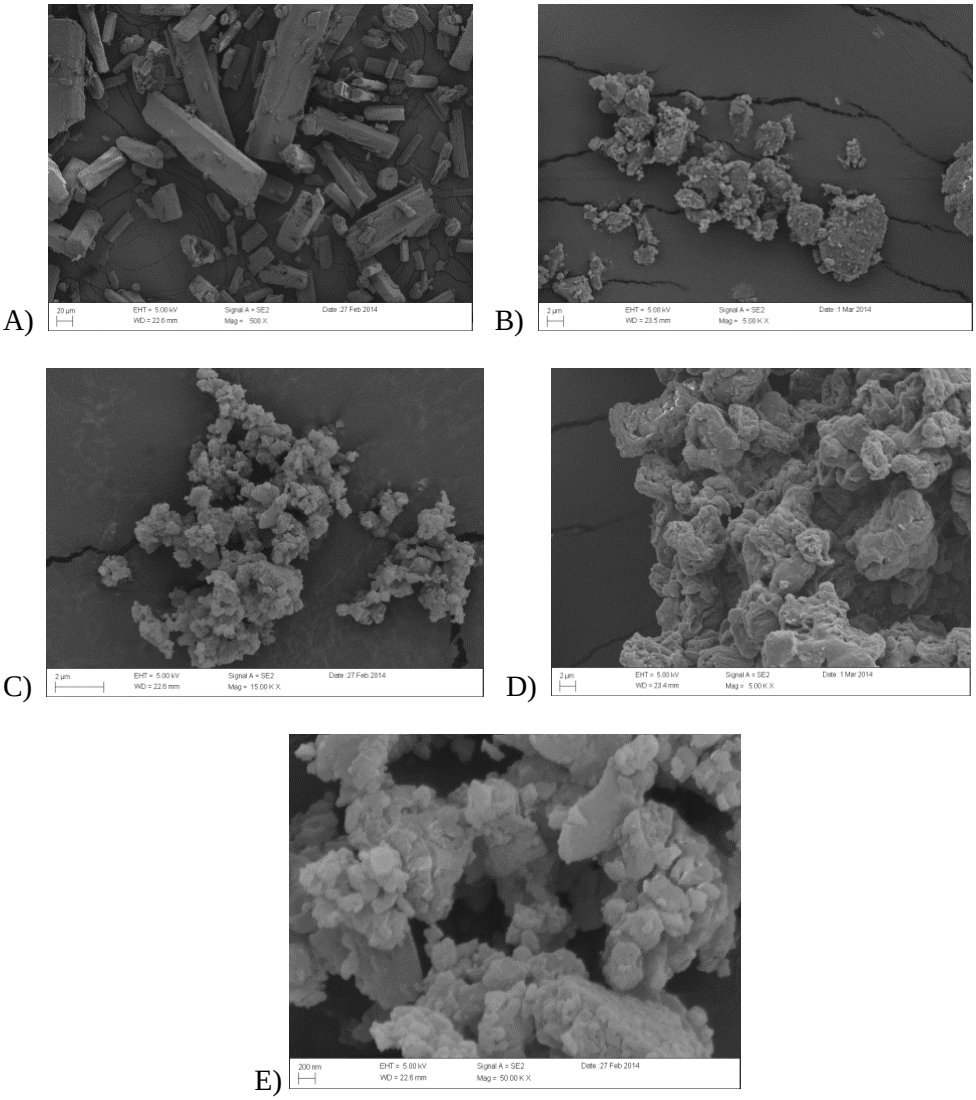

Figure 5. 1 Scanning electron microscopy images of (A) RF form I, (B) RFMS, and (C) RFNS, (D) RFMS under a higher resolution and (E) RFNS, under a higher resolution.

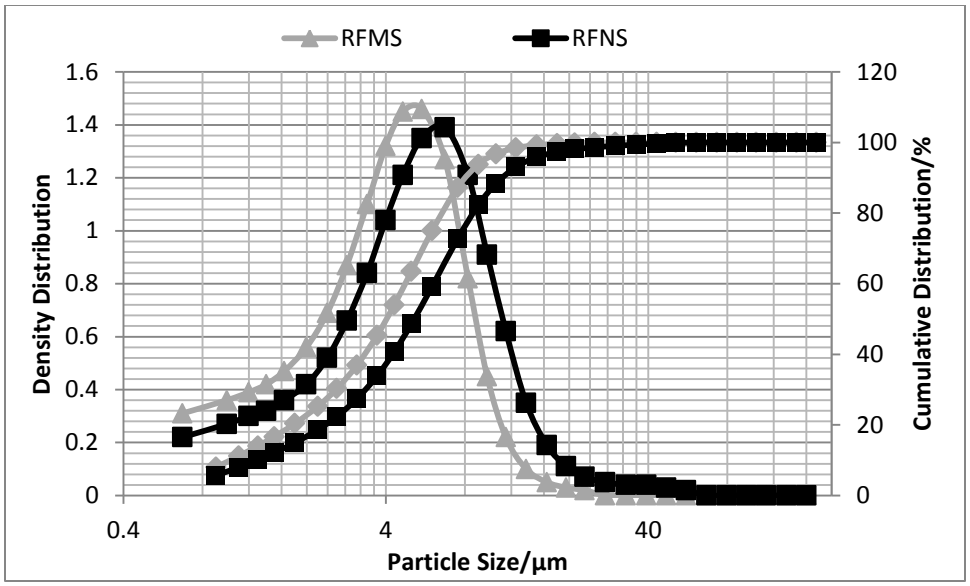

Figure 5.2 Particle size distribution of RFMS and RFNS.

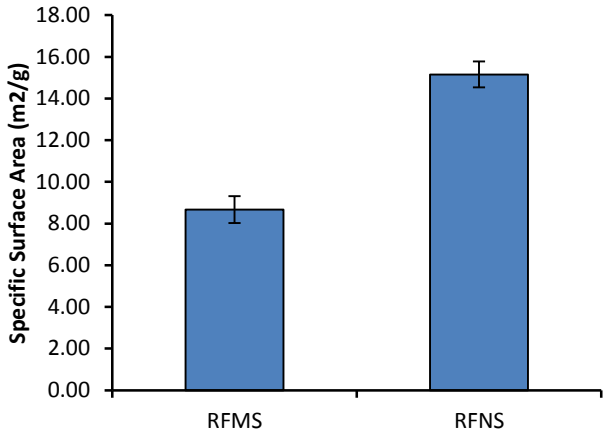

Figure 5.3 BET surface area and density of micronized rifampicin (RFMS) and nanosized rifampicin (RFNS)

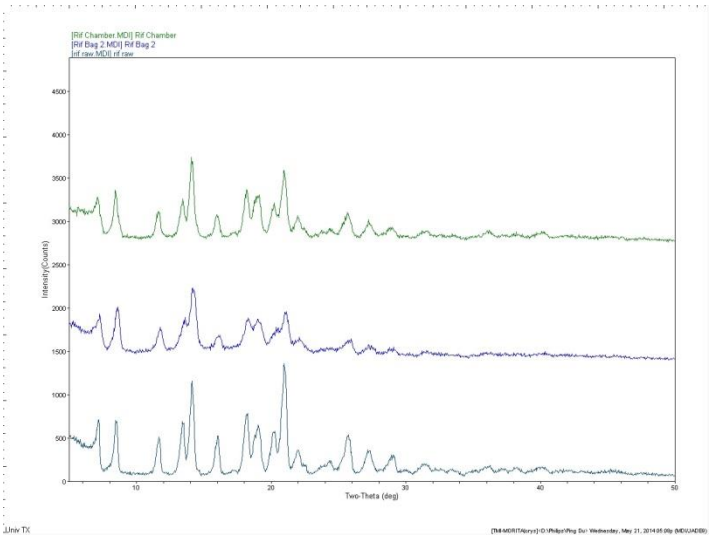

Figure 5.4 Powder X-ray diffractograms of (a) RF form I, (b) RFNS, (c) RFMS.

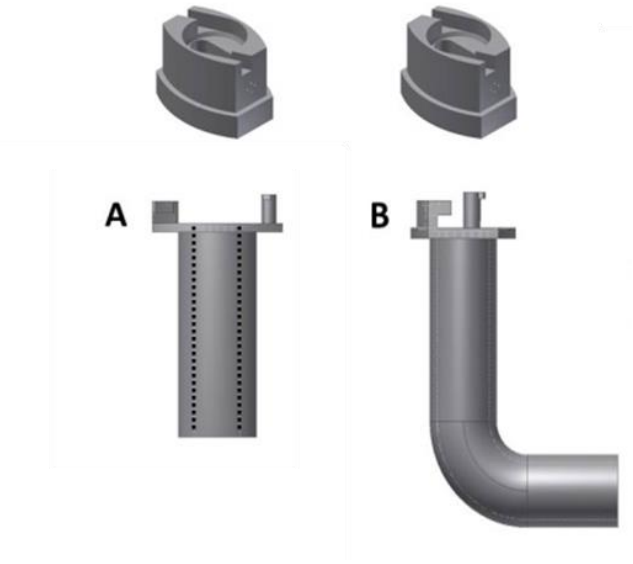

Figure 5.5 A) Original device and B) modified device with bent inhaler tube and reduced air inlet passage.

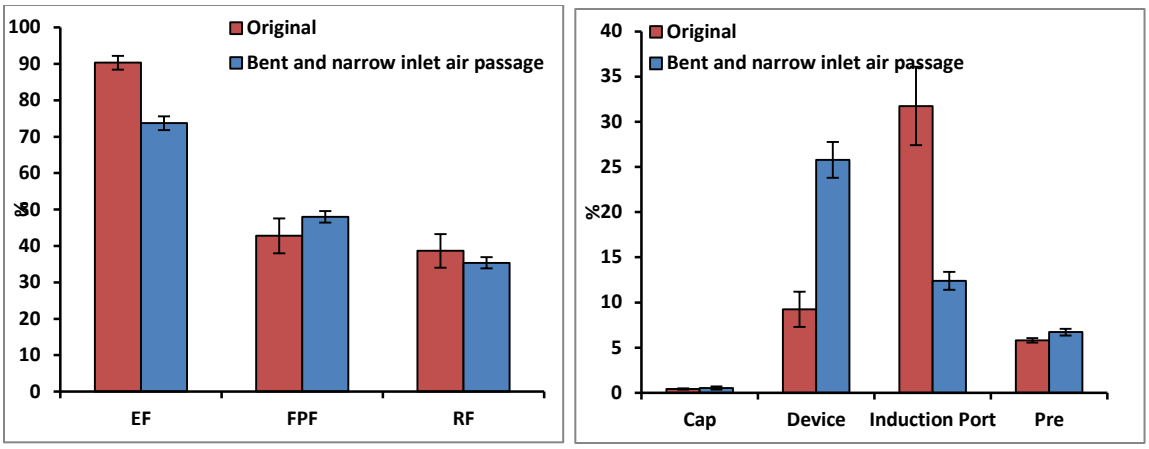

Figure 5.6 Effect of bent mouthpiece on (a) *in vitro* aerosol performance and (b) aerosol deposition of GL 212-250 μm mixed formulation on each stage of the next generation impactor (n=3).

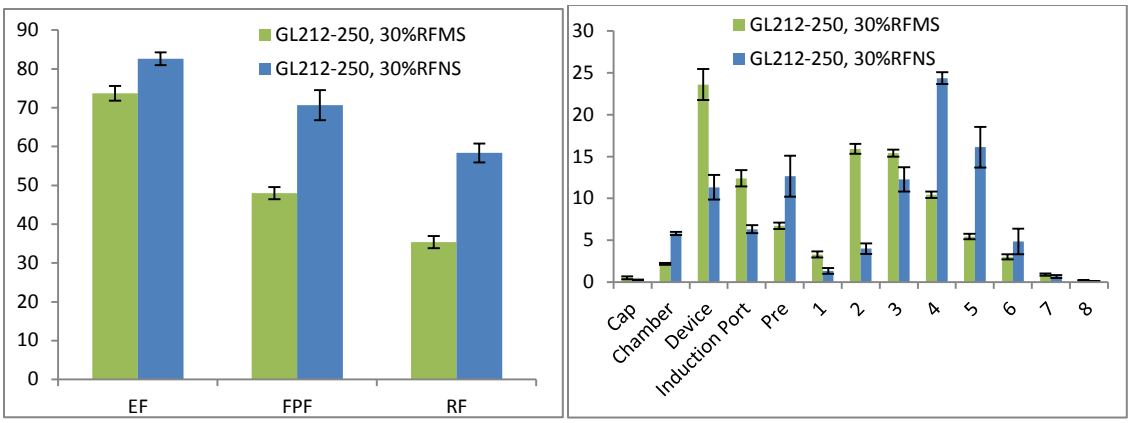

Figure 5.7 Effect of rifampicin size on (a) *in vitro* aerosol performance and (b) aerosol deposition of GL 212-250 μm mixed formulation on each stage of the next generation impactor via modified inhaler (n=3)

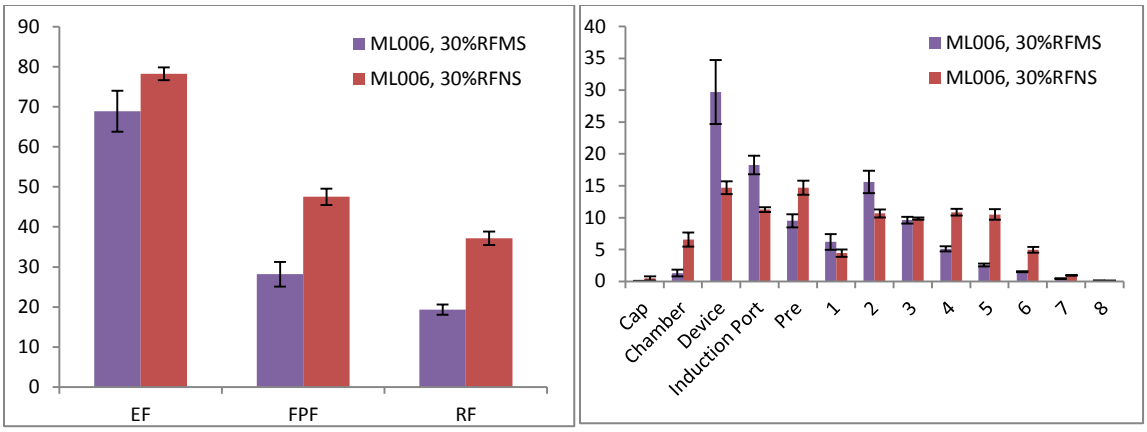

Figure 5.8 Effect of rifampicin size on (a) in vitro aerosol performance and (b) aerosol deposition of ML006 mixed formulation on each stage of the next generation impactor via modified inhaler (n=3)

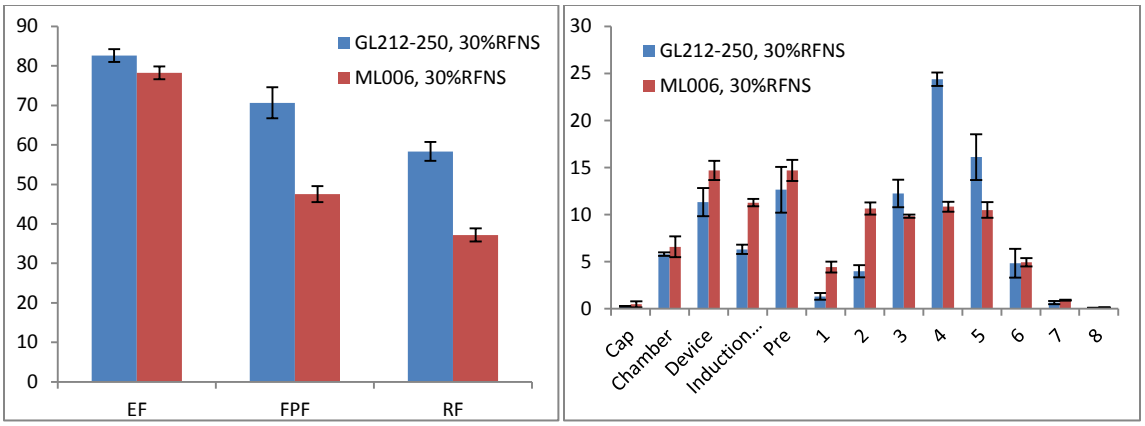

Figure 5.9 Effect of carrier lactose on (a) *in vitro* aerosol performance and (b) aerosol deposition of 30% RFNS based formulation on each stage of the next generation impactor via modified inhaler (n=3)

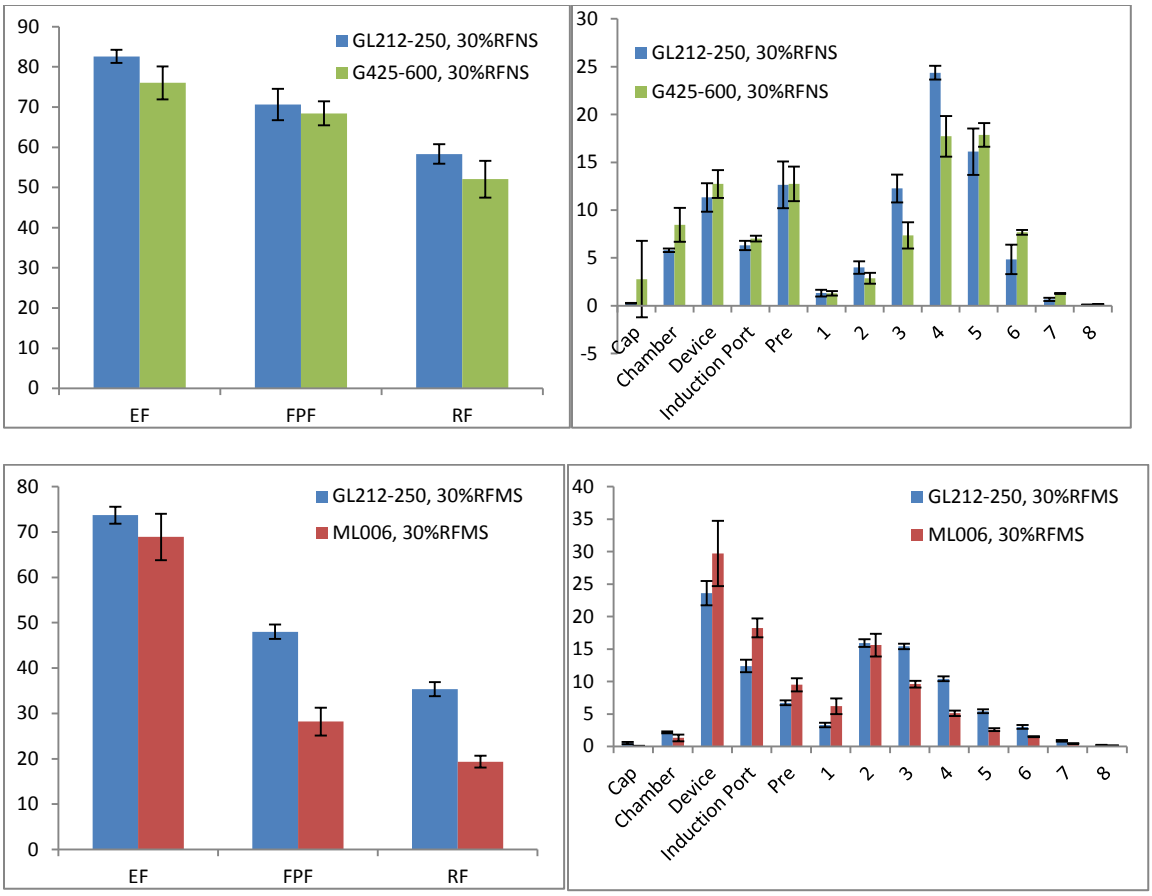

Figure 5.10 Effect of carrier lactose on (a) *in vitro* aerosol performance and (b) aerosol deposition of 30% RFMS based formulation on each stage of the next generation impactor via modified inhaler (n=3)

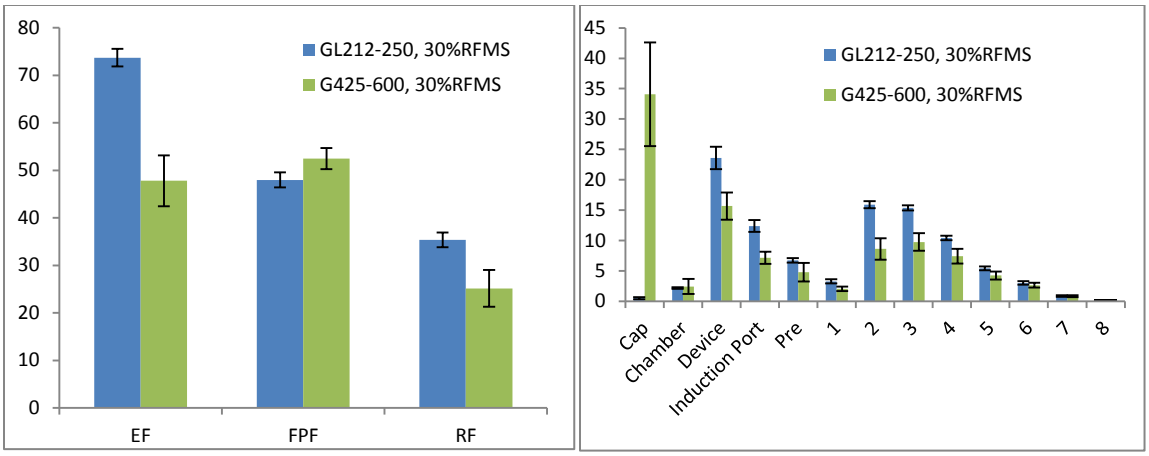

Figure 5.11 Effect of granulated lactose size on (a) *in vitro* aerosol performance and (b) aerosol deposition of 30% RFMS based formulation on each stage of the next generation impactor via modified inhaler (n=3)

5.8 REFERENCES

1. Global tuberculosis control: surveillance, planning, financing: WHO report 2012.

2. Lusignani LS, Quaglio G, Atzori A, Nsuka J, Grainger R, Palma MDC, et al. 2013. Factors associated with patient and health care system delay in diagnosis for tuberculosis in the province of Luanda, Angola. BMC Infectious Diseases 13:168.

3. Becher RD, Hoth JJ, Rebo JJ, Kendall JL, Miller PR. 2012. Locally derived versus guideline-based approach to treatment of hospital-acquired pneumonia in the trauma intensive care unit. Surg Infect (Larchmt). 13:352-9.

4. 2015. Nationwide survey of anti-tuberculosis drug resistance in Japan. Int J Tuberc Lung Dis. 19:157-62.

5. Joukhadar C, Derendorf H, Muller M. 2001. Microdialysis. A novel tool for clinical studies of anti-infective agents. Eur J Clin Pharmacol. 57:211-9.

6. Herkner H, Muller MR, Kreischitz N, Mayer BX, Frossard M, Joukhadar C, et al. 2002. Closed-chest microdialysis to measure antibiotic penetration into human lung tissue. Am J Respir Crit Care Med. 165:273-6.

7. Muttil P, Wang C, Hickey AJ. 2009. Inhaled drug delivery for tuberculosis therapy. Pharm Res. 26:2401-16.

8. Dube D, Agrawal GP, Vyas SP. 2012. Tuberculosis: from molecular pathogenesis to effective drug carrier design. Drug Discov Today. 17:760-73.

9. Schreiber J, Zissel G, Greinert U, Schlaak M, Muller-Quernheim J. 1999. Lymphocyte transformation test for the evaluation of adverse effects of antituberculous drugs. Eur J Med Res. 4:67-71.

10. Hagerman JK, Hancock KE, Klepser ME. 2006. Aerosolised antibiotics: a critical appraisal of their use. Expert Opin Drug Deliv. 3:71-86.

11. Smyth HD, Hickey AJ. Advances in Delivery Science and Technology: Controlled Release Society; 2011.

12. Giry K, Pean JM, Giraud L, Marsas S, Rolland H, Wuthrich P. 2006. Drug/lactose co-micronization by jet milling to improve aerosolization properties of a powder for inhalation. Int J Pharm. 321:162-6.

13. Zhang Y, Wang X, Lin X, Liu X, Tian B, Tang X. High azithromycin loading powders for inhalation and their in vivo evaluation in rats. Int J Pharm. 395:205-14.

14. Son YJ, McConville JT. 2011. A new respirable form of rifampicin. Eur J Pharm Biopharm. 78:366-76.

15. Young PM, Wood O, Ooi J, Traini D. 2011. The influence of drug loading on formulation structure and aerosol performance in carrier based dry powder inhalers. Int J Pharm. 416:129-35.

16. Suarez S, O'Hara P, Kazantseva M, Newcomer CE, Hopfer R, McMurray DN, et al. 2001. Respirable PLGA microspheres containing rifampicin for the treatment of tuberculosis: screening in an infectious disease model. Pharm Res. 18:1315-9.

17. O'Hara P, Hickey AJ. 2000. Respirable PLGA microspheres containing rifampicin for the treatment of tuberculosis: manufacture and characterization. Pharm Res. 17:955-61.

18. Sung JC, Padilla DJ, Garcia-Contreras L, Verberkmoes JL, Durbin D, Peloquin CA, et al. 2009. Formulation and pharmacokinetics of self-assembled rifampicin nanoparticle systems for pulmonary delivery. Pharm Res. 26:1847-55.

19. Pilcer G, Amighi K. 2010. Formulation strategy and use of excipients in pulmonary drug delivery. Int J Pharm. 392:1-19.

20. Suarez S, O'Hara P, Kazantseva M, Newcomer CE, Hopfer R, McMurray DN, et al. 2001. Airways delivery of rifampicin microparticles for the treatment of tuberculosis. J Antimicrob Chemother. 48:431-4.

21. Kou X, Chan LW, Steckel H, Heng PW. 2012. Physico-chemical aspects of lactose for inhalation. Adv Drug Deliv Rev. 64:220-32.

22. Du P, Du J, Smyth HD. 2014. Evaluation of Granulated Lactose as a Carrier for DPI Formulations 1: Effect of Granule Size. AAPS PharmSciTech. 15:1417-28.

23. Kawashima Y, Serigano T, Hino T, Yamamoto H, Takeuchi H. 1998. Effect of surface morphology of carrier lactose on dry powder inhalation property of pranlukast hydrate. 172:188.

24. Li J, Tao L, Buckley D, Tao J, Gao J, Hubert M. 2013. The Effect of the Physical State of Binders on High-Shear Wet Granulation and Granule Properties: A Mechanistic Approach to Understand the High-Shear Wet Granulation Process. Part IV. The Impact of Rheological State and Tip-speeds. J Pharm Sci. 102:4384-94.

25. Fujiwara M, Dohi M, Otsuka T, Yamashita K, Sako K. 2013. Influence of binder droplet dimension on granulation rate during fluidized bed granulation. Chem Pharm Bull (Tokyo). 61:320-5.

26. Ogawa T, Uchino T, Takahashi D, Izumi T, Otsuka M. 2012. Pharmaceutical production of tableting granules in an ultra-small-scale high-shear granulator as a pre-formulation study. Drug Dev Ind Pharm. 38:1390-3.

27. Mangwandi C, Adams MJ, Hounslow MJ, Salman AD. 2012. An investigation of the influence of process and formulation variables on mechanical properties of high shear granules using design of experiment. Int J Pharm. 427:328-36.

28. Saleem IY, Smyth HD. 2010. Micronization of a soft material: air-jet and micro-ball milling. AAPS PharmSciTech. 11:1642-9.

29. Saleem I, Smyth H, Telko M. 2008. Prediction of dry powder inhaler formulation performance from surface energetics and blending dynamics. Drug Dev Ind Pharm. 34:1002-10.

30. Agrawal S, Ashokraj Y, Bharatam PV, Pillai O, Panchagnula R. 2004. Solid-state characterization of rifampicin samples and its biopharmaceutic relevance. Eur J Pharm Sci. 22:127-44.

31. Csiszar E, Fekete E, Toth A, Bandi E, Koczka B, Sajo I. 2013. Effect of particle size on the surface properties and morphology of ground flax. Carbohydr Polym. 94:927-33.

32. Ward GH, Schultz RK. 1995. Process-induced crystallinity changes in albuterol sulfate and its effect on powder physical stability. Pharm Res. 12:773-9.

33. Descamps M, Willart JF, Dudognon E, Caron V. 2007. Transformation of pharmaceutical compounds upon milling and comilling: the role of T(g). J Pharm Sci. 96:1398-407.

34. Du P, Du J, Smyth HDC. Evaluation of granulated lactose as a carrier for DPI formulations 2: Effect of Drug Loading.

35. Han X, Ghoroi C, Dave R. 2013. Dry coating of micronized API powders for improved dissolution of directly compacted tablets with high drug loading. Int J Pharm. 442:74-85.

36. Hirst PH, Bacon RE, Pitcairn GR, Silvasti M, Newman SP. 2001. A comparison of the lung deposition of budesonide from Easyhaler, Turbuhaler and pMDI plus spacer in asthmatic patients. Respir Med. 95:720-7.

37. Dickhoff BH, de Boer AH, Lambregts D, Frijlink HW. 2005. The interaction between carrier rugosity and carrier payload, and its effect on drug particle redispersion from adhesive mixtures during inhalation. Eur J Pharm Biopharm. 59:197-205.

APPENDIX A: *In vitro* models with simulated tear flow for screening topical ocular formulations

Abstract

The objective of this work was to establish an *in vitro* ocular clearance model to simulate specifically the physiological process of lacrimation and tear flow in the eye to enable screening for sustained release topical ophthalmic formulations. A solution formulation and gel-forming solution formulation, with extensive prior in vivo pharmacokinetic data were selected as model formulations used to assess the eye clearance model. Both formulations had an equivalent strength of timolol (Timolol Maleate Ophthalmic Solution and Timolol GFS™). The experiments were performed with simulated induced lacrimation and tear flow. In the study, using Transwell™ diffusion cells, 200 µl basolateral and 60 µl apical samples were taken and replaced with blank medium every 15 minutes for 3 hours. We evaluated the utility of the polycarbonate membrane (PC) model and a model air-liquid interfacial epithelium cell culture model for evaluating timolol retention, clearance and permeation. Transepithelial electrical resistance (TEER) values were measured before and after treatment to assess the integrity of the polycarbonate membrane (PC) and cell layers throughout the experiments. UV spectrophotometer was used to measure all the samples at a wavelength of 295 nm. The *in vitro* results of timolol elimination and diffusion had good correlation

with published in vivo pharmacokinetic data. The developed *in vitro* model shows potential for screening retention and absorption of topical ocular formulations.

Keywords

timolol; ocular drug delivery; polycarbonate membrane model; cell model; induced lacrimation; simulated tear flow; diffusion; elimination; precorneal residence; IVIVC

A.1 INTRODUCTION

In 2009, the global ophthalmic pharmaceutical market size reached $14 billion (US).[1, 2] It is expected that the overall market of ophthalmic therapeutics will grow consistently and considerably during the next decade.[2] Eye drops, accounted for 90% of marketed ophthalmic formulations, is the most convenient noninvasive administration and patient compliance route.[3-5] An eye drop solution is instilled to the eye to treat anterior segment diseases. The anterior segment diseases include, but not limited to, glaucoma, allergic conjunctivitis, anterior uveitis and cataract.

Although topical instillation is very popular, the bioavailability is notoriously poor, typically less than 5%.[2, 6] This is a consequence of sophisticated eye structure and effective eye clearance system.[7] Of the anterior segment, the cornea layer is the main barrier for topically applied drugs, which comprises the epithelium, stroma and endothelium layers.[8] Even though the stroma and endothelium constitute 80-90% of the total cornea mass and volume, the cornea epithelium is the permeation rate-limiting barrier of hydrophilic drugs. This is because the cornea epithelium is composed with two to three layers of flattened superficial cells, and wing cells, as well as a single layer of columnar basal cells. The superficial cells also adhere to each other via desmosomes and are enrcircled by tight junctions.[9] In addition to permeation barriers, therapeutic agents are rapidly removed from the eye surface via lacrimation,[10] nasolacrimal drainage, blinking reflex, tear turn over, tear flow (4 µl/min) and clearance from the vasculature in the conjunctiva.[10, 11] Whereas, increasing the dosing frequency of eye drops to overcome

clearance significantly reduces patient compliance, especially to patients with glaucoma (REFS – see Matt). Collectively, these represent significant challenges to the clinically effective delivery of drugs at the appropriate therapeutic dose to the target ocular tissue efficiently. In response to these well known barriers, efforts have been made to overcome the permeability barriers and clearance mechanisms, so as to improve drug contact time, and thus improve ocular bioavailability of therapeutics. These approaches for topical delivery to anterior segment include gel or gel-forming technologies, pro-drug development with improved physicohemical properties for permeation enhancement, solubilization agents, nanoparticle technologies, and microdroplets, among others.[4] As more therapeutic candidates are identified and existing drugs are reformulated, it is essential to have cost effective, predictive, and simple tools available to screen, op evaluate and these systems prior to in vivo testing. Although animal studies and *ex vivo* studies with excised cornea tissue from animals are widely used,[12, 13] they have well recognized disadvantages that include high costs, uncontrolled variability, are of different species, and the presence of ethical issues.[13, 14] The success of in vitro cell models such as EpiOcular® and others illustrates the potential of using human cell based 3D models in ocular drug delivery screening.

Several *in vitro* cell models consisted with cornea epithelium cells and 3D reconstituted human cornea equivalents have been developed (REFS). Several were initially developed to enable testing of the potential for eye irritation.[15] There are also some cornea models or 3D cornea equivalents developed and used in drug absorption and metabolism studies.[13, 14, 16, 17] Up to now, however, no *in vitro* models have been established with induced tear flow or tear dilution for the evaluation of both precorneal

residence and diffusion of topical ophthalmic formulations.[11] Since the low precorneal residence time, caused by induced lacrimation, eye blink, tear dilution and constant tear flow,[10] also prevents the absorption of ocular formulations besides the barrier of tight cornea, low precorneal retention should be included in the *in vitro* models to improve the model. Therefore, the objective of this study was to develop a simple *in vitro* screening tool that can be used for evaluation of precorneal residence and absorption of topical ocular formulations simultaneously. Our hypothesis is that modified diffusion models that simulate induced lacrimation, tear fluid clearance rates/volumes will allow good correlation with ophthalmic *in vivo* pharmacokinetic data.[18] Induced lacrimation is commonly experienced when applying topical ocular formulations (e.g. eye drops) to the eyes. Generally, 60 µl is the induced lacrimation drainage volume.[10]

To address these goals, we used a well characterized system (timolol formulations) to evaluate our developed *in vitro* membrane based screening tool. Commercially available timolol marketed as Timolol Maleate Ophthalmic Solution (0.5%),[19] and Timolol GFS (0.5%)[20] were used. Timolol Maleate Ophthalmic Solution is the traditional simple eye drop, while Timolol GFS stands for timolol maleate gel forming solution. Upon contact with the precorneal tear film, Timolol GFS forms a gel with increased precorneal contact time and improved absorption through the cornea.[21] These Timolol Maleate Ophthalmic Solution and Timolol GFS have been investigated in an *in vivo* rabbit model previously.[22] Our developed in vitro model attempted to provide simple methodology to allow simulation of (1) induced lacrimation as a result of drop instillation into the eye, (2) lacrimal drainage, (3) baseline lacrimation and tear flow, and (4) permeation from the apical surface.

A.2 EXPERIMENTAL

A.2.1 Materials

The two formulations evaluated in this study were Timolol Maleate Ophthalmic Solution (0.5%) and Timolol GFS (0.5%) (Falcon Pharmaceuticals, Ltd, Texas, USA).[19, 20] All other chemicals and solvents were of reagent grade. The Calu-3 Lung Epithelium Cells were purchased from ATCC. Polycarbonate membrane (Whatman® Schileicher&Schuell) used had 50 nm pore size. 12-Well Transwell® Inserts were (surface area, 4.7 cm^2; pore size, 0.4 mm; Transwell Clear; Sigma, USA) purchased from Sigma.

Transwell®, the permeable supports was used to provide the air-liquid interface for epithelial cells to differentiate to higher levels with morphology and function close to the *in vivo* counterparts.[32] It is consisted with donor chamber and receiver chamber, from which the apical sample and basolateral sample are withdrawn for 'precorneal residence' and diffusion analysis.[31] Transwell® with clear inserts was chosen to provide better cell visibility and allow for assessment of monolayer formation.[31]

A.2.2 Polycarbonate (PC) Model

The Nuclepore Track-Etch Polycarbonate Membranes (0.05 μm) (Whatman Scheicher&Schuell) were glued underneath the transwell inserts to mimic the artificial

precorneal membrane. The TEER value of the PC membrane was measured by Millipore (Millicell®ERS) to be around 20-25 Ω●cm^2.

A.2.3 Cell Culture

Calu-3 Lung Epithelium Cell lines (purchased from ATCC®) with passage number of 13-15 were seeded on the transwell inserts at a concentration of 90,000 cells/cm^2 and were grown in the standard medium. Both the receiver chamber and donor chamber were filled with the standard medium, Minimum Essential Medium (MEM, Sigma, USA) supplemented with 10% heat-inactivated fetal bovine serum (FBS), 100 U/ml penicillin and 100 μg/ml streptomycin (all purchased from Sigma, USA).

Through the entire culture period, the cells were kept at 37℃ in a humidified atmosphere containing 5% CO_2. The cells become confluent 5-7 days later. After that, the medium was removed from the donor chamber to expose the cells to an air-liquid interface for further differentiation. The TEER value of the cell layers was monitored at the same time. It was reported that the epithelial models with the transepithelial electrical resistance (TEER) around 200 to 1300 Ω●cm^2 had good correlation with bovine cornea and human cornea equivalents in permeation coefficient of timolol maleate.[32] TEER is usually used to characterize the expression of functional tight junctions. Meantime, the culture medium in the receiver chamber was changed every other day. The cells were kept at the air-liquid interface for another 7-20 days until the TEER value arrived at around 200-400 Ω●cm^2.

A.2.4 Permeation Experiments (Diffusion and Elimination) with PC Membrane

The permeation experiments through PC membrane were performed with Timolol Maleate Ophthalmic Solution (0.5%) and Timolol GFS (0.5%). As shown in Figure A.1, the permeation studies were initiated by adding 500 µl PBS medium to the receiver chamber (Figure A.1A) and 30 µl normal saline solutions to the donor chamber (Figure. 1B). The culture plate was tilted to 15-20 °degree when sampling and adding happened at the donor chamber, which was used to facilitate the fluid spreading across the apical surface. Two drops (~ 60-100 µl) of Timolol Maleate Ophthalmic Solution (0.5%) and Timolol GFS (0.5%) were administered into the middle of the donor chamber (Figure A.1C), immediately followed with 30 µl normal saline added at the fixed position of the donor chamber to mimic the induced lacrimation (Figure A.1D).[10] Aliquots of 200 µl were withdrawn from the receiver chamber (Figure. 1E) and an equal volume of blank PBS (Figure A.1F) was replaced. Meanwhile, aliquots of 60 µl aliquots of sample were taken out (Figure A.1G) from the donor chamber to simulate the drainage of the eye drop formulations due to the tear flow from induced lacrimation. At the same time, an equal volume of blank normal saline was added to the fixed position of the donor chamber (Figure A.1H). Every 15 minutes for 3 hours afterwards, aliquots of 200 µl were withdrawn (Figure A.1E) from the receiver chamber and replaced with an equal volume of blank PBS (Figure A.1F). Similar, aliquots of 60 µl were withdrawn from the donor chamber (Figure A.1G) and replaced with an equal volume of blank normal saline

(Figure A.1H) every 15 minutes for 3 hours. The culture plate was kept in the incubator during the rest time. The experiments were performed in triplicate.

A.2.5 Permeation Experiments (Diffusion and Elimination) with In vitro Cell Models

The permeation studies of Timolol Maleate Ophthalmic Solution (0.5%) and Timolol GFS (0.5%). across *in vitro* cell models were carried out. The experiment procedure was similar to the study with PC membrane model (Figure A.1). The study was initiated by adding 500 µl MEM with 2% FBS to the receiver chamber (Figure A.1A) and 30 µl MEM with 2% FBS to the donor chamber (Figure A.1B). Two drops (around 60-100 µl) of Timolol Maleate Ophthalmic Solution (0.5%) and Timolol GFS (0.5%) were administered to the middle of the donor chamber (Figure A.1C). The culture plate was tilted to 15-20 ° degree and 30 µl of MEM with 2% FBS was added at the fixed position of the donor chamber slowly to simulate the induced lacrimation (Figure A.1D). Aliquots of 200 µl medium were withdrawn from the receiver chamber (Figure A.1E) and an equal volume of blank medium was replaced (Figure A.1F). Meanwhile, aliquots of 60 µl fluid were taken out from the donor chamber from the fixed position to simulate the drainage of the eye drop formulations due to the tear flow from induced lacrimation (Figure A.1G). Also an equal volume of blank medium was added at the fixed position of the donor chamber (Figure A.1H). Aliquots of 200 µl were withdrawn from the receiver chamber and replaced with an equal volume of blank medium every 15 minutes for 3 hours from then on. The culture plate was put in the incubator at the rest time. In addition, aliquots of

60 µl were withdrawn from the donor chamber from the fixed bottom side and replaced with an equal volume of blank medium from the fixed top side every 15 minutes for 3 hours also. The experiments were performed in triplicate. Care should be taken during instillation, sampling and replacing with blank medium, in case the artificial membrane was disturbed.

A.2.6 Drug Quantitation

UV spectrophotometer (infinite reader M200, TECAN) with a wavelength of 295 nm was used to detect the concentration of timolol in all samples. For PC membrane study, blank PBS and normal saline solutions were used as the control groups for the collected samples from diffusion and elimination studies, respectively. For Cell model study, MEM with 2% FBS was used as the control for detection. TM Solution and TM GFS dissolved in control solutions with different dilution factors were measured as standard samples for calculation in PC membrane and cell model experiments.

A.2.7 Kinetic Data and Statistical Analysis

For both *in vitro* PC membrane and cell model studies, timolol mass acquired from the absorption and elimination experiments were plotted versus the sample collection time, respectively. The following kinetic parameters were calculated: eliminated timolol concentration at the apical surface from donor chamber 1 minute after dose administration (C_{1min}); eliminated timolol concentration at the apical surface from donor

chamber 15 minute after dose administration (C_{5min}); area under the timolol eliminated concentration vs. time curve (AUC), calculated from time = 1 min to the end of the observation times; peak time (t_{max}); peak timolol concentration (C_{max}) in the diffusion study; area under the timolol diffusion concentration vs. time curve (AUC), calculated from time = 1 min to the end of the observation times; mean residence time (MRT) of timolol on apical surface, calculated from the ratio of the area under the first moment curve (AUMC, concentration and time vs. time from t=0 to 180 min) to AUC (Equation: MRT = AUMC/AUC). The AUC and AUMC values were both calculated using the linear trapezoidal rule. Statistical significance between TM GFS group and TM Solution group was determined with one-way t-test (* indicates $P < 0.05$, ** indicates $P < 0.005$).

A.3 RESULTS

A.3.1 'Precorneal' retention of PC membrane model

Timolol Maleate Solution (TM Solution) and Timolol GFS (TM GFS) with equivalent strength (5mg/ml Timolol) were used.[19, 20] As mentioned in the method section, 30 µl normal saline was instilled across the 'precorneal' one minute after drug dosing to simulate the induced lacrimation and then 60 µl apical fluid was immediately withdrawn to simulate lacrimation drainage.[10] Induced lacrimation is commonly experienced when applying topical ocular formulations (e.g. eye drops) to the eyes. Generally, 60 µl is the induced lacrimation drainage volume.[10] The repeating steps after induced lacrimation mimic 'constant tear flow'. The normal tear flow rate is reported to be 4 µl/min, therefore 60 µl was instilled and withdrawn every 15 minutes in the study to simulate 'constant tear flow'. Relevant kinetic data of timolol concentration on the apical surface are listed in Table A.1. As seen from Table A.1, TM Solution had a larger washed away timolol concentration (3.40 ± 0.12 µg/µl) than TM GFS (2.65 ± 0.37 µg/µl) by induced lacrimation drainage (~1 min). However, at 15 min, the timolol concentration of TM Solution washed away by 'constant tear flow' become smaller (0.90 ± 0.08 µg/µl) than TM GFS (1.44 ± 0.12 µg/µl). Actually, timolol amounts of TM Solution at apical surface from 15 minutes to 3 hours (the end of the experiments) were all smaller than that of TM GFS, demonstrated by Figure A.2. Figure A.2 presents the elimination kinetic curve from 'constant tear flow' (timolol concentration in aliquots withdrawn from apical surface of donor chamber versus sampling time, starting at 15 minutes for 3 hours). It was clearly

shown that timolol amounts (Figure A.2) of both formulations (TM Solution and TM GFS) decreased significantly during 'constant tear flow' phase, while TM Solution had a lower timolol content starting at 15 minutes and stayed at a lower amount for 3 hours. Specifically, in the case of TM Solution, the timolol concentration decreased from 1.44±0.12 μg/μl to undetectable value in less than 90 min. The undetected time for TM GFS was longer, less than 120 min. Thus, TM Solution had a lower residence concentration than TM GFS on the artificial 'corneal' of PC membrane model. Due to the lower residence concentration, the area under the elimination curve (AUC) for TM solution (39.07 ± 4.31 min*μg/μl) was merely half of that for TM GFS (63.27 ± 4.31 min*μg/μl), accompanied by a shorter MRT (17.4 ± 0.3 min vs. 23.9 ± 0.9 min).

A.3.2 Diffusion across 'corneal' of PC membrane model

The total absorption and diffusion rate of timolol across artificial 'corneal' of PC membrane model were plotted versus the sampling time, respectively (Figure A.3A and Figure A.3B). As shown in Figure A.3A, after administration of the two formulations, timolol permeated through the PC membrane immediately and the amount of absorption increased rapidly in the receiver chamber during the first 15 minutes. Although slowly, the absorption of the two formulations still increased after 15 minutes, and plateaued at around 60 minutes. Nevertheless, the final accumulated basolateral timolol in the receiver chamber from TM solution (94.46 ± 5.51 μg) was much smaller than TM GFS (156.62 ± 27.94 μg). The different absorption amount could be explained by their different diffusion rates. The rate of diffusion peaked at 15 min for both formulations, but the peak

timolol concentration was 0.29 ± 40.02 μg/μL for TM solution and was 0.68 ± 0.05 μg/μL for TM GFS. As a result of the different diffusion rate, the area under rate of diffusion curve (AUC) of TM GFS (18.02 ± 2.36 min*μg/μL) was statistically and significantly different ($p^* < 0.05$) from the AUC of TM Solutions (6.61 ± 0.48 min*μg/μL) (Table A.2).

A.3.3 'Precorneal' retention and diffusion across 'corneal' of cell model

Timolol Maleate Solution (TM Solution) and Timolol GFS (TM GFS) with equivalent strength (5μg/μl Timolol) were also used in the Cell model study. Figure A.4 presents, for the two formulations under study, the elimination kinetic curve versus time. The timolol washed away by the induced lacrimation (1 min after administration) showed significant difference between TM GFS (114.21±16.14 μg) and TM Solution (159.60±13.48 μg). Similar to the PC model, in the cell model TM GFS also had higher timolol concentration in the elimination study (starting at 15 minutes for 3 hours) under 'constant tear flow' than TM Solution (Figure A.4), thus TM GFS had a higher 'precorneal' residence concentration even though similar MRT compared to TM Solution. The higher 'precorneal' residence is also confirmed by a larger area under elimination curve (AUC) for TM GFS (Table A.3). Elimination kinetic parameters reported in Table A.3 show that the area under elimination curve (AUC) of TM GFS (60.31 ± 8.18 min*μg/μl) was 1.17 fold of TM Solution (51.40 ± 2.97 min*μg/μl).

The diffusion results of the two formulations in cell model were also similar to the diffusion in the PC membrane model. The total absorption and rate of diffusion of the two timolol formulations across cell model were plotted versus the sampling time in Figure A.5A and Figure A.5B. According to Figure A.5A, TM GFS had a higher absorption across (93.60 ± 4.12 μg vs. 38.31 ± 0.92 μg) the artificial 'corneal' of the cell model and (Figure A.5B) a larger peak timolol concentration (0.25 ± 0.03μg/μL vs. 0.08 ± 0.00 μg/μL) than TM Solution. Consequently, TM GFS had a larger area under the rate of diffusion curve (AUC) than TM Solution (9.43 ± 0.81 min*μg/μL vs. 3.35 ± 0.19 min*μg/μL). Also, the diffusion rate of both formulations peaked at 15 minutes (Table A.4).

A.4 DISCUSSION

A.4.1 'Precorneal' retention of PC membrane model

The washing step in the PC membrane model simulated 'induced lacrimation' and 'constant tear flow', in order to differentiate formulations based on the retention time on the 'corneal'. The timolol cleared from the apical surface by the 60 µl 'induced lacrimation drainage' accounted for almost half of the total timolol elimination of the entire 'precorneal' study for the formulations in study. Nevertheless, different timolol amount was eliminated from the two formulations, under 'simulated induced lacrimation'. The mass of timolol washed away by the 'induced lacrimation drainage' was 203.85±7.09 µg for TM Solution and 158.88±21.92 µg for TM GFS (the ratio is more than 2:1), respectively (Table A.5). If percentage of timolol cleared away by 'induced lacrimation drainage' of total eliminated timolol was calculated, the value for TM Solution was 71% but 49% for TM GFS. Since larger amount of timolol was cleared by the 'induced lacrimation' from TM Solutions than from TM GFS (Table A.5), less timolol left on the 'precorneal' rendered less timolol capable of being cleared away from applied TM Solutions via 'constant tear flow'. Table A.5 showed that timolol mass washed away by 'constant tear flow' from applied TM Solutions was 84.41 ± 4.01 µg, but was 163.37 ± 30.47 µg from TM GFS.

Different retention results, as discussed above, demonstrated that 'induced lacrimation drainage' was less efficient in eliminating timolol from applied TM GFS than from TM solution, which could be explained by the gelling properties of TM GFS. It was

known that TM GFS contains GELRITE gellan gum, a purified anionic heteropolysaccharide derived from gellan gum. With a cation present, the aqueous solution of GELRITE tends to gel.[21] In this study, once upon contact with the cations in the normal saline, TM GFS tended to form rigid gels. Consequently, the timolol trapped in the gel would become harder to clear away by tear fluid than simple timolol solutions. Different retention performance of the two ophthalmic formulations detected by the PC model with 'simulated tear flow' suggested that the initial washing step applied in the *in vitro* model successfully simulated the 'induced lacrimation' for screening formulations with different residence time.

A.4.2 Diffusion across 'corneal' of PC membrane model

Overall, the diffusion trends of the two formulations were similar, but the absorption amount and bioavailability were different. As shown in Table A.6, TM GFS had higher timolol absorption percentage (33%) than TM Solution (25%). The higher bioavailability of TM GFS was relevant with a lower total elimination percentage (67% vs. 75%) from 'induced lacrimation' and 'constant tear flow' than TM Solution.

Although TM GFS had a higher timolol total elimination mass (322.26 ± 10.03 μg) than TM Solution (288.26 ± 10.90 μg) in Table A.6, the total timolol absorption from TM GFS was still larger than TM Solution (156.62 ± 27.94 μg vs. 94.46 ± 5.51 μg). The discrepancy of the low elimination percentage with the high elimination mass could be explained by dosing variation. Even though both two droplets of the two formulations

(TM Solutions and TM GFS) were applied in the study, the shape and volume of the droplets from the two bottles could be different owing to their different viscosity. Table A.6 also showed that the total recovered timolol mass from TM GFS (478.88 ± 37.94 μg) and TM Solutions (382.72 ± 6.97 μg) were slightly different. Therefore, the exact amount of timolol instilled from TM GFS could be slightly higher than TM Solution, resulting in a higher total eliminated timolol mass. Since the absolute amount of timolol applied was different from the formulations in study, total absorption percentage and elimination percentage are better criterion than absorption and elimination mass in evaluating the retention and diffusion properties of applied timolol formulations.

A.4.3 Epithelium cell model versus polycarbonate membrane (PC) model

Cell model in this study could also differentiate TM solution and TM GFS in induced lacrimation drainage, total absorption, and total elimination. TM Solution had a higher percentage of (Table A.7) induced lacrimation drainage (61% vs. 46%), (Table A.7) a higher percentage of total elimination (90% vs. 78%) and (Table 8) a lower percentage of total absorption (10% vs. 22%) than TM GFS.

Although the overall trends of the two models (PC model and Cell model) in terms of precorneal retention and diffusion were similar, the absolute values were slightly different due to different transport resistance. Because PC membrane model had a TEER value merely around 20-25 $\Omega \bullet cm^2$, corresponding to a small transport resistance, the majority of the timolol could pass through the PC membrane model within the first 15

min (Figure A.3). While the established epithelium cell model in this study had a high TEER value around 200-400 $\Omega \bullet cm^2$, thus timolol could not diffuse easily through the cell membrane, resulting in a continuous but slow timolol accumulation after the peak time (Figure A.5).

Due to the high transport resistance, the overall accumulation of timolol in the receiver chamber of the cell model is less than that of the PC membrane model. As shown in Figure A.6A and Figure A.6B, the absorption percentage was smaller and the elimination percentage was larger in the cell model than that in the PC membrane model for both formulations. Despite the difference in elimination percentage and absorption percentage, the initial elimination percentage was similar for both models (Figure A.6C). Thus, the effect of initial washing applied in PC model and Cell model was equivalent in differentiating the timolol formulations in terms of 'induced lacrimation drainage'.

A.4.4 Correlation with published pharmacokinetic data

The kinetics of timolol solution and "in situ" gelling formulation (Timoptic® XE) was investigated previously with the pigmented rabbits.[32] Although not exactly the same, the elimination studies of the *in vivo* rabbits have similar kinetic curves with than of PC model and cell model. In the diffusion study, the t_{max} values obtained from Timolol Maleate Solution and Timolol GFS were both around 15 min for the established two *in vitro* models, a little different from the *in vivo* data, which are 30 min and 60 min, respectively.[33] There are two potential reasons for the slight difference. Firstly, the

transport resistance values of the *in vitro* models were not high enough. The epithelial models with the transepithelial electrical resistance (TEER) around 200 to 1300 Ω●cm^2 was reported to have good correlation with bovine cornea and human cornea equivalents in permeation coefficient of timolol maleate. But actually, HCE-T model with TEER around 1300 Ω●cm^2 had the best correlation. In our research, cell model had a TEER around 200-400 Ω●cm^2, which is at the lowest range of acceptable TEER value for a good correlation. The PC model's TEER was merely 20-25 Ω●cm^2. So, the TEER of both in vitro models were much smaller than that of HCE-T model. Another reason

Additionally, Timolol Solution and Timoptic® XE have also been investigated by ex vivo rabbit corneas with simulated tear flow.[34] The relative timolol delivered from Timoptic® XE was 2.36 fold of Timolol Solution in the end of diffusion study. This number was 1.32 of the PC membrane model and 2.2 of the Cell model, calculated by the ratio of TM GFS absorption percentage with TM Solution absorption percentage (Table A.6 and Table A.8).

Although the two models were not established with cornea epithelium cell lines, the two models had similar diffusion and elimination profiles, and both correlated well with *in vivo* and ex vivo pharmacokinetic study. Considering the source of human cornea or tedious maintenance of animal, the two *in vitro* models provided an extremely simple and easy way to fast screen ocular topical formulations with prolonged residence time, compared to ex vivo human cornea model and sophisticated 3D models. Among them, PC model is much cheaper and easier to build up than epithelium cell model. But Cell

model is more accurate than PC model, proved by a relatively accurate value of relative timolol delivered.

Nevertheless, there are still some shortcomings of these two models. Firstly, the two formulations Timolol Maleate Solution and Timolol GFS used were not brand name drugs, merely generic drugs. So, *in vitro* evaluations of two different brand name drugs of timolol were still needed in the future study to further confirm the two *in vitro* models. Moreover, since the *in vitro* models in this study were consisted with polycarbonate (PC) membrane or Calu-3 lung epithelium cells only, they don't possess the binding sites on the cornea cell lines. Thus, these two *in vitro* models are not adequate to screen ocular formulations specifically attaching to the binding sites on cornea epithelium layers for longer precorneal retention. To solve these problems, cornea epithelium cell model or three dimensional human cornea equivalents should be applied.

A.5 CONCLUSION

Development of a simple, efficient and convenient model for screening topical ocular formulations is important for the ocular formulation development and advancement of ocular delivery. The *in vitro* models in this study, which used polycarbonate (PC) membrane and epithelium cell lines, show clear differences in elimination and diffusion results of the two different and well-studied formulations. Moreover, the two models also have good correlation in both elimination and diffusion with the *in vivo* animal study and *ex vivo* corneal study of timolol.[10, 35] Last but not the least important, the two models, especially the PC model, are much cheaper and easier to establish than current models. Therefore, the washing step with simulated tear flow is an improvement of current existing *in vitro* cell models in mimicking the induced lacrimation and tear flow.[32] In conclusion, the two models developed in this project are potential tools for screening ocular formulations ahead of large scale animal studies.

A.6 TABLES

Table A.1 Statistical Data of Timolol eliminated from Donor Chamber after administration in PC study.

Eye Drops	C_{1min} (µg/µL)	C_{15min} (µg/µL)	AUC(min*µg/µL)	AUC_{rel}	MRT(min)
TM Solution	3.40 ± 0.12	0.90 ± 0.08	39.07 ± 4.31	1	17.4 ± 0.3
TM GFS	2.65 ± 0.37*	1.44 ± 0.12**	63.27 ± 4.31	1.62	23.9 ± 0.9

Table A.2 Statistical Data of Rate of Diffusion of the two formulations through PC model

Eye Drops	**C_{max} (µg/µL)**	**t_{max} (min)**	**AUC(min*µg/µL)**
TM Solution	0.29 ± 0.02	15	6.61 ± 0.48
TM GFS	0.68 ± 0.05**	15	18.02 ± 2.36**

Table A.3 Timolol eliminated from Donor Chamber after administration with Cell Model.

Eye Drops	**C_{1min} (µg/µl)**	**C_{15min} (µg/µL)**	**AUC(min*µg/µL)**	**AUC_{rel}**	**MRT(min)**
TM Solution	3.62 ± 0.31	1.18 ± 0.07	51.40 ± 2.97	1	11.1 ± 0.1
TM GFS	2.59 ± 0.37**	1.37 ± 0.22	60.31 ± 8.18	1.17	11.0 ± 0.2

Table A.4 Rate of Diffusion of timolol across Cell Model.

Eye Drops	**C_{max}(µg/µL)**	**t_{max}(min)**	**AUC(min*µg/µL)**
TM Solution	0.08 ± 0.00	15	3.35 ± 0.19
TM GFS	0.25 ± 0.03**	15	9.43 ± 0.81**

Table A.5 Eliminated timolol in PC Membrane Study (timolol amount at the apical surface)

Eye Drops	Induced Lacrimation Drainage	Normal Constant Tear Flow	Total Elimination
TM Solution	203.85 ± 7.09 µg (71%)	84.41 ± 4.01 µg (29%)	288.26 ± 10.90 µg (100%)
TM GFS	158.88 ± 21.92 µg* (49%)	163.37 ± 30.47 µg (51%)	322.26 ± 10.03 µg* (100%)

One way T-test, p*<0.05, p**<0.005

Table A.6 Recovered timolol from PC Membrane Study

Eye Drops	Total Absorption	Total Elimination	Total Mass
TM Solution	94.46 ± 5.51 µg (25%)	288.26 ± 10.90 µg (75%)	382.72 ± 6.97 µg (100%)
TM GFS	156.62 ± 27.94 µg* (33%)	322.26 ± 10.03 µg* (67%)	478.88 ± 37.94 µg* (100%)

One way T-test, p*<0.05, p**<0.005

Table A.7 Eliminated timolol in Cell Model Study

(timolol amount at the apical surface)

Eye Drops	Induced Lacrimation Drainage	Normal Constant Tear Flow	Total Elimination
TM Solution	217.05 ± 18.34 μg (61%)	140.03 ± 11.12 μg (39%)	357.08 ± 15.12 μg (100%)
TM GFS	155.32 ± 2.59 μg** (46%)	181.49 ± 24.64 μg (54%)	336.81 ± 10.96 μg (100%)

One way T-test, p*<0.05, p**<0.005

Table A.8 Recovered timolol from Cell Model Study

Eye Drops	Total Absorption	Total Elimination	Total Mass
TM Solution	38.31 ± 0.92 µg (10%)	357.08 ± 15.12 µg (90%)	395.39 ± 14.29 µg (100%)
TM GFS	93.60 ± 4.12 µg** (22%)	336.81 ± 10.96 µg (78%)	430.41 ± 7.77 µg* (100%)

One way T-test, p*<0.05, p**<0.005

A.7 FIGURES

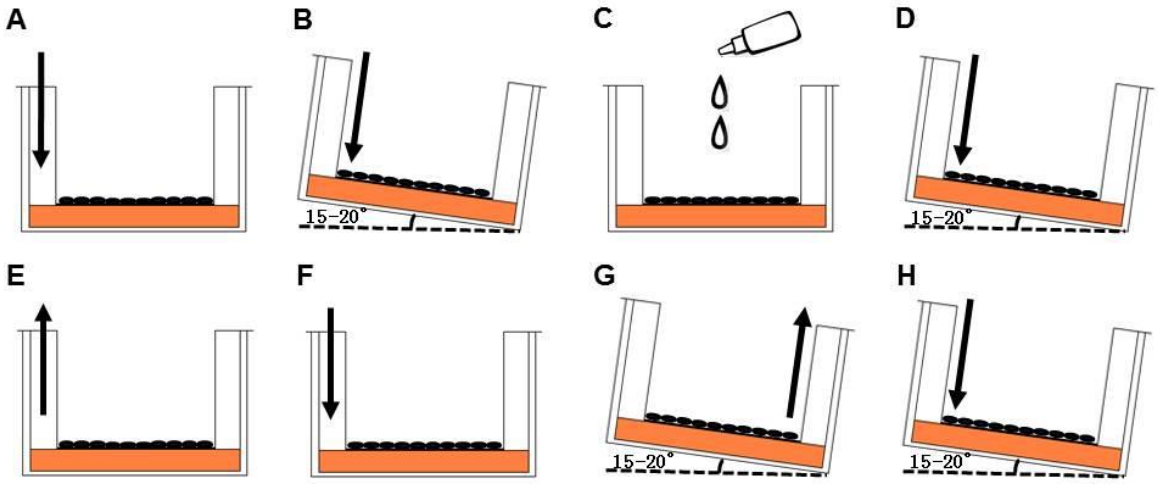

Figure A.1 Diffusion and elimination studies with established in vitro models; A) Add 500 µl medium solution to the receiver chamber; B) Apply 30 µl isotonic solution to provide moisture environment of 'precorneal'; C) Instill 2 droplets of eye drops; D) Apply 30 µl isotonic solution to simulate induced lacrimation, immediately (~ 1 min) after administration of eye drops; E) Sample 200 µl fluid from receiver chamber for diffusion studies; F) Replace with 200 µl blank solution in the receiver chamber; G) Meanwhile, withdraw 60 µl fluid from donor chamber to simulate induced lacrimation drainage; H) Replenish with 60 µl blank solution in the donor chamber; Repeat E), F), G), and H) steps every 15 min for 3 hrs for diffusion studies and to simulate 'constant tear flow', respectively.

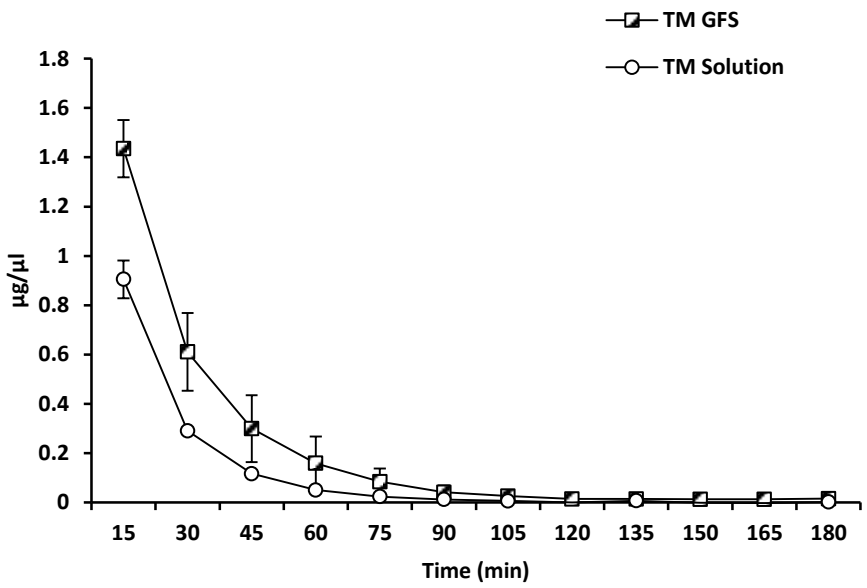

Figure A.2 Apical surface concentration of timolol with the PC membrane model

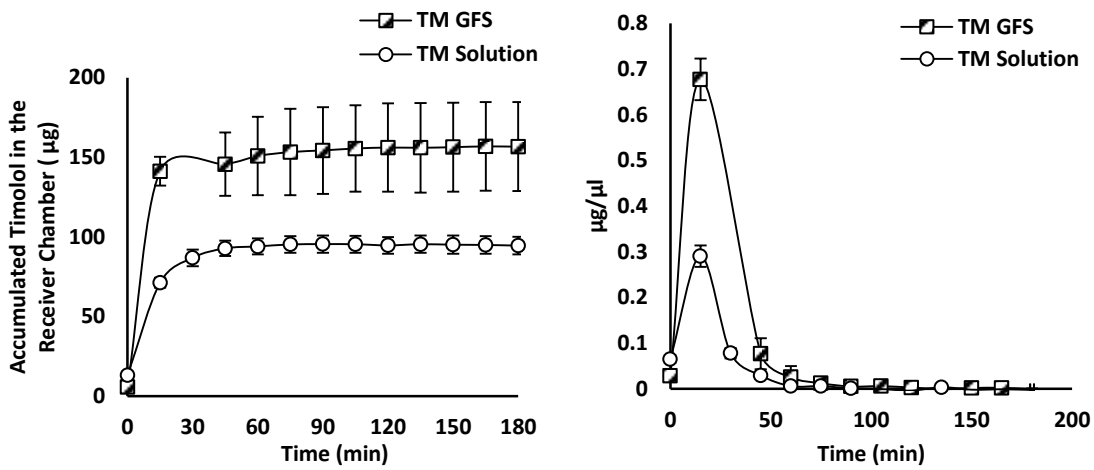

Figure A.3 A) Total absorption, B) Rate of diffusion of the two timolol formulations across PC membrane model.

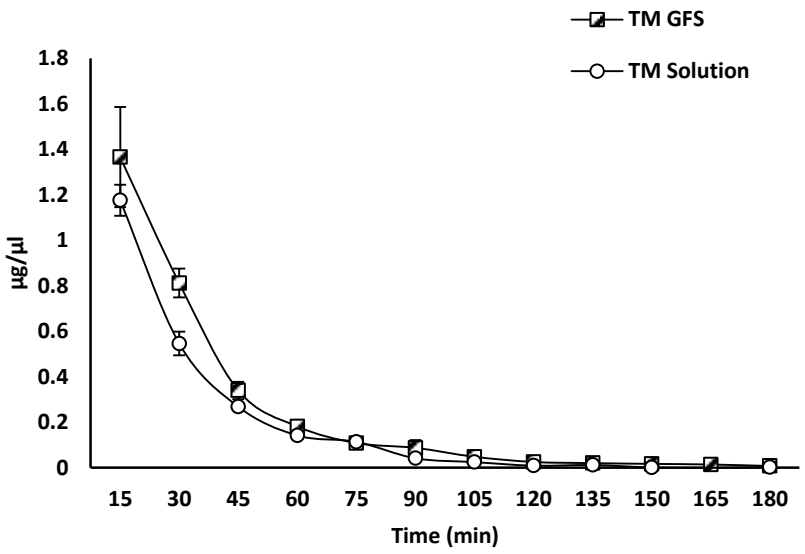

Figure A.4 Apical surface concentration of timolol with Cell Model from 15 minutes to 3 hours.

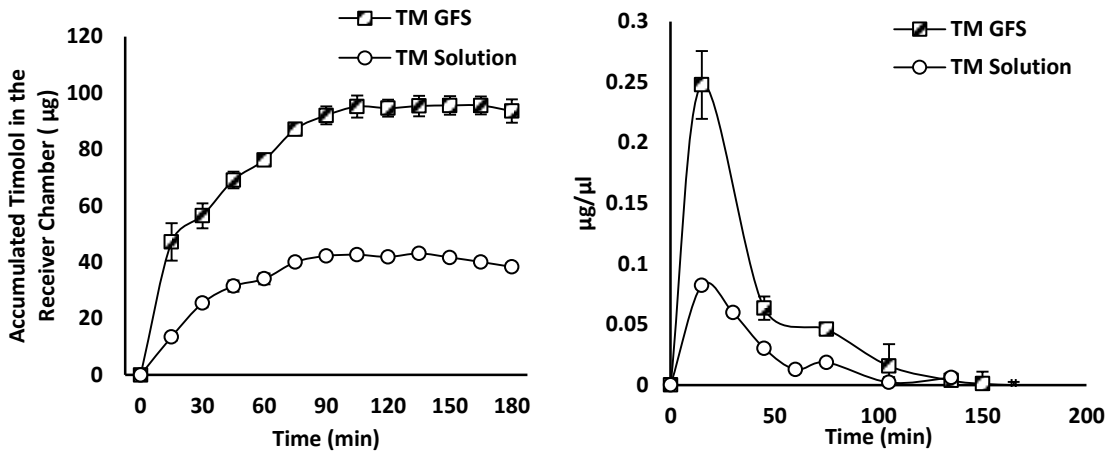

Figure A. 5 A) Total absorption, B) Rate of diffusion of the two timolol formulations across cell model. (0-30 min, increase sampling frequency)

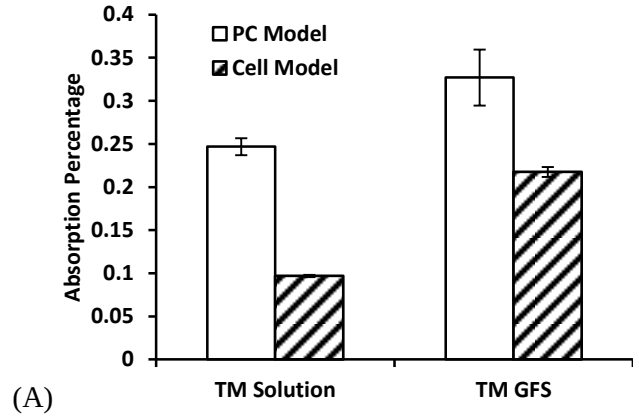

(A)

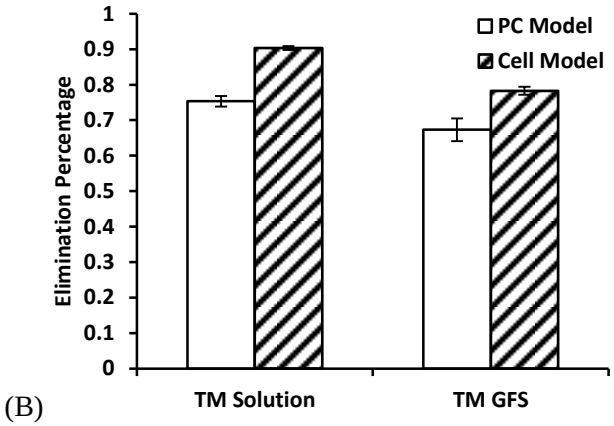

(B)

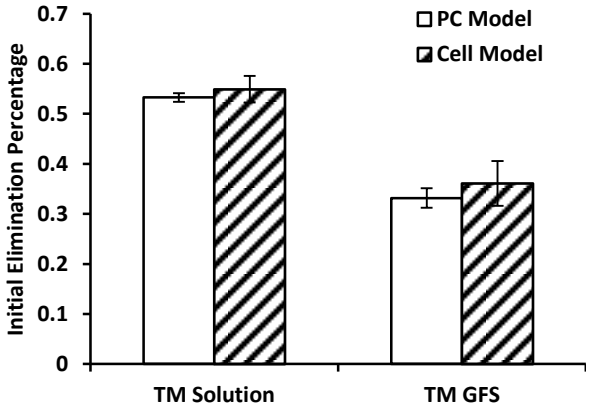

(C)

Figure A. 6 Comparison between the PC Model and Cell Model in A) absorption ratio, B) elimination ratio and C) initial elimination ratio.

A.8 REFERENCES

1. Huml RA, Chance K. 2009. Key Challenges to US Topical Ocular Drug Development. Science & Technology.

2. Kompella UB, Kadam RS, Lee VH. 2011. Recent advances in ophthalmic drug delivery. Ther Deliv. 1:435-56.

3. Gupta D. Review on ocular drug delivery.

4. Patel A, Cholkar K, Agrahari V, Mitra. AK. 2013. Ocular drug delivery systems: An overview. World J Pharmacol 2:47-64.

5. Weiner AL, Gilger BC. 2010. Advancements in ocular drug delivery. Vet Ophthalmol. 13:395-406.

6. Gaudana R, Jwala J, Boddu SH, Mitra AK. 2009. Recent perspectives in ocular drug delivery. Pharm Res. 26:1197-216.

7. Hornof M, Toropainen E, Urtti A. 2005. Cell culture models of the ocular barriers. Eur J Pharm Biopharm. 60:207-25.

8. DelMonte DW, Kim T. 2011. Anatomy and physiology of the cornea. J Cataract Refract Surg. 37:588-98.

9. Reichl S, Kolln C, Hahne M, Verstraelen J. 2011. In vitro cell culture models to study the corneal drug absorption. Expert Opin Drug Metab Toxicol. 7:559-78.

10. Gaudana R, Ananthula HK, Parenky A, Mitra AK. 2010. Ocular drug delivery. AAPS J. 12:348-60.

11. Liu Q, Wang Y. 2009. Development of an ex vivo method for evaluation of precorneal residence of topical ophthalmic formulations. AAPS PharmSciTech. 10:796-805.

12. Lee YC, Simamora P, Yalkowsky SH. 1997. Effect of Brij-78 on systemic delivery of insulin from an ocular device. J Pharm Sci. 86:430-3.

13. Reichl S. 2008. Cell culture models of the human cornea - a comparative evaluation of their usefulness to determine ocular drug absorption in-vitro. J Pharm Pharmacol. 60:299-307.

14. Chang JE, Basu SK, Lee VH. 2000. Air-interface condition promotes the formation of tight corneal epithelial cell layers for drug transport studies. Pharm Res. 17:670-6.

15. Jung KM, Lee SH, Ryu YH, Jang WH, Jung HS, Han JH, et al. 2011. A new 3D reconstituted human corneal epithelium model as an alternative method for the eye irritation test. Toxicol In Vitro. 25:403-10.

16. Dey S. 2011. Corneal cell culture models: a tool to study corneal drug absorption. Expert Opin Drug Metab Toxicol. 7:529-32.

17. Elliott NT, Yuan F. 2011. A review of three-dimensional in vitro tissue models for drug discovery and transport studies. J Pharm Sci. 100:59-74.

18. Toropainen E, Ranta VP, Talvitie A, Suhonen P, Urtti A. 2001. Culture model of human corneal epithelium for prediction of ocular drug absorption. Invest Ophthalmol Vis Sci. 42:2942-8.

19. Timolol Maleate Ophthalmic Solution USP STERILE, 0.25% and 0.5%. FALCON PHARMACEUTICALS. In: COPYRIGHT © 2004 FALCON PHARMACEUTICALS, EDITOR. Fort Worth, Texas 76134 USA.

20. Timolol GFS (timolol maleate ophthalmic gel forming solution), 0.25% and 0.5%. In: COPYRIGHT © 2008 FALCON PHARMACEUTICALS, EDITOR. Fort Worth, Texas 76134 USA.

21. STERILE OPHTHALMIC GEL FORMING SOLUTION. TIMOPTIC-XE® 0.25% AND 0.5% (TIMOLOL MALEATE OPHTHALMIC GEL FORMING SOLUTION). In: COPYRIGHT © 2009 ATON PHARMA I, editor. Lawrenceville, NJ 08648, USA2009.

22. Burgalassi S, Chetoni P, Panichi L, Boldrini E, Saettone MF. 2000. Xyloglucan as a novel vehicle for timolol: pharmacokinetics and pressure lowering activity in rabbits. J Ocul Pharmacol Ther. 16:497-509.

23. Benediktsdottir BE, Arason AJ, Halldorsson S, Gudjonsson T, Masson M, Baldursson O. 2013. Drug delivery characteristics of the progenitor bronchial epithelial cell line VA10. Pharm Res. 30:781-91.

24. Toropainen E, Ranta VP, Vellonen KS, Palmgren J, Talvitie A, Laavola M, et al. 2003. Paracellular and passive transcellular permeability in immortalized human corneal epithelial cell culture model. Eur J Pharm Sci. 20:99-106.

25. Cozens AL, Yezzi MJ, Kunzelmann K, Ohrui T, Chin L, Eng K, et al. 1994. CFTR expression and chloride secretion in polarized immortal human bronchial epithelial cells. Am J Respir Cell Mol Biol. 10:38-47.

26. Wan H, Winton HL, Soeller C, Stewart GA, Thompson PJ, Gruenert DC, et al. 2000. Tight junction properties of the immortalized human bronchial epithelial cell lines Calu-3 and 16HBE14o. Eur Respir J. 15:1058-68.

27. Manford F, Tronde A, Jeppsson AB, Patel N, Johansson F, Forbes B. 2005. Drug permeability in 16HBE14o- airway cell layers correlates with absorption from the isolated perfused rat lung. Eur J Pharm Sci. 26:414-20.

28. Pibalpakdee P, Wongratanacheewin S, Taweechaisupapong S, Niumsup PR. 2012. Diffusion and activity of antibiotics against Burkholderia pseudomallei biofilms. Int J Antimicrob Agents. 39:356-9.

29. Stephens JR, Beveridge JS, Latham AH, Williams ME. 2010. Diffusive flux and magnetic manipulation of nanoparticles through porous membranes. Anal Chem. 82:3155-60.

30. Shlyonsky V. 2013. Ion permeability of artificial membranes evaluated by diffusion potential and electrical resistance measurements. Adv Physiol Educ. 37:392-400.

31. Transwell® Permeable Supports Selection and Use Guide. CORNING. Corning Incorporated Life Sciences. NY. 14831.

32. Liu Q, Wang Y. 2009. Development of an ex vivo method for evaluation of preconrneal residence of topical ophthalmic formulations.m AAPS PharmSciTech. 10(3): 796-805.

33. Oh C, Saville BA, Cheng YL, Rootman DS. 1995. A compartmental model for the ocular pharmacokinetics of cyclosporine in rabbits. Pharm Res. 12:433-7.

34. Rowe TE, Akande JA, Reed K. 2007. Measurement and Prediction of Timolol Diffusion with and Without Simulated Tear Flow.

35. Rowe TE, Akande JA, Reed K. 2010. Measurement and Prediction of Timolol Diffusion with and Without Simulated Tear Flow. Poster 2452.

VITA

Ping Du received her professional degree in College of Pharmacy and master degree in Chemical Biology from Peking University, China. In May 2011, she attended graduate school in Pharmaceutics Division, College of Pharmacy at The University of Texas at Austin having Dr. Hugh D. C. Smyth as the supervisor. During her four years' graduate study in UT-Austin, Ping has achieved various accomplishments in academic research. As a graduate student, she has authorized in high-quality and leading international journals 1 book chapter, 1 review paper, and 2 research publications, as well as 5 research manuscripts ready to submit and publish. Ping also has presented 9 conference papers about her research and dissertation work in prestigious international conferences. In 2013 and 2014, Ping did two summer internship in Boehringer Ingelheim Inc. and Genentech, Inc. working on projects relevant with her dissertation project to apply the knowledge and science acquired from UT-Austin into practice. Apart from her excellent academic achievements, Ping also has held several leadership roles in the student organizations. She has been the secretary/treasurer and chair of AAPS UT-Austin Student Chapter and also secretary and president of Pharmacy Graduate Student Association. Because of Ping's excellent performance, she was awarded various fellowships for successive three years, including 2011-2012 professional development award from the University of Texas at Austin, 2012-2013 The Dr. Michael and Carrie Crowley and Dr. Jason and Kasey Vaughn Graduate Fellowship, 2012-2013 The Dr. Feng Zhang & Dr. James McGinity Graduate Fellowship, 2013-2014 The James W.

McGinity Graduate Fellowship, 2013-2014 The Williams & McGinity Graduate Fellowship and 2013-2014 The Dr. Feng Zhang & Dr. James McGinity Graduate Fellowship. Additionally, in 2014 she was also nominated by UT-Austin for Howard Hughes Medical Institute (HHMI) Fellowship. Only 5 graduate students in UT-Austin were nominated for this fellowship that year.

Permanent email address: du.ping@utexas.edu

This dissertation was typed by the author.